ÖVERSPÄNNING FRÅN ENFASANSLUTNA SOLPANELER

RAPPORT 2018:506

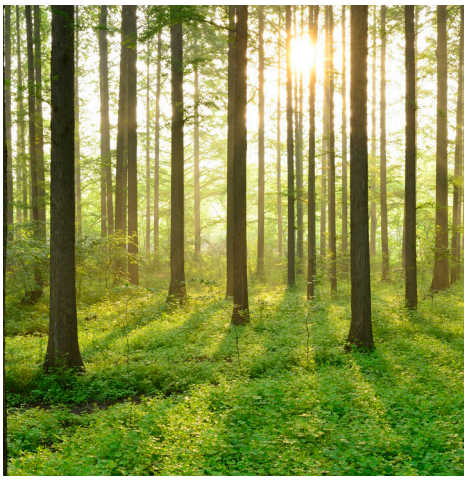

SMARTA ELNÄT

Energiforsk

Överspänning från enfasanslutna solpaneler

Overvoltage due to single-phase connected PV

MATH BOLLEN

ISBN 978-91-7673-506-0 | © Energiforsk juni 2018

Energiforsk AB | Telefon: 08-677 25 30 | E-post: kontakt@energiforsk.se | www.energiforsk.se

Förord

Anslutning av solkraft till lågspänningsnätet kommer att påverka elnätets presentande på ett antal olika sätt. Påverkan på vågformsdistorsion har inte studerats så mycket men när det införs smarta-elnätsteknologi för att kunna ansluta mer solkraft kommer det att oftare uppstå situationer då övertonsnivåerna blir oacceptabla. Utöver de vanliga spänningsvariationerna (10-minuters rms värden) ska det också tas med att spänningsvågen blir distorderad. I detta projekt kommer det att utföras mätningar och beräkningar för att bedöma hur distorsionen kommer att ändras vid anslutning av ökade mängder solkraft till lågspänningsnät. Beräkningsmetoder kommer att utvecklas och tillämpas på två befintliga lågspänningsnät i Sverige. Det kommer att behandlas båda övertoner (under 2 kHz) och supratoner (över 2 kHz).

Projektet *Övertoner i lågspänningsnät vid anslutning av solpaneler*, ingår i programmet Smarta Elnät, ger kvantitativ information om den förväntade distorsionen i lågspänningsnät med stora mängden solkraft, samt underlag för at bedöma om det behövs åtgärder för att begränsa distorsionen.

Math Bollen från Luleå tekniska universitet, Skellefteå har varit projektledare för projektet. Ett extra stort tack också till referensgruppen, som på ett mycket givande sätt har bidragit till projektet:

- Sara Johansson, Vattenfall Energy Trading AB
- Nicklas Fredlund, Elverket Vallentuna AB
- Tokhir Gafurov, Mälarenergi AB
- Oscar Willén, She AB
- Andres Feurst, Öresundskraft AB
- Malin Westman, Skellefteå Kraft AB

Programmets Smarta Elnät programstyrelse, som initierat, följt upp och godkänt projektet, består av följande ledamöter:

- Peter Söderström, Vattenfall Eldistribution AB (ordförande)
- Torbjörn Solver, Mälarenergi AB (vice ordförande)
- Mira Rosengren Keijser, Svenska kraftnät
- Patrik Björnström, Sveriges ingenjörer (Miljöfonden)
- Kristina Nilsson, Ellevio AB
- Björn Ållebrand, Trafikverket
- Ferruccio Vuinovich, Göteborg Energi AB
- Per-Olov Lundqvist, Sandviken Energi AB
- Claes Wedén, ABB AB
- Daniel Köbi, Jämtkraft AB
- Hannes Schmied, NCC AB
- Mats Bergström, Umeå Energi Elnät AB
- Magnus Sjunnesson, Öresundskraft AB
- Henric Johansson, Jönköping Energi AB
- David Håkansson, Borås Elnät AB
- Peter Addicksson, HEM AB
- Matz Tapper, Energiföretagen Sverige (adjungerad)
- Anders Fredriksson, Energiföretagen Sverige (adjungerad)

Sammanfattning

Denna rapport behandlar påverkan av enfasanslutna solcellsinstallationer på överspänning i lågspänningsnät. Två befintliga nät valdes för att tillämpa en nyutvecklad stokastisk planeringsmetod.

Acceptansgränsen visades vara begränsad för dessa två nät under de antaganden som gjordes. Det visades emellertid också att flera av de parametervärden som används har stor påverkan på resultaten. Detta gäller särskilt för produktionen per installation, percentilen som används i prestandaindexen och bakgrundspänningen. Acceptansgränsen från studierna i denna rapport är sannolikt en underskattning.

Ett antal åtgärder har studerats för att öka acceptansgränsen. De mest lovande är: koordinerat anslutning av växelriktare till fas med lägst spänning innan anslutning; nedstyrning av produktion eller energilagring nära installationerna; kondensator eller reaktor nära distributionstransformatorn. Den första metoden kan tillämpas på ett enkelt sätt utan mycket investering. Metoden kräver dock en mätning för vilken det behövs riktlinjer.

Planeringsmetoden har visat sig vara användbar för att utvärdera behovet av åtgärder och för att jämföra åtgärder.

Användningen av tidsserier av produktion och konsumtion är ett alternativ till den stokastiska planeringsmetoden. Detta kräver data över ett antal år, eftersom det finns betydande variationer mellan åren.

Ytterligare insamling av data från både produktions- och konsumtionsställen behövs. Tidsupplösning bör vara minst 10 minuter. Användning av timvärden är inte tillräcklig för att beräkna acceptansgränser gällande överspänning och underspänning.

Summary

This report addresses the impact of single-phase connected PV installations to overvoltage in low-voltage distribution networks. Two existing networks were selected to apply a newly developed stochastic planning method.

The hosting capacity was shown to be limited for the two networks under the assumptions made. It was however also shown that several of the parameter values used have a strong influence on the results. This especially holds for the estimated size of the production per installation, the percentile value used in the performance index, and the range of the background voltage. The hosting capacity values found in the studies presented in this report are most likely and underestimation.

Several mitigation methods have been studied to increase the hosting capacity. The most promising ones are: coordinated connection of inverters to the phase with the lowest pre-connection voltage; curtailment of production or energy storage close to the PV installations; and capacitor bank or shunt reactor close to the distribution transformer. The first one appears rather simple; it can be applied without much investment. The method does however require a measurement for which some guidelines are needed.

The hosting-capacity based planning tool was shown to be a useful tool for evaluating the need for mitigation actions and for comparing mitigation actions.

The use of time series of production and consumption is an alternative to the stochastic method. This requires data over a number of years, as there are significant year-to-year variations.

Further collection of data from both production and consumption sites is needed. Time resolution should be at least 10 minutes. Using hourly data is not enough for hosting-capacity studies concerning overvoltage and undervoltage.

Innehåll

1 Inledning, översikt och slutsatser

1.1 BAKGRUND

Anslutning av solkraft till ett lågspänningsnät leder till en spänningsökning för kunderna anslutna till detta nät. Fenomenet är känt och har diskuterats tidigare för både vindkraft och solkraft och för distribuerad generering i allmän[1,2,3,4]. När mängden ansluten solkraft orsakar en spänningsökning som överstiger överspänningsgränsen har man nått den så kallade acceptansgränsen[5]. För att då kunna ansluta ytterligare solkraft behövs åtgärder för att minska spänningshöjningen.

Spänningsökningen är större vid enfasig anslutning av solkraft än vid trefasig anslutning. Det visas i rapporten att den är ungefär sex gånger större vid enfasig anslutning. Acceptansgränsen blir därmed också mindre om solcellsanläggningen ansluts till enbart en fas. Projektet som beskrivs i denna rapport riktar sig mot de enfasigt anslutna solcellsanläggningar, vilka spänningsökningar de leder till, vad acceptansgränsen är och vilka möjliga åtgärder det finns. Det har gjorts en del mätningar i projektet och en del av dessa kommer också att presenteras i rapporten.

Bidraget från projektet är:

- Systematiska beräkningsmetoder för att kunna jämföra olika metoder för att hantera spänningsvariationer i elnätet från lokala förnyelsebara energikällor på ett stokastiskt sätt. Grunden till metoden utvecklas i ett tidigare projekt om obalans på grund av enfasig ansluta solcellsanläggningar[6].
- Tillämpning av metoderna på två svenska lågspänningsnät.
- Tillämpning av metoderna för att kunna kvantifiera huruvida vissa åtgärder kan minska risken för överspänningar.

Projektet utfördes parallellt, och med gemensam referensgrupp, med två andra projekt inom Energiforsk: Övertoner och supratoner från solkraft ansluten till lågspänningsnät, som utfördes av Luleå tekniska universitet; och Mellansnabba spänningsvariationer på grund av solkraft, som utfördes av STRI.

---

[1] Tonkoski, R., Turcotte, D., & El-Fouly, T. H. (2012). Impact of high PV penetration on voltage profiles in residential neighborhoods. IEEE Transactions on Sustainable Energy, 3(3), 518-527.
[2] Katiraei, F., & Aguero, J. R. (2011). Solar PV integration challenges. IEEE Power and Energy Magazine, 9(3), 62-71.
[3] Bollen, M. H., & Hassan, F. (2011). Integration of distributed generation in the power system (Vol. 80). John wiley & sons.
[4] Jayasekara, N., & Wolfs, P. (2010, December). Analysis of power quality impact of high penetration PV in residential feeders. In Power Engineering Conference (AUPEC), 2010 20th Australasian Universities (pp. 1-8). IEEE.
[5] Deuse, J., Grenard, S., & Bollen, M. (2008). EU-DEEP integrated proect: technical implications of the" hosting-capacity" of the sytem for DER. International Journal of Distributed Energy Resources, 4(1), 17-34.
[6] D. Schwanz, M. Bollen, S. Rönnberg, Obalans från enfasanslutna solpaneler, Energiforsk Rapport 2015:130, July 2015.

Resultat från dessa två projekt, samt från två tidigare projekt, kommer att sammanfattas och diskuteras i en gemensam rapport.

1.2 EXEMPELNÄT OCH BERÄKNINGSMETODEN

Simuleringar i projektet utfördes till största delen för två lågspänningsnät i norra Sverige: ett landsbygdsnät med 6 kunder och ett stadsnät med 28 kunder. Både nät och komponentdata finns beskriven i detalj i kapitel 2. Där beskrivs även modellen som används för att räkna ut spänningarna vid anslutning av solpaneler. Modellen bygger på transferimpedansmatrisen för spänningar mellan fas och nolla. Matrisen anger hur mycket spänningarna (de komplexa spänningarna) ändras på ett visst ställe i nätet på grund av en ström någonstans i nätet.

1.3 ACCEPTANSGRÄNS SOM ETT PLANERINGSVERKTYG

Från impedansdata för ungefär 50 000 lågspänningskunder beräknades det en fördelning av acceptansgränsen för anslutning av solkraft, enfasig och trefasig. Acceptansgränsen beräknades för tillåten spänningsökning på 3 % och 5 %. Resultat visas i Tabell 1 och detaljerna finns i Avsnitt 3.1.

Tabell 1. Andel av kunder som inte klarar acceptansgränserna av 3 kW eller 6 kW.

Tillåten spänningsökning	5%	3%	5%	3%
Acceptansgräns mindre än	3 kW		6 kW	
Enfas anslutning (% av kunder)	4.6%	17.8%	25.3%	50.6%
Trefas anslutning (% av kunder)	0.002%	0.05%	0.04%	0.5%

En planeringsmetod som bygger på acceptansgränsen har använts och vidareutvecklats i projektet. Metoden består av följande steg:

i) Uppskatta spänningsvariationerna i lågspänningsnätet utan produktion eller förbrukning, under de timmar på året som produktionen från solenergi kan vara hög. Dessa är de spänningsvariationer som kommer från mellanspänningsnätet.
ii) Uppskatta intervallet av den lägsta förbrukningen under de timmarna på året som produktionen från solenergi kan vara hög.
iii) Uppskatta produktionen per anläggning under den 10-minutersperioden med högst effekt från alla installationer tillsammans. Detta är inte detsamma som den maximala produktionen per anläggning, men det kan betecknas som en "maximal produktion efter mångfald" (”after-diversity-maximum-production”) bredvid en "minsta konsumtion efter mångfald".
iv) Lägg slumpmässigt till solkraftanläggningar hos kunderna fördelat över faserna och beräkna fördelningen av högsta spänningen med ökande mängd solkraft.
v) Definiera ett prestationsindex för nätet, en lämplig gräns för detta index och bestäm acceptansgränsen.

En detaljerad beskrivning av metoden återfinns i kapitel 3.

Eftersom regelverket för spänningsvariationer utgår från 10-minutersvärden behövs samma 10-minuters tidsupplösning för bakgrundspänning och förbrukning.

Metoden kan användas för att uppskatta acceptansgränsen i planeringsstadiet. Utfallet av uppskattningen, tillsammans med uppskattningar av framtida tillväxt av antalet kunder med solkraft, ger återkoppling till nätoperatören om behovet av nätinvesteringar. Som ett exempel visas fördelningsfunktionen av spänningen för de två exempelnäten med 6-kW enfasanslutna solcellsanläggningar i Figur 1 och Figur 2.

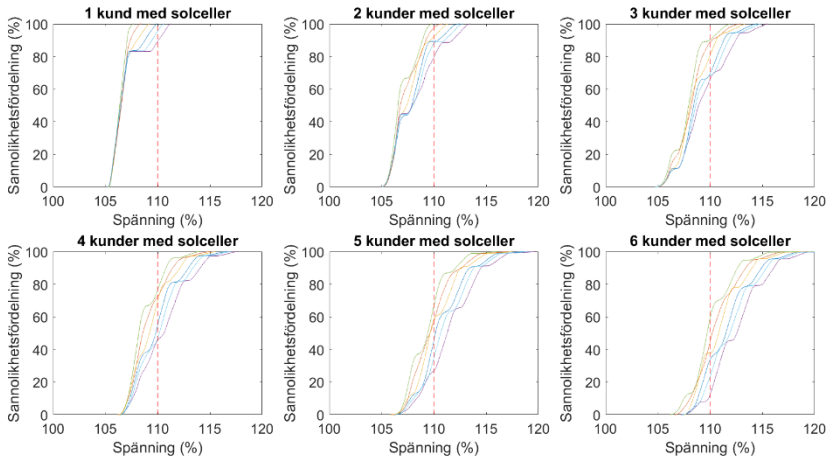

Figur 1. Sannolikhetsfördelningen för värsta överspänning i sex-kunders nät vid ökad andel kunder med solkraft.

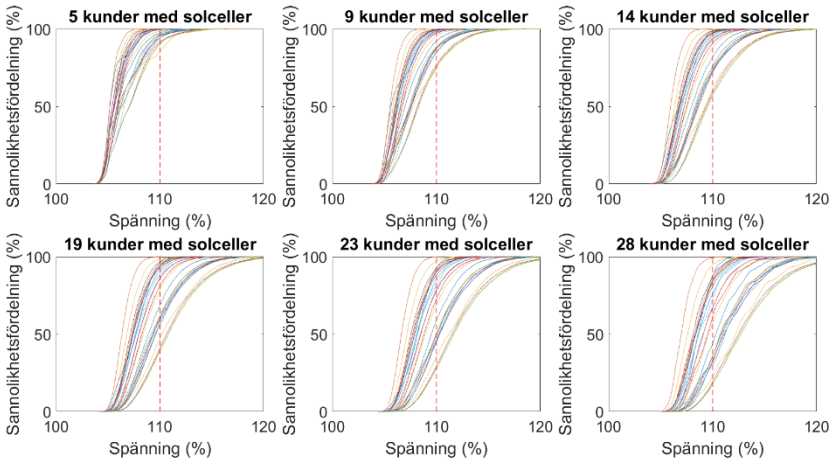

Figur 2. Sannolikhetsfördelningen för värsta överspänning i 28-kunders nät vid ökad andel kunder med enfasig-ansluten solkraft (PV).

Från sannolikhetsfördelningen har det beräknats ett prestandaindex, som motsvarar 90-percentil av fördelning för överspänningen. Indexen visas, som funktion av antalet kunder med solkraft, i Figur 3 och Figur 4, för de två exempelnäten.

Acceptansgränsen blir ungefär 1 kund med solceller för 6-kunders nät och ungefär 3 kunder med solceller för 28-kunders nät.

Resultat visas på ett något annorlunda sätt i Figur 5. Här visas att acceptansgränsen nås först hos kund nummer 24 och strax efter det för kunderna 17, 18 och 19.

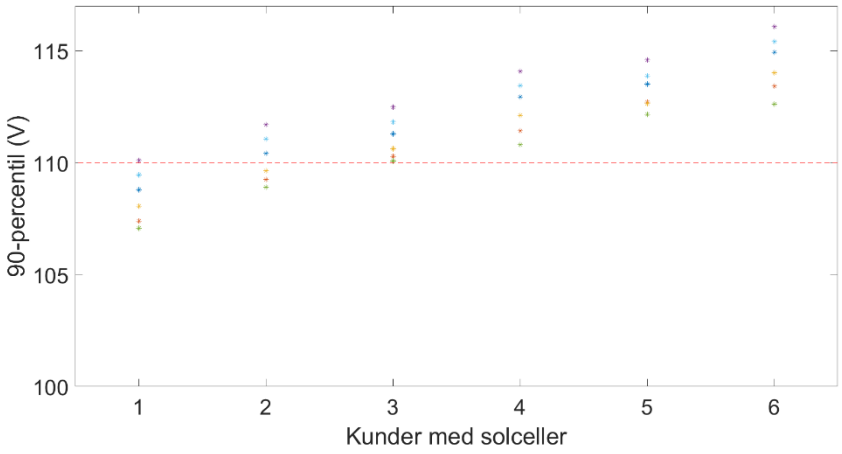

Figur 3. Prestandaindex (90-percentil av överspänningen) för sex-kunders nät.

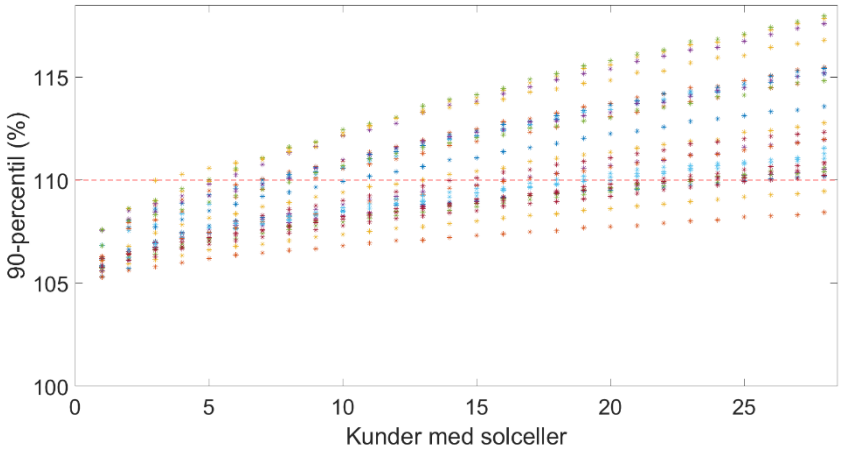

Figur 4. Prestandaindex (90-percentil av överspänningen) för 28-kunders nät.

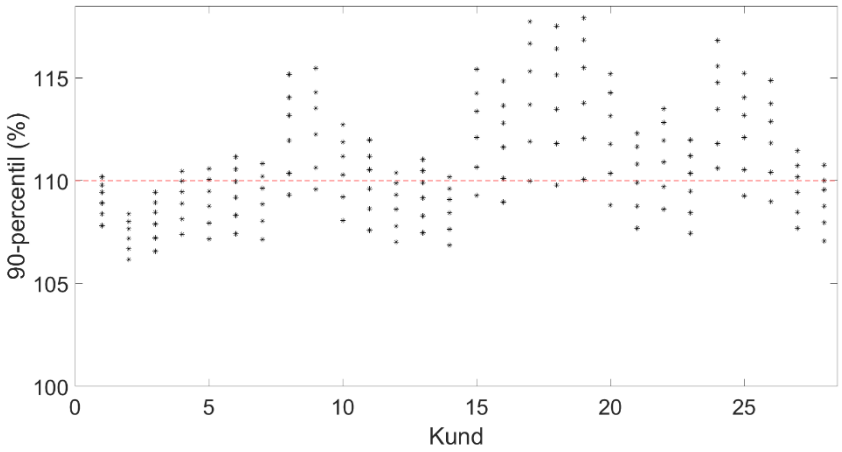

Figur 5. Prestandaindex för kunderna i 28-kunders nät, 5, 9, 14, 19, 23 och 28 kunder med enfasig-ansluten solkraft.

Enfasinstallationer som matar in en effekt på 6 kW ger ett bidrag till överspänning som leder till att för 90-procentilen nås överspänningsgränsen på 110 % redan för ett litet antal kunder med solkraft. Detta är troligen ett extremt fall och den faktiska acceptansgränsen kan vara betydligt större av två skäl:

- Det förväntas inte att alla installationer kommer att mata in 6 kW effekt samtidigt. För en installationsstorlek lika med 4 kW ökar acceptansgränsen avsevärt. Mer data behövs för att göra en noggrannare studie, till exempel på förväntad storlek på växelriktare och installerad effekt, men också på skillnader i produktion mellan paneler, skillnader i lutningsvinkel och riktning osv.
- 90 percentilen är en hög percentil. För 75 percentilen ökar acceptansgränsen också. Valet av percentilvärdet är starkt relaterat till den mängd risk som nätoperatören och andra intressenter är beredda att ta.

En detaljerat känslighetsanalys för 28-kunders nät visas i Avsnitt 3.5.2.

För att kunna tillämpa denna metod i större utsträckning bör information lämnas tillgänglig om lågspänningskunders förbrukning och spänningsnivåer i mellanspänningsnät med en tidsupplösning på minst 10 minuter. Det behövs mätningar på flera ställen i lågspänningsnät för att kunna samla in relevant information.

Enfasanslutna solcellsanläggningar ökar inte bara risken för överspänning; de medför också risk för underspänning. Underspänning kan uppstå när hög inmatad effekt i en fas sammanfaller med hög konsumtion i någon av de andra faserna.

Att ansluta alla växelriktare i samma fas ger hög överspänning redan för ett fåtal kunder med solkraft. Sannolikheten att sådant inträffar är dock så låg att det inte behövs ta med i planeringen annars än på ett stokastiskt sätt.

1.4 DISKUSSION OCH STUDIE AV ETT ANTAL ÅTGÄRDER

Ett antal åtgärder för att öka acceptansgränsen har studerats i denna rapport och resultat visas i detalj i kapitel 4 och till en del (vad gäller koordinerad anslutning) i kapitel 3.

Att minska transformatorns impedans har mycket begränsad påverkan på överspänningen och acceptansgränsen och är ingen lämplig åtgärd. Se Avsnitt 4.1.1.

Uppgradering av serviskablarna från 10 mm² till 25 mm² har stor påverkan för de flesta kunder. Denna uppgradering förbättrar dock endast spänningen för kunderna med solcellsanläggning; det gör inget för att minska påverkan på andra kunder. Se avsnitt 4.1.2.

Uppgradering av matarkabeln har ytterligare positiv inverkan på spänningen både för kunder med solcellsanläggning och för andra kunder. Se avsnitt 4.1.3.

Användningen av en automatisk lindningskopplare i distributionstransformatorn har förmågan att öka acceptansgränsen mycket. Den resulterande ökningen beror starkt på den använda spänningsstyrningsalgoritmen och inställningarna. Risken för överspänning bör balanseras mot risken för underspänning under perioder med hög konsumtion. Simuleringar i kapitel 3 har visat att spänningsintervallet (skillnad i spänningsnivå mellan högsta och lägsta fas-till-neutral spänning för någon av kunderna) ligger inom 20 % även om nästan alla kunder har solceller. Detta innebär att det i teorin är möjligt att öka acceptansgränsen hela vägen genom att använda en lämplig kontrollalgoritm. Ytterligare studier och algoritmutveckling behövs här. Se avsnitt 4.2.

Användningen av ett kopplat kondensatorbatteri (Avsnitt 4.3) eller shuntreaktor (Avsnitt 4.4) på lågspänningssidan av distributionstransformatorn skapar 2,5 % extra överspänningsmarginal med den tillhörande ökningen av acceptansgränsen. Ytterligare studier behövs kring oavsiktliga negativa konsekvenser, särskilt kring risken för att lågspänningskondensatorbanken förstärker kopplingstransienter som kommer från högre spänningsnivåer.

Energilagring hos kunderna (Avsnitt 4.7) och begränsning av produktionen (Avsnitt 4.8) är lösningar som ger en minskad överspänning och ökning av acceptansgränsen. Om produktionen kan minskas till max 2,5 kW kan alla kunder utrustas med enfasanslutna solcellsanläggningar utan att överspänningsgränsen överskrids.

Lagring i närheten av distributionstransformatorn (Avsnitt 4.5) och reaktiv-effektstyrning (Avsnitt 4.9) vid omriktarens anslutningspunkt är inga lämpliga lösningar.

Koordinerad anslutning (anslutning av enfasomriktaren till fasen med lägsta spänningen innan anslutning) är ett bra och enkelt sätt att möjliggöra att mycket mer solcellsanläggningar kan anslutas enfasiga. I simuleringarna används spänningen vid hög produktion, låg förbrukning och hög bakgrundsspänning för att jämföra med. Denna spänning är vanligtvis inte tillgänglig under installationen. Vissa riktlinjer måste utvecklas för att fastställa "fas med lägsta spänning" på ett

snabbt och enkelt sätt. Trots dessa osäkerheter rekommenderas att börja sprida denna metod, eftersom det inte finns några tecken på att koordinerad anslutning kan leda till sämre spänningskvalitet än slumpmässig anslutning. Se Avsnitt 3.3.3 och 3.5.3.

1.5 MÄTNING AV FÖRBRUKNING OCH PRODUKTION

Det har gjorts mätningar av spänning och förbrukning hos två lågspänningskunder och mätningar av produktion för två solcellsanläggningar.

Mätningarna presenteras i detalj i kapitel 5. Mätningarna visar att olika fördelningar måste användas för att uppskatta risken för överspänning och underspänning. Högsta och lägsta 10 minuters värden under en period av några timmar mitt på dagen under sommartid behövs för detta. Av mätningarna hos två kunder (10 minuters värden) bestämdes följande intervall för användning i simuleringar:

- För beräkning av överspänning är en rimlig fördelning av förbrukning mellan 0 och 250 W per kund per fas, och för bakgrundspänningen mellan 238 V och 242 V.
- För beräkning av underspänning är en rimlig fördelning av förbrukning mellan 1000 och 2500 W per kund per fas och för bakgrundspänningen mellan 232 V och 236 V.

Sannolikhetsfördelningsfunktionen för bakgrundspänning och förbrukning bör beräknas över årets soliga perioder (timmarna mitt på dagen, april till augusti), inte över hela året. Det visas också att timvärden inte är lämplig för acceptansgränsstudier med tanke på överspänning och underspänning. Det är igen relaterat till att regelverket och gränsvärden utgår från 10-minutersvärden.

Mätningarna av produktionen visar att höga produktionsnivåer kan inträffa under vilken dag som helst under perioden april till och med augusti.

De två produktionsenheterna, på ett avstånd av ca 500 m från varandra, visar en stark korrelerad men inte identisk produktion på en 10-minuters skala.

1.6 ANVÄNDNING AV TIDSERIER

Tidserier räknades ut för spänningen hos kunder med solkraft, genom att kombinera mätningar (spänning innan anslutningen; solkraftproduktionen) med beräkning av spänningshöjningen. Resultat visas i kapitel 6. Acceptansgränsen (över en period på bara några månader) överskrids (max spänning över 110 % av nominellt) för endast tre kunder med solkraft i sex-kunders nätet. Detta motsvarar rimligen väl resultaten från kapitel 3, där acceptansgränsen visas vara en eller två kunder med solkraft. Den korta mätperioden ger en underskattning av den högsta spänningen och därmed en överskattning av acceptansgränsen.

Data från två olika år (2016 och 2017) ger olika resultat för överspänningsstatistik. Att använda data från bara ett år är alltså otillräckligt för att göra en noggrann uppskattning av acceptansgränsen. Data över flera år bör användas, men det

kräver långa mätperioder. Planeringsmetoden i kapitel 3 och 4 lider inte av denna nackdel, även om metoden kräver visst resultat från mätningar som input.

När man tar med aggregeringen mellan två anläggningar (mätningar erhållna för båda installationerna ca 500 m separerade) i beräkningar blir överspänning och underspänning mindre. Denna allmänna trend förväntas, eftersom det alltid kommer att finnas någon påverkan av aggregeringen så solcellsanläggningarna är spridda geografiskt. Ytterligare studier behövs för att verifiera storleken av aggregeringen och för att få allmänna riktlinjer.

1.7 SLUTSATSER

Båda exempelnät som studeras i denna rapport har en låg acceptansgränsen för enfasanslutna solcellsanläggningar. Det visades också under studierna att flera av de parametervärden som används har ett starkt inflytande på resultaten. Detta gäller speciellt för uppskattad storlek av maxeffekt hos anläggningen, det procentuella värdet som används i prestandaindexet och intervallet för spänningen utan förbrukning och produktion. Värden på acceptansgränsen som presenteras i denna rapport är sannolikt något av en underskattning.

Flera åtgärder har studerats för att öka acceptansgränsen. De mest lovande är: koordinerad anslutning av växelriktare till fasen med lägsta spänning innan anslutningen; nedstyrning av produktion eller energilagring nära solcellsanläggningar, och kondensatorbatteri eller shuntreaktor nära distributionstransformatorn. Den första åtgärden verkar ganska enkel; den kan tillämpas utan mycket investering. Metoden kräver dock en mätning och vissa riktlinjer behövs för denna mätning och det rekommenderas att sådana utvecklas.

Det acceptansgräns-baserade planeringsverktyget har visat sig vara ett användbart verktyg för att utvärdera behovet på åtgärder och för att jämföra åtgärder.

Ytterligare insamling av data från både produktion och konsumtion behövs. Tidsupplösning bör vara minst 10 minuter. Användning av timvärden är inte tillräcklig för acceptansgränsberäkningar avseende överspänning och underspänning.

1.8 RAPPORTENS INNEHÅLL

Resten av rapporten är skriven på engelska och innehåller detaljer av modellerna, beräkningarna och beräkningsresultat.

Kapitel 2 ger detaljer av modellerings- och beräkningsmetoden som har använts och introducerar de två exempelnät som används i beräkningarna.

Kapitel 3 visar resultat av själva acceptansgränsberäkningarna. Kapitlet börjar med en jämförelse mellan enfas och trefas anslutna solcellsanläggningar vad gäller acceptansgräns för spänningshöjning hos en anläggning. Planeringsmetoden beskrivs och tillämpas på båda exempelnäten. Framförallt överspänning studeras men även en liten delstudie om risken för underspänning.

I Kapitel 4 används metoden för att jämföra ett antal åtgärder, vid distributionstransformatorn, i kabelnätet, och vid solcellsanläggningarna.

Kapitel 5 och Kapitel 6 visar resultat från mätningar och från simuleringar med tidserier.

Alla figurer som visas i Kapitel 1, visas också i ett senare kapitel. Tabell 2 ger relationen mellan figurerna, som ger läsaren möjlighet att kolla på mer detaljer av beräkningarna som resulterade i figuren.

Tabell 2, figurer och tabell i Kapitel 1 och i senare kapitel

.. i Kapitel 1	.. i senare kapitel	Avsnitt i senare kapitel
Tabell 1	Table 3-3	Section 3.1
Figur 1	Figure 3-6	Section 3.3.1
Figur 2	Figure 3-15	Section 3.5.1
Figur 3	Figure 3-8	Section 3.3.1
Figur 4	Figure 3-16	Section 3.3.1
Figur 5	Figure 3-17	Section 3.3.1

1.9 PROJEKTDELTAGARE

Huvudförfattaren till denna rapport och projektledare har varit Math Bollen (Elkraftteknik, Luleå tekniska universitet). Utöver det har de följande personerna bidragit till projektet men bland annat insamling och analys av data; data om exempelnät; delar av beräkningar; samt allmänna diskussioner: Tatiano Busatto, Mikael Byström; Cecilia Karlsson (examensarbetare Umeå universitet); Anders Larsson; Martin Lundmark; Enock Mulenga; Sarah Rönnberg; Daphne Schwanz, Mats Wahlberg (MWG Power samt Skellefteå Kraft elnät).

En referensgrupp skapades till projektet med följande deltagare: Oscar Willén, Sala-Heby Energi Elnät; Sara Johansson, Gotland Elnät; Nicklas Fredland, Elverket Vallentuna Elnät; Tokhir Gafurov, Mälarenergi; Andreas Feurst, Öresundskraft; Malin Westman, Skellefteå Kraft Elnät.

2 Modelling and Example Networks

This chapter introduces the modelling approach used, the calculation methods and the two example networks used in this project.

2.1 CALCULATION METHOD USED

2.1.1 Transfer impedance matrix for phase-to-neutral voltages

The calculation method used for the study presented in this report is formed around the "transfer impedance matrix". The elements of the transfer impedance matrix, the "transfer impedances", give the change in complex voltage at one location, due to an injected current at another location.

$$U_k = Z_{kl} \cdot I_l \tag{1}$$

Where U_k is the phase-to-neutral voltage at location k, I_l the current injected from neutral to phase at location l, and Z_{kl} the transfer impedance. When $k = l$, the source impedance between phase and neutral is obtained; we will include the source impedance in the general concept of "transfer impedance".

With multiple sources of injected current, the voltage at location k is equal to the "background voltage" U_0 plus the contributions from all sources:

$$U_k = U_0 + \sum_{l=1}^{N} Z_{kl} \cdot I_l \tag{2}$$

Note that all variables in this expression are complex variables. This expression is referred to as the "superposition principle"; it is a reformulation of the definition of linearity. The underlying assumption made in this study is therefore that the system is linear.

2.1.2 Node voltages against the reference node

The transfer matrix for phase-to-neutral voltages is obtained from a more basic transfer impedance matrix: the one relating the voltage and current against a reference node; typically referred to as 0 (zero). Like for the phase-to-neutral voltages, a matrix of transfer impedances can be defined also for voltage and currents in this case. This one is also referred to as the "node impedance matrix" and it can be obtained easily by inverting the "node admittance matrix". The node admittance matrix can in turn be obtained from the branch impedances in a straightforward way as will be explained in the next section.

2.1.3 Creating the node admittance matrix

The node admittance matrix is built from the branch impedances through a recursive algorithm. Each branch adds values to a small number of elements in the matrix.

Consider an impedance Z_{branch} between nodes n and k. The corresponding branch admittance is obtained as the inverse of the branch impedance:

$$Y_{branch} = \frac{1}{Z_{branch}} \quad (3)$$

Adding this branch to the network requires updating two diagonal and two off-diagonal elements of the node admittance matrix:

$$Y_{nn} := Y_{nn} + Y_{branch} \quad (4)$$

$$Y_{kk} := Y_{kk} + Y_{branch} \quad (5)$$

$$Y_{nk} := Y_{nk} - Y_{branch} \quad (6)$$

$$Y_{kn} := Y_{kn} - Y_{branch} \quad (7)$$

(In words: add Y_{branch} to the diagonal elements and subtract Y_{branch} from the off-diagonal elements.)

Consider a branch with impedance Z_{branch} between node k and the reference node (0). The branch admittance is again

$$Y_{branch} = \frac{1}{Z_{branch}} \quad (8)$$

In this case, only the diagonal element needs to be updated

$$Y_{kk} := Y_{kk} + Y_{branch} \quad (9)$$

The initial values of all elements of the matrix are zero; after adding all branches as described above, the node admittance matrix is obtained.

2.1.4 Calculating the phase-to-reference node-impedance matrix

The phase-to-reference node-impedance matrix $\boldsymbol{Z}$ is obtained as the matrix inverse of the node-admittance matrix $\boldsymbol{Y}$ from Section 2.1.3.

$$Z = \frac{1}{Y} \quad (10)$$

This is not an efficient way of calculating the node-impedance matrix: especially for large networks, much more efficient methods are available. However, the kind of distribution networks that are studied in this project are rather small and the time needed to do the inversion did not show to be the limiting factor. The transfer-impedance matrix only needs to be calculated once, for thousands up to hundreds of thousands of voltage calculations.

2.1.5 Calculating the phase-to-neutral node-impedance matrix

Once the phase-to-reference node-impedance matrix is known, the voltage between a node and the reference node can be calculated due to current injected into one or more nodes. Such a model is however not the most convenient one when considering the voltage rise due to single-phase connected inverters. The voltage of interest is between the phase and the local neutral. The injected current (due to the produced power) is flowing out of the local neutral into one of the

phases. To simplify the calculations, a so-called "phase-to-neutral impedance matrix" is calculated from the phase-to-reference impedance matrix obtained in Section 2.1.3 and 2.1.4.

Consider a network with a "sending bus" and a "receiving bus", each consisting of four nodes. The nodes are numbered as shown in Figure 2-1. A current I_{an} is injected between neutral and phase a, at the sending end. We are interested in the voltage between phase and neutral (an, bn, cn) at sending and receiving end.

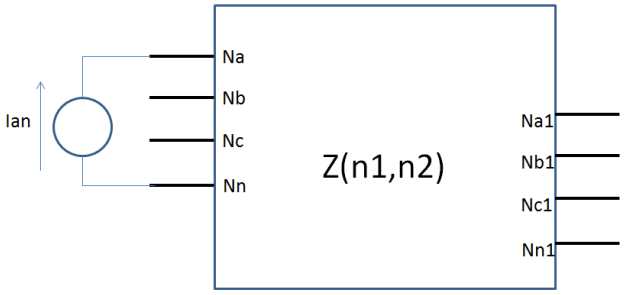

Figure 2-1. Definition of "phase-to-neutral transfer impedance matrix", with sending node (left) and receiving node (right).

Seen from the network, there are two currents being injected, at busses N_a and N_n, with opposite sign:

$$I(N_a) = I_{an}$$
$$I(N_n) = -I_{an} \quad (11)$$

The voltage between phase A (a) and neutral (n) is found as follows

$$U_{an} = U(N_a) - U(N_n) \quad (12)$$

Using the superposition principle and the definition of the node impedance matrix, we get:

$$U(N_a) = Z(N_a, N_a) \cdot I(N_a) + Z(N_a, N_n) \cdot I(N_n) \quad (14)$$

$$U(N_n) = Z(N_n, N_a) \cdot I(N_a) + Z(N_n, N_n) \cdot I(N_n) \quad (15)$$

The "input impedance" between "a" and "n" is defined as

$$Z_{an} = \frac{U_{an}}{I_{an}} \quad (16)$$

Combining the above expressions gives:

$$Z_{an} = Z(N_a, N_a) - Z(N_a, N_n) - Z(N_n, N_a) + Z(N_n, N_n) \quad (17)$$

The same can be done for the transfer impedance to the same phase at the receiving node:

$$Z_{an-an1} = \frac{U_{an1}}{I_{an}} \tag{18}$$

Using the same notations as before gives:

$$Z_{an-an1} = Z(N_{a1}, N_a) - Z(N_{a1}, N_n) - Z(N_{n1}, N_a) + Z(N_{n1}, N_n) \tag{19}$$

The transfer impedance to another phase at the sending end is defined as:

$$Z_{an-bn} = \frac{U_{bn}}{I_{an}} \tag{20}$$

The voltage between phase B and neutral is found as:

$$U_{bn} = U(N_b) - U(N_n) \tag{21}$$

Using the superposition principle and the definition of the node impedance matrix, the following expressions are obtained:

$$U(N_b) = Z(N_b, N_a) \cdot I(N_a) + Z(N_b, N_n) \cdot I(N_n) \tag{22}$$

$$U(N_n) = Z(N_n, N_a) \cdot I(N_a) + Z(N_n, N_n) \cdot I(N_n) \tag{23}$$

Resulting in:

$$Z_{an-bn} = Z(N_b, N_a) - Z(N_b, N_n) - Z(N_n, N_a) + Z(N_n, N_n) \tag{24}$$

The transfer impedance to another phase at the receiving end, is defined as:

$$Z_{an-bn1} = \frac{U_{bn1}}{I_{an}} \tag{25}$$

Using

$$U_{bn1} = U(N_{bn1}) - U(N_{n1}) \tag{26}$$

And

$$U(N_{bn1}) = Z(N_{bn1}, N_a) \cdot I(N_a) + Z(N_{bn1}, N_n) \cdot I(N_n) \tag{27}$$

$$U(N_{n1}) = Z(N_{n1}, N_a) \cdot I(N_a) + Z(N_{n1}, N_n) \cdot I(N_n) \tag{28}$$

Give the following expression for this transfer impedance:

$$Z_{an-bn1} = Z(N_{bn1}, N_a) - Z(N_{bn1}, N_n) - Z(N_{n1}, N_a) + Z(N_{n1}, N_n) \tag{29}$$

Using the following notation:

N_s: sending node phase

N_{sn}: sending node neutral

N_r: receiving node phase

N_{rn}: receiving node neutral

the following general expression appears:

$$Z_{tr} = Z(N_r, N_s) - Z(N_r, N_{sn}) - Z(N_{rn}, N_s) + Z(N_{rn}, N_{sn}) \tag{30}$$

This expression has been used to obtain the "phase-to-neutral transfer impedance matrix" from the "phase-to-reference transfer impedance matrix".

In a network with N busses (each consisting of three phases and neutral), the phase-to-reference transfer impedance matrix consists of $4 \cdot N$ nodes; the phase-to-neutral transfer impedance matrix consists of $3 \cdot C$ nodes, where C is the number of customers. It is assumed thereby that injected currents only occur with customers and that the interest only is in the three phase-to-neutral voltages with customers. The calculation approach remains the same when injected currents and voltages at other busses are to be considered.

2.1.6 Series element model

The low-voltage distribution networks modelled in this study consist mainly of series elements: cables, lines and transformers. The model used allows for shunt elements (capacitor banks, loads) as well, but these are not used in this study. Instead, both consumption and production are modelled per phase as a current source.

All series elements are modelled as a 4x4 element (with 4 input nodes and 4 output nodes), as explained in Section 2.1.5. However, in the data used for the calculations, a limited number of parameters are used. The assumptions made are:

- There is no coupling between the phases between the two terminals of a series element, i.e. the current that enters in phase A also leaves in phase A
- The positive-sequence and negative-sequence impedances are the same

Two complex parameters are used to characterize this 4x4 connection: the series impedance (resistance and reactance) of the phase conductor Z_p; the series impedance (resistance and reactance) of the neutral conductor Z_n.

These two impedances can be related to the positive and zero-sequence series impedances in the following way:

$$Z_{pos} = Z_p \tag{31}$$

$$Z_{zero} = Z_p + 3Z_n \tag{32}$$

In some studies (e.g. the one presented in Section 3.1), a distinction is made between an "earth-fault impedance" and a "short-circuit impedance". Those are related to the impedances used in this study through the following expressions:

$$Z_{short} = Z_p \tag{33}$$

$$Z_{earth} = Z_n + Z_p \tag{34}$$

These impedances are also the ones given in standards like SS 421 1405, which was used to obtain the cable data for the example network.

The distribution transformer and the 10-kV source impedance are modelled in the same way. The zero-sequence impedance of a distribution transformer is somewhat smaller than the positive-sequence impedance; the zero-sequence impedance of the 10-kV network does not contribute to the zero-sequence source impedance as seen at the low-voltage terminals of the distribution transformer.

2.1.7 Calculating the voltage magnitude

The complex phase-to-neutral voltage at the customer terminals is obtained using the following matrix expression:

$$U_{cust} = U_0 + Z_{pn}(I_{prod} - I_{cons}) \quad (35)$$

Where, U_{cust} is the vector with voltages at the customer terminals (of length $3C$, with C the number of customers), U_0 the vector with background voltages (the voltages in the low-voltage network without any consumption or production), Z_{pn} the phase-to-neutral transfer impedance matrix, I_{prod} the vector of currents injected by the PV inverters, and I_{cons} the vector of currents taken out by the consumption.

The currents are calculated from the active and reactive power (consumed or produced) assuming that the voltage at the customer terminals equals the nominal voltage of 230 V.

The consumption has a non-zero value for all customers and all phases. The production is non-zero only for customers and phases with PV connected.

The voltages obtained from the above expression are complex variables. The voltage magnitude is obtained as the absolute value of the complex voltage.

2.1.8 Probability distribution functions

To obtain the probability distribution function of the voltage magnitude, a Monte-Carlo simulation approach has been used. The voltage magnitudes for all phases with all customers have been calculated (using the methods described in the previous sections) for up to one million randomly selected cases. The following random variables have been used as input:

- The customers with PV (the number of customers with PV is given as input, but not which customers have PV);
- The phase at which the PV inverter is connected;
- The background voltage;
- The consumption for each customer and each phase.

A typical number of runs used in the study is between 10 000 and 100 000.

The Monte-Carlo simulation, including the voltage calculations and the calculation of the phase-to-neutral transfer impedance matrix has been implemented in Matlab.

2.2 LOW-VOLTAGE EXAMPLE NETWORKS

For validation, the proposed model is applied to two Swedish networks. Both networks were selected based on criteria of complexity and application. Cable parameters (as defined in Section 2.1.5) for both networks are listed in Table 2-1.

The first network, illustrated in Figure 2-2, is a typical countryside grid where a few houses, spread over a few hundred meters, are connected to a single transformer. Detailed data is given in Table 2-2 and Table 2-3, where CB stands for “customer bus”.

The second network, shown in Figure 2-3, is a suburban grid with 28 customers connected to a 500-kVA transformer. This type of network is typical for a suburban region where some tens of houses are connected to the same distribution transformer. The data related to this network is presented in Table 2-4 and Table 2-5.

The source impedance at 10 kV is as follows:

For the 6-customer grid: 1.0736 + j 2.1325 Ω

For the 28-customer grid: 0.4174 + j 0.7977 Ω

The zero-sequence impedance of the transformer is assumed equal to the positive-sequence impedance.

Table 2-1. Cable and line impedances

Type	Description	Short-circuit impedance (Ω/km)	Earth-fault impedance (Ω/km)	Susceptance (μS/km)
1	EKKJ-3x10/10	1.830 + *j*0.087	3.660 + *j*0.103	94.25
2	N1XE-4x10	1.830 + *j* 0.087	3.660 + *j*0.175	31.42
3	ALUS-4x25	1.200 + *j* 0.090	2.400 + *j*0.180	128.04
4	ALUS-4x50	0.641 + *j* 0.085	1.282 + *j*0.170	157.80
5	N1XV-4x50	0.641 + *j* 0.081	1.282 + *j*0.161	31.42
6	N1XE-4x50	0.641 + *j* 0.081	1.282 + *j*0.161	31.42
7	N1XE-4x150	0.206 + *j* 0.078	0.412 + *j*0.156	31.42
8	AKKJ-3x150/41	0.206 + *j* 0.074	0.649 + *j*0.076	251.33
9	AKKJ-3x240/72	0.125 + *j* 0.073	0.378 + *j*0.076	282.74
10	FKKJ-3x35/16	0.524 + *j* 0.079	1.674 + *j*0.086	188.50
11	N1XV-4x10	1.830 + *j* 0.087	3.660 + *j*0.175	31.42

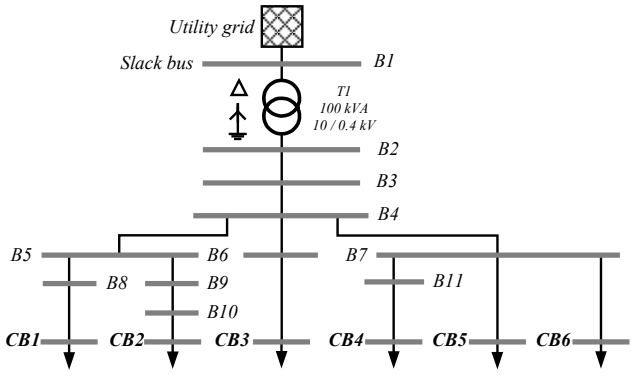

Figure 2-2. Single-line diagram for the 6-Customer network

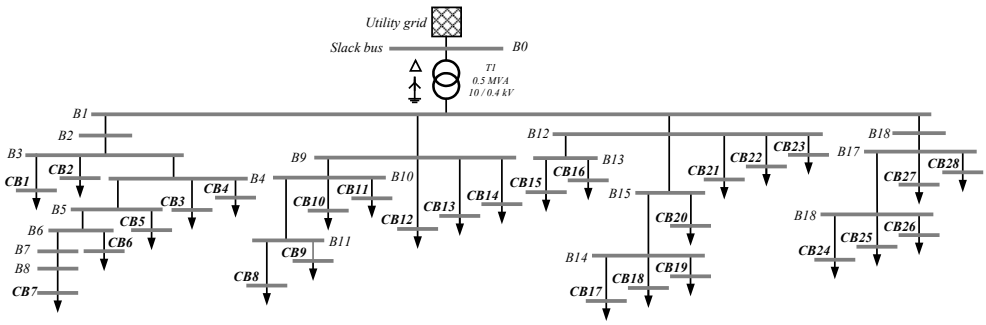

Figure 2-3. Single-line diagram for the 28-Customer network

Table 2-2. Transformer Data for the 6-Customer Network

Power	100 kVA
Voltage	10/0.4 kV
Connection	Dyn11
Positive sequence impedance	4 %
Source impedance at 10 kV	1.0736+j2.1325 Ω

Table 2-3. Cable and Line Data for the 6-Customer Network

N1	N2	Type	Length (m)	N1	N2	Type	Length (m)
B2	B3	5	14.0	B7	B11	2	54.4
B3	B4	4	108.0	B7	CB5	1	8.9
B4	B5	4	26.9	B7	CB6	2	79.5
B4	B6	4	46.0	B8	CB1	1	41.5
B4	B7	3	1.9	B9	B10	3	0.1
B5	B8	4	41.2	B10	CB2	1	17.0
B5	B9	4	0.1	B11	CB4	1	41.3
B6	CB3	1	31.0				

Table 2-4. Transformer Data for the 28-Customer Network

Power	500 kVA
Voltage	10/0.4 kV
Connection	Dyn11
Positive sequence impedance	4.9 %
Source impedance at 10 kV	0.4174+j0.7977 Ω

Table 2-5. Cable and Line Data for the 28-Customer Network

N1	N2	Type	Length (m)	N1	N2	Type	Length (m)
B1	B2	7	15.0	B11	CB9	1	37.8
B2	B3	8	77.9	B1	B12	8	196.9
B3	CB1	1	68.7	B12	CB21	1	33.8
B3	CB2	1	24.9	B12	CB22	1	65.7
B3	B4	8	56.0	B12	CB23	1	17.0
B4	CB3	1	22.4	B12	B13	10	89.5
B4	CB4	1	48.9	B13	CB15	1	42.7
B4	B5	8	64.1	B13	CB16	1	27.7
B5	CB5	1	28.2	B12	B14	10	71.0

N1	N2	Type	Length (m)	N1	N2	Type	Length (m)
B5	B6	8	67.4	B14	CB20	1	21.2
B6	CB6	1	23.1	B14	B15	10	58.6
B6	B7	8	52.3	B15	CB17	11	28.9
B7	B8	7	1.2	B15	CB18	11	21.7
B8	CB7	6	34.2	B15	CB19	11	33.0
B1	B9	9	270.1	B1	B16	8	157.0
B9	CB12	1	29.8	B16	B17	8	50.6
B9	CB13	1	46.1	B17	CB28	1	22.9
B9	CB14	1	23.4	B17	CB27	1	41.8
B9	B10	8	86.0	B17	B18	10	93.4
B10	CB10	1	47.2	B18	CB24	1	76.2
B10	CB11	1	27.7	B18	CB25	1	37.4
B10	B11	10	96.1	B18	CB26	1	28.5
B11	CB8	1	29.9				

3 Hosting-Capacity Estimation

This chapter introduces (in Section 3.2) a planning approach based on the hosting-capacity concept. The hosting capacity is the maximum amount of new production or new consumption that can be connected without unacceptably deteriorating the reliability or voltage quality of the grid. In the planning stage, many uncertainties remains, making it not straightforward to estimate the hosting capacity. The used approach compares a high percentile of the worst-case voltage with an overvoltage limit.

The approach has been applied to the two example networks introduced in Chapter 2, for three distributions of PV inverters over the phases:

- Uniform distribution (referred to here as "random connection"), where each phase has the same probability of having a PV inverter connected.
- All inverters in the same phase.
- Coordinated connection, where each new inverter is connected to the phase with the lowest voltage before connection.

The chapter starts with some general statistics on voltage rise and hosting capacity for single-phase and three-phase connected PV.

3.1 SOURCE IMPEDANCE AND HOSTING CAPACITY

Data was obtained of the source impedance (short-circuit impedance and earth-fault impedance) for about 50 000 low-voltage customers with a Swedish distribution network operator. All customers had fuse sizes between 16 A and 35 A. The values of the source impedance are shown in Figure 3-1 and Figure 3-2.

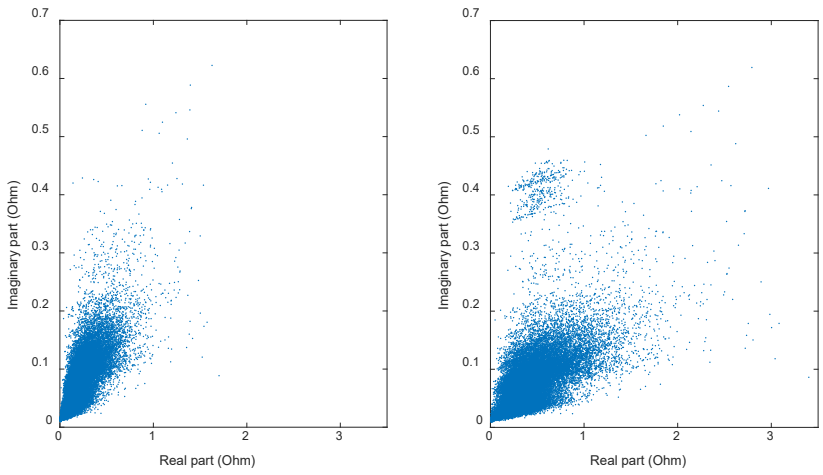

Figure 3-1. Real and imaginary part of the short-circuit impedance (left) and the earth-fault impedance (right) for 50 000 low-voltage customers.

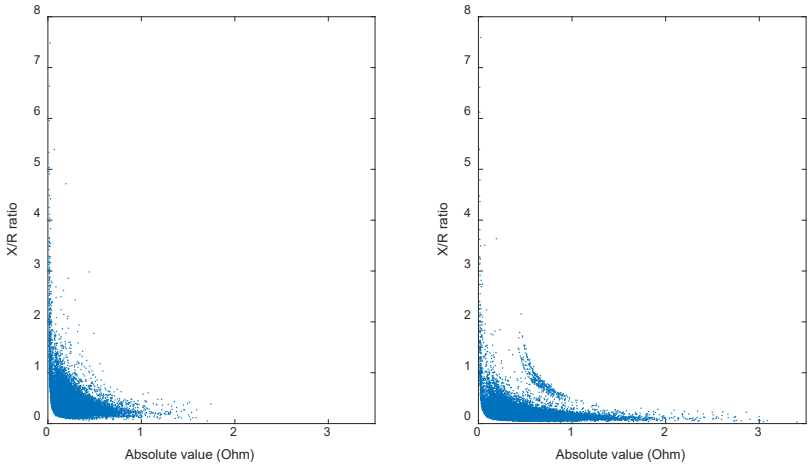

Figure 3-2. Absolute value and X/R ratio of the short-circuit impedance (left) and the earth-fault impedance (right) for 50 000 low-voltage customers.

As a reference, the high percentage values of the earth-fault impedance in a number of European countries are presented in Table 3-1[7]. The IEC reference impedance, for testing of equipment against emission of fast voltage variations, is equal to 0.4+j0.25 Ω. A substantial amount of customers in Figure 2-1 has an earth impedance bigger than the reference impedance.

Table 3-1. High percentile values of impedance in European low-voltage networks (in Ohm).

	Percentage of customers			
	98%	95%	90%	85%
Belgium		0.63+j0.33	0.32+j0.17	0.28+j0.15
France		0.55+j0.34	0.45+j0.25	0.34+j0.21
Germany		0.45+j0.25	0.36+j0.21	0.31+j0.17
Ireland	1.47+j0.64	1.26+j0.60	1.03+j0.55	0.94+j0.43
Italy		0.59+j0.32	0.48+j0.26	0.44+j0.24
Netherlands		0.70+j0.25	0.41+j0.21	0.30+j0.18
Switzerland		0.60+j0.36	0.42+j0.25	0.30+j0.18
United Kingdom	0.46+j0.45		0.25+j0.23	
USSR		0.63+j0.30	0.50+j0.26	
IEC reference impedance			0.40+j0.25	

The voltage rise ΔU due to a current I with (displacement) power factor $\cos\phi$ is in good approximation equal to:

$$\Delta U = RI\cos\phi + XI\sin\phi \qquad (36)$$

Where $R + jX$ is the relevant source impedance. For solar power, the power factor is close to unity. If we further assume that the voltage is close to the nominal

[7] G.S. Finlay, Relationships between network impedances, test impedances and power quality, Improving distribution power quality and transmission optimisation conference – Amsterdam 15 January 1998.

voltage, the (relative) voltage rise due to an injected power P can be approximated by the following expression:

$$\Delta u = \frac{\Delta U}{U_{nom}} \approx \frac{(R \cdot P)}{U_{nom}^2} \quad (37)$$

For a single-phase-connected installation, the resistive part of the earth-fault impedance should be used; for a three-phase connected unit, the resistive part of the short-circuit impedance. The active power in the above equation is the active power per phase; the voltage is the phase-to-neutral voltage. For a three-phase connected installation, the rated power is three times the value per phase.

The voltage rise has been calculated for single-phase and three-phase-connected installations with 6 kW injected power, for each of the 50 000 customers. The results are shown in Figure 3-3. The voltage rise is significantly less for a three-phase connected inverter than for a single-phase connected inverter. Not only is the injected power per phase just one third, also the short-circuit impedance is less than the earth-fault impedance.

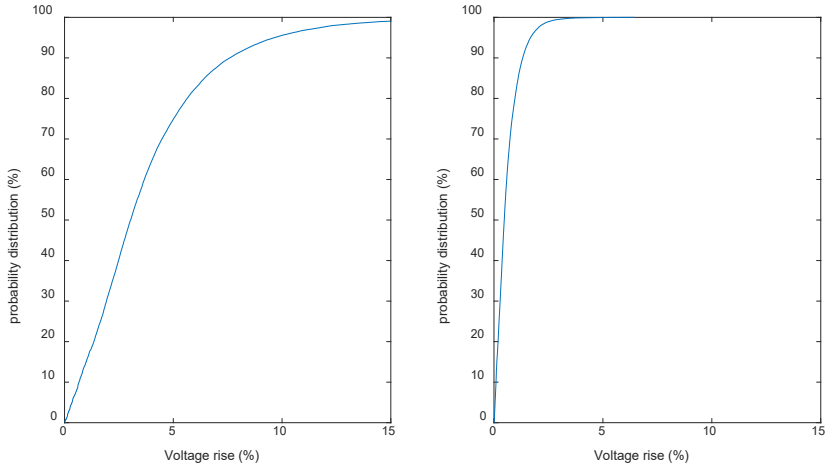

Figure 3-3. Probability distribution function (CDF) of the rise due to a 6-kW PV inverter: single-phase connected (left) and three-phase connected (right).

For many customer locations, a 6-kW single-phase-connected PV installation would result in unacceptable voltage rise. Table 3-2 shows the percentage of customer locations at which the voltage rise would exceed certain values, for both single-phase and three-phase connection.

Table 3-2. Percentage of customer locations with voltage rise exceeding certain values, upon connection of 6 kW PV.

	3%	5%	10%
Single-phase connection	51%	25%	4.6%
Three-phase connection	0.5%	0.04%	0.002%

For three-phase connection, a voltage rise above 3% is unlikely. However, for single-phase connection of a 6-kW inverter the voltage rise will exceed 3% at half of the customer locations.

The voltage rise for single-phase and three-phase connection is compared in Figure 3-4. The black diagonal line in the figure corresponds to a factor of six between the two values. A conclusion from the figure is that the voltage rise due to single-phase connection is about six times the voltage rise due to three-phase connection.

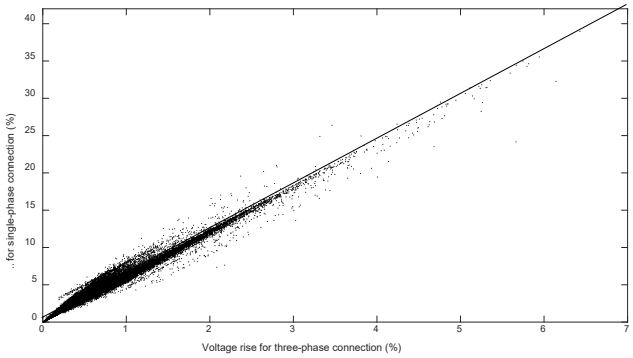

Figure 3-4. Relation between voltage rise due to single-phase and three-phase connection of 6 kW PV with 50 000 customer locations.

Instead of calculating the voltage rise for a given size of installation, one can calculate the installation size for a given voltage rise. Assume a maximum-permissible voltage rise, Δu_{max}, above which it is not allowed to connect a production unit. The hosting capacity is in that case the size of production unit that gives a voltage rise equal to the maximum-permissible rise:

$$\Delta u_{max} = \frac{(R \cdot P_{max})}{U_{nom}^2} \tag{38}$$

The hosting capacity is obtained from the following expression:

$$P_{max} = \frac{\Delta u_{max}}{R} \cdot U_{nom}^2 \tag{39}$$

This is again the active power per phase, so that it has to be multiplied by three for a three-phase installation. Statistical results, using the same dataset as in Figure 3-1, are shown in Figure 3-5.

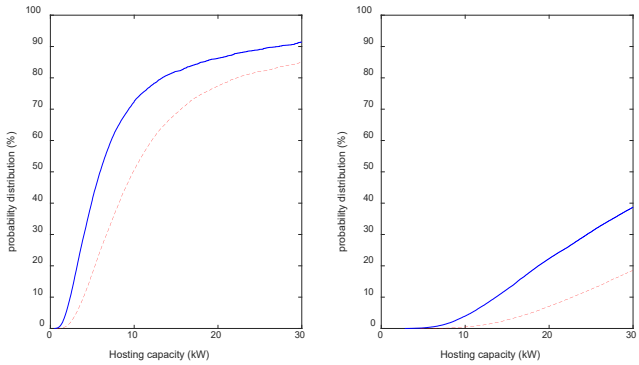

Figure 3-5. Probability distribution (CDF) for the hosting capacity with single-phase connected (left) and three-phase connected (right) installations; permitted voltage rise equal to 3% (blue solid) and 5% (red dotted).

The figure shows that the hosting capacity is higher for three-phase connections. This corresponds with the earlier conclusion that the voltage rise is less for such a connection.

From the probability distribution shown in Figure 3-5, the number of customer locations with insufficient hosting capacity has been calculated. The results are shown in Table 3-3.

Table 3-3. Percentage of customer locations with insufficient hosting capacity to connect 3 kW or 6 kW installations, given a permissible voltage rise of 3% or 5%, for single-phase and three-phase connection.

Permissible voltage rise	5%	3%	5%	3%
Required hosting capacity	3 kW		6 kW	
Single-phase connection	4.6%	17.8%	25.3%	50.6%
Three-phase connection	0.002%	0.05%	0.04%	0.5%

3.2 A PLANNING-BASED HOSTING-CAPACITY APPROACH

The hosting-capacity-based planning approach used in this study, consists of the following steps:

i) Estimate the no-load voltage variations in the low-voltage distribution network during those hours of the year that the production from solar power may be high. These are the voltage variations originating from the medium-voltage network.
ii) Estimate the range of the lowest consumption during those hours of the year that the production from solar power may be high.
iii) Estimate the production per installation, during the 10-minute period with the highest impact from all installations together. This is not the same as the maximum production per installation, but it can be referred to as an "after diversity maximum production", next to an "after diversity minimum consumption".
iv) Add solar power installations in a random way and calculate the distribution of worst-case voltage with increasing amount of solar power.
v) Define a performance index for the network, an appropriate limit for this index, and determine the hosting capacity.

This approach for distribution-system planning can be seen as an adapted version of the classical approach, where an "after diversity maximum consumption" is compared with the capacity of lines, cables and transformers.

The difference between the planning approach used here, and the time-series approach often used in other studies, is that the used approach immediately considers the worst-case during a longer period, like several years. Distribution-network planning is largely about making sure that the network can cope with for example the highest current through a transformer. It is this worst case that matters. However, also the worst-case value can be treated as a random variable, which is the base for the planning approach used here. Probability distributions are used, for example for the consumption. These are not the same as the probability distributions obtained from time series. Instead, they are the range of values during those hours of the year that the worst-case situation can occur. Some further discussion on this is part of Chapter 5, including the way of estimating the range of item ii) and iii) above from time series of voltage and current.

The result of the calculations is thus not the probability distribution of the voltage magnitude, but instead the probability distribution of the worst-case voltage magnitude. Alternatively, one may consider this as the probability distribution obtained over a range of possible futures, all with a different worst-case value. Important advantages of the approach used here, are:

i) The approach fits closely to existing planning approaches used by distribution companies.
ii) A limited amount of input data is needed.
iii) The results are such that they can be interpreted relatively easy by distribution companies.
iv) Different kinds of uncertainties can be added without changing the basic approach.
v) Any power-system analysis tool can be used to perform the actual calculations.

The limitation of the approach is that it requires certain assumptions, like in step (i) and (ii) above. In practical planning studies, these assumptions might become more based on expert opinions than on actual reproducible studies. Different persons may obtain different results. Such is however common in practical planning studies for distribution grids. With the proposed approach, the assumptions become clearly visible and might trigger further studies.

3.3 OVERVOLTAGE IN THE 6-CUSTOMER RURAL NETWORK

3.3.1 Random spread of inverters over the phases

The risk of overvoltage due to the introduction of single-phase-connected PV has been studied for the six-customer rural network. The following input data has been used for obtaining probability distribution functions of the highest voltage after connection of single-phase PV:

i) Each installation is connected single-phase and each installation produces 6 kW.
ii) The consumption per customer per phase, during the worst case, is uniformly distributed between 0 and 250 W. This range was obtained from measurements of 10-min values of two customers (one in the rural network and one in the suburban network) and the study of hourly consumption from other customers (see Chapter 5). The worst case, when considering the risk of overvoltage, is when consumption is low and production is high. High production will likely last a period of one or two hours around noon. The regulation in most European countries sets limits to 10-min values of rms voltage. The lowest 10-min consumption values during one or two-hour periods were considered to obtain the range from 0 to 250 W. Only measurement values around noon during the summer months were used here.
iii) The no-load voltage in the low-voltage network, during the worst case, is uniformly distributed between 238 V and 242 V. The highest 10-min values during one or two-hour periods around noon in the summer months (as obtained from the same measurements) were used to obtain this distribution.

All the random variables in the model are non-correlated. It is further assumed that the PV installations are randomly distributed over the customers and over the phases. The network model used is a simple, linear one, consisting of the node-impedance matrix calculated from the positive and zero-sequence series impedance of the different branches. Positive-sequence and negative-sequence impedances are considered equal. The difference between positive and zero-sequence impedance is considered in the calculations. From the injected and consumed power for each customer and phase, a current vector is calculated. This vector is multiplied with the node-impedance matrix to obtain the vector with phase-to-neutral voltages for all customers and phases. All calculations are performed in Matlab. More details of the model and calculations used are found in Chapter 2.

A Monte-Carlo simulation is used to generate a large number of combinations of customers and phases with PV. For each combination, the highest phase-to-ground voltage is calculated for each customer. The probability distribution for this voltage is shown in Figure 3-6. In this case, each distribution was obtained from 10,000 samples. The probability distribution is presented in the form of the “probability distribution function” also known as “cumulative distribution function” of “CDF”.

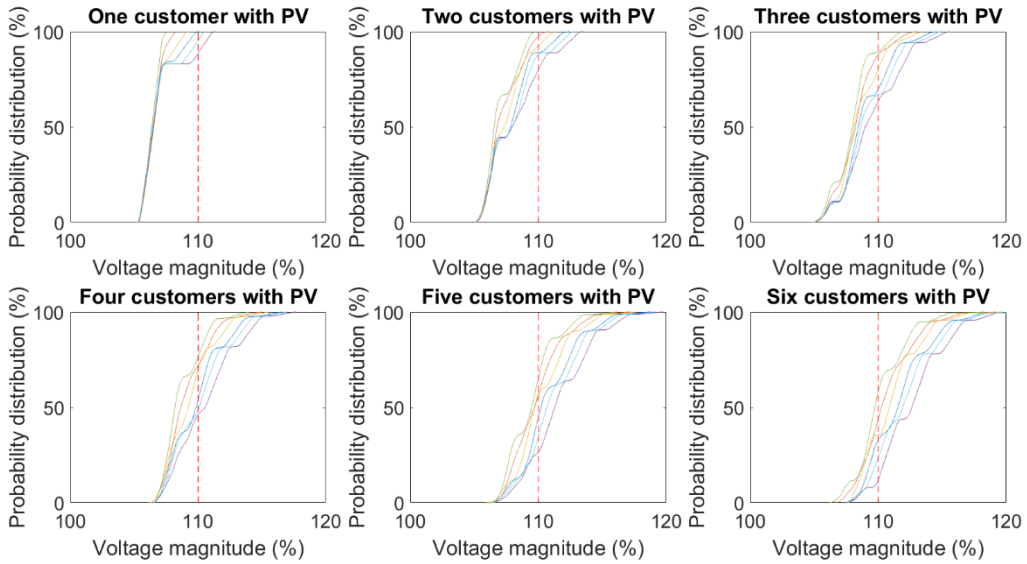

Figure 3-6. Probability distribution (CDF) for the highest voltage (worst-case voltage) for increasing amount of single-phase connected solar power in the 6-customer rural network. The different colours refer to the six different customers. The red dashed vertical line is the overvoltage limit at 110% of the nominal voltage.

The plots show how the distribution shifts towards higher voltage magnitudes with increasing amount of solar power. The probability that the overvoltage limit (110% of nominal voltage) is exceeded increases because of this. Already for one customer with PV, there is a small probability that the voltage with one of the customers exceeds the overvoltage limit as can be seen in Figure 3-6 (top left).

An important advantage of the hosting capacity approach is its transparency: a well-defined performance index is compared with a well-defined limit. The same should hold when the hosting capacity is used as a planning tool. In this example, the 90th percentile of the distribution shown in Figure 3-6 has been used as an index and 110% of nominal voltage as a limit. The index value with increasing amount of solar power is shown in Figure 3-7, where each point is the result of 100,000 simulations. The results are shows for each of the six customers. When one of the 90th percentiles exceeds the 110% limit for one of the customers, the hosting capacity has been exceeded. The hosting capacity is in this case equal to only one customer with PV.

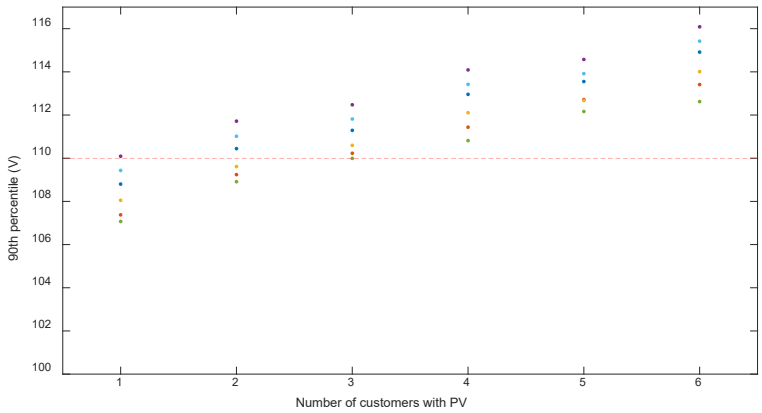

Figure 3-7. 90th percentile of the worst-case overvoltage as a function of the number of customers with PV in the 6-customer rural network.

Figure 3-8 shows the performance index when it is assumed that each PV installation injects 4 kW instead of 6 kW during the worst case. The resulting hosting capacity is three customers. An example of the impact of the choice of performance index is shown in Figure 3-9, where the 75th percentile is used instead of the 90th percentile. The production per installation is again assumed to be 6 kW. The resulting hosting capacity is two customers with PV. In the latter example, it is clear that the increase in hosting capacity goes together with an increase in risk. However, even for the example in Figure 3-8, the risk of overvoltage increases, as installations may contribute more than 4 kW to the worst case. The choice of model, data, etc. with hosting-capacity calculations is strongly related to the risks that the different stakeholders are willing to take.

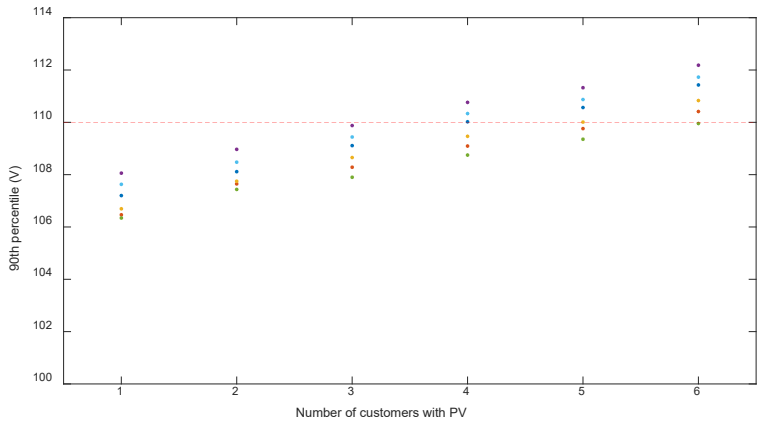

Figure 3-8. 90th percentile of the worst-case overvoltage as a function of the number of customers with PV in the 6-customer rural network; 4 kW production per PV installation.

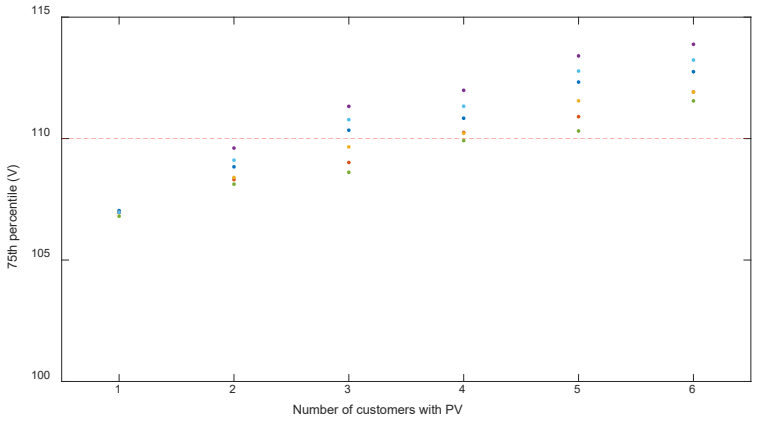

Figure 3-9. 75th percentile of the worst-case overvoltage as a function of the number of customers with PV in the 6-customer rural network.

3.3.2 All inverters connected to the same phase

An extreme case would be all solar power inverters connected to the same phase. This has been modelled injecting the power in the A phase for all customers with PV. The results are shown in Figure 3-10. As expected, the overvoltage becomes higher, and already for three customers with PV is it almost certain that the 110% overvoltage limit will be exceeded as seen in Figure 3-10 (top right).

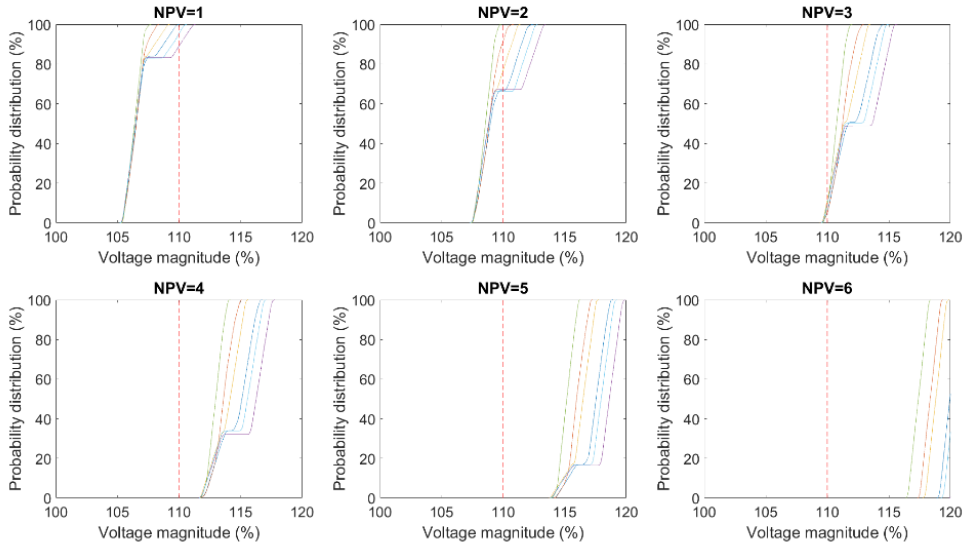

Figure 3-10. Probability distribution function for the highest voltage for increasing amount of solar power in the 6-customer rural network, when all single-phase inverters are connected to the same phase.

3.3.3 Coordinated connection of inverters

Instead of random connection, a study was done where each inverter was connected to the phase with the lowest voltage before connection. Results are shown in Figure 3-11 and Figure 3-12. The order in which the inverters are connected plays a role now; before every connection the three phase-to-neutral voltages at the new customer with PV were calculated; the PV was connected to the phase with the lowest phase-to-neutral voltage. For one customer with PV, the

result is the same as for the earlier cases, as there is nothing to coordinate. For more customers with PV, the risk of overvoltage stays about the same, with a small step between three and four, as the fourth inverter does not compensate the voltage rise from the first three.

It is also concluded from the figures that even with coordinated connection, there is a risk that the 110% overvoltage limit will be exceeded. Note that again this is based on 6 kW per installation and the 90th percentiles.

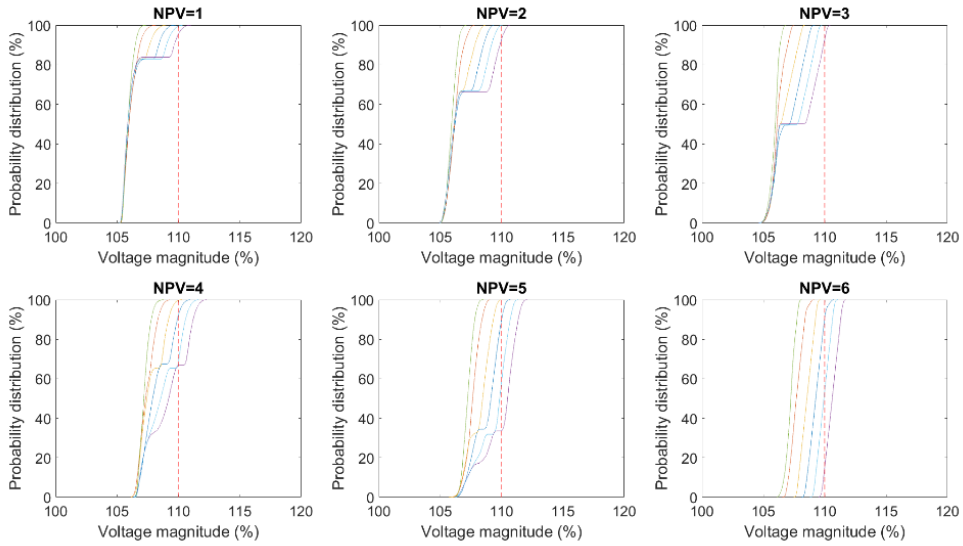

Figure 3-11. Probability distribution function for the highest voltage for increasing amount of solar power in the 6-customer rural network; coordinated connection of inverters.

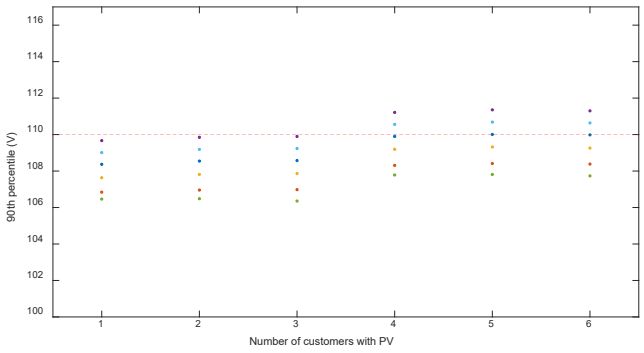

Figure 3-12. 90th percentile of the worst-case overvoltage as a function of the number of customers with PV in the 6-customer rural network; coordinated connection of inverters.

3.4 UNDERVOLTAGE IN THE 6-CUSTOMER RURAL NETWORK

The appearance of overvoltage due to solar power connected to the distribution grid is discussed in many publications [1-4] to name a few. As was shown in Section 3.1, this is the case for both single-phase and three-phase connected inverters. Single-phase inverters may also result in undervoltages: a voltage rise will occur in the phase to which the inverter is connected; an undervoltage in the other two phases. Examples of this are shown in Section 4.9.2 and Section 4.9.4.

3.4.1 Random spread of inverters over the phases

When considering the risk of undervoltage, other distributions have to be considered for the no-load and no-PV voltages than when considering the risk of overvoltage. Undervoltage occurs in the phases without PV during periods with high production and at the same time high consumption and low no-load voltages. High production can occur, like before, around noon during the summer months. Instead of the lowest consumption and the highest no-load voltage, the highest consumption and the lowest no-load voltage during the sunny hours of the year should be used as input to the calculation. From the same data as in Section 3.3, the following input data to the hosting-capacity calculation has been used:

i) Consumption: 1000 W–2500 W per customer per phase. Note again that this is not a typical consumption but an estimation of the amount of consumption that may occur during a worst case for undervoltage due to PV.
ii) No-load voltage: 232 V–236 V.

Like before, 6 kW production per PV installation has been assumed. The resulting probability distributions are shown in Figure 3-13. Compared to the figures in Section 3.3 (risk of overvoltage), the lowest of the three voltages for each customer has been used as input to the probability distribution function. The results show that a voltage drop may occur due to solar power, but values less than 95% of nominal during hours of high production are very unlikely. Undervoltage does not set the hosting capacity in this network. However, when the highest consumption occurs during periods with high solar power production, undervoltage may be a bigger concern than overvoltage.

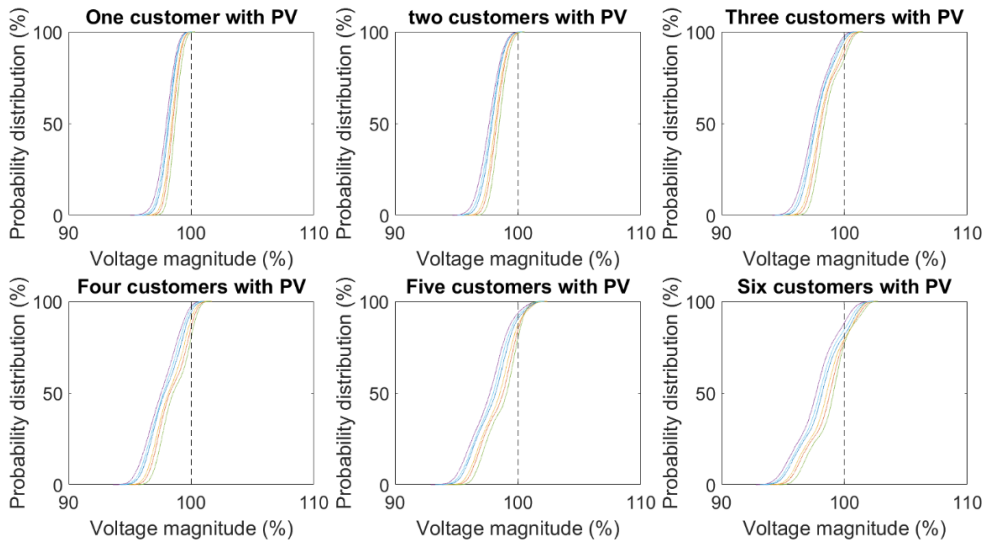

Figure 3-13. Probability distribution (cumulative distribution function) for the lowest voltage (worst-case voltage) for increasing amount of single-phase connected solar power in the 6-customer rural network. The different colours refer to the six different customers. The black dashed vertical line is the nominal voltage.

3.4.2 All inverters in the same phase

The calculations in Section 3.4.1 have been repeated for the case when all inverters are connected to the same phase. The results are shown in Figure 3-14. The voltage becomes lower than with random connection, but the risk of unacceptable undervoltage (below 90%) remains very low.

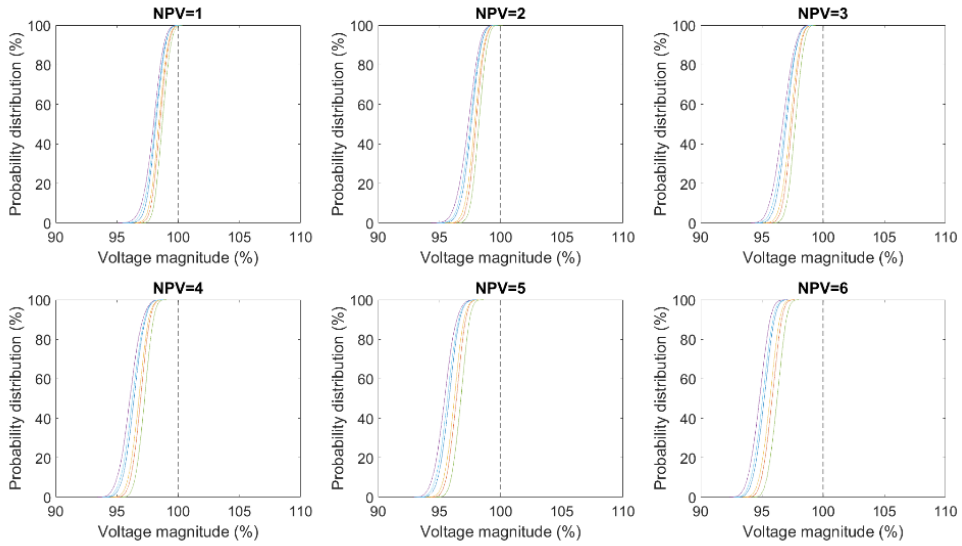

Figure 3-14. Probability distribution for the lowest voltage for increasing amount of single-phase connected solar power in the 6-customer rural network. All inverters are connected to the same phase.

3.5 OVERVOLTAGE IN THE 28-CUSTOMER URBAN NETWORK

3.5.1 Random spread of inverters over the phases

The calculations presented in the previous two sections have been repeated for the 28-customer suburban network. The distributions for no-load voltage and consumption are the same as used for the rural network. The results are shown in Figure 3-15 and Figure 3-16. The hosting capacity, using the same values as before, equals three customers (see Figure 3-16).

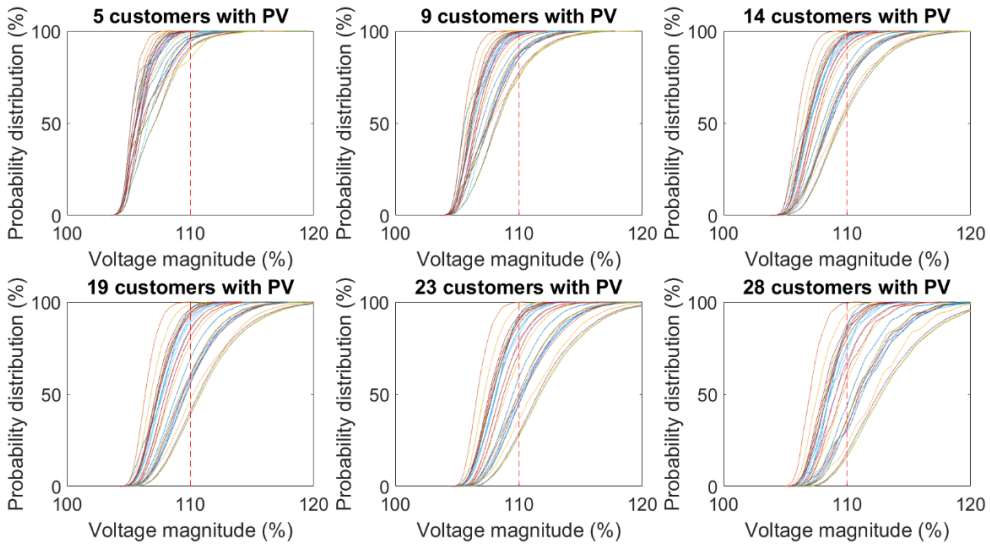

Figure 3-15. Probability distribution (CDF) for the highest voltage (worst-case voltage) for increasing amount of single-phase connected solar power in the 28-customer suburban network.

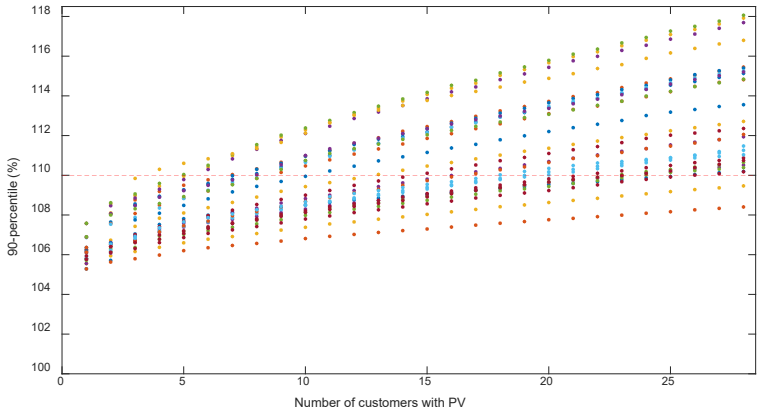

Figure 3-16. 90th percentile of the worst-case overvoltage as a function of the number of customers with PV in the 28-customer suburban network.

The results are presented in a somewhat different way in Figure 3-17. The horizontal axis now gives the customer number; the dots indicate the 90th percentile of the worst-case overvoltage for an increasing number of customers with PV (from bottom to top). The figure shows which customers are most likely to show high overvoltage with a high penetration of solar power in this network: customers 17, 18 and 19, followed by 8, 9, 24, 25 and 26.

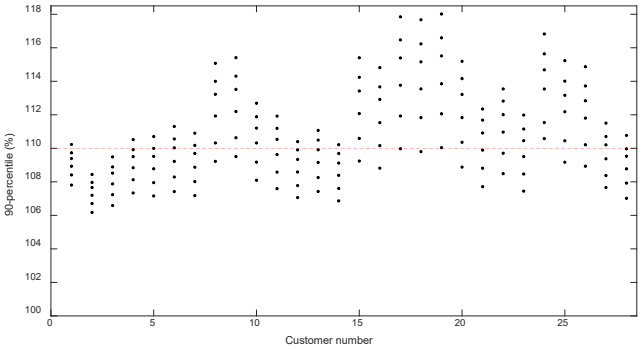

Figure 3-17. 90th percentile of the worst-case overvoltage for the customers on the 28-customer network, for 5, 9, 14, 19, 23 and 28 (bottom to top) customers with PV.

3.5.2 Sensitivity analysis

To illustrate how different parameters affect the outcome of the calculation, a sensitivity analysis has been done. The results of this are shown in Table 3-4. The hosting capacity turns out to be most sensitive to the percentile used and to the produced power per installation. The percentile used is a matter of how much risk the network operator is willing or even allowed to take in the planning stage. This remains largely an unexplored but very important area. The value of the produced power used in the calculation depends on the size of the individual installations and on the spread in tilt direction and angle between the installations. Some specific studies, with more detailed models covering these uncertainties, are needed for a more accurate estimation of the hosting capacity.

Table 3-4. ***Sensitivity Analysis of the Hosting Capacity.***

Case	Parameter	Default Value	New Value	Hosting capacity
0				3 customers
1	Produced power per installation	6 kW	7 kW	2 customers
2			5 kW	6 customers
3			4 kW	11 customers
4	Percentile	90th	95th	1 customer
5			85th	5 customers
6			75th	8 customers
7	load per customer per phase	[0, 250 W]	[0, 150 W]	3 customers
8			[0, 350 W]	3 customers
9	No-load voltage	[238 V, 242 V]	[240 V, 244 V]	2 customers
10			[239 V, 243 V]	2 customers
11			[237 V, 241 V]	4 customers
12			[236 V, 240 V]	6 customers

3.5.3 Voltage range

The voltage range over all customers and phases is a measure for how close a low-voltage network is to its limits. This range has been calculated as the difference between the lowest and the highest voltage anywhere with a customer. This is presented in Figure 3-18 for increasing number of customers with PV and in Figure

3-19 as a function of the number of customers with PV. We will use this information when discussing distribution transformers with on-load tap changers in Section 4.2.

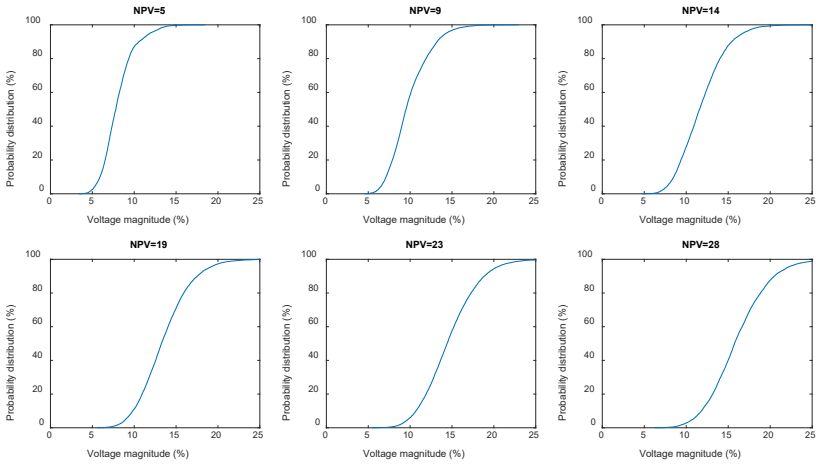

Figure 3-18. Range of voltage for the 28-customer network with increasing penetration of single-phase-connected PV.

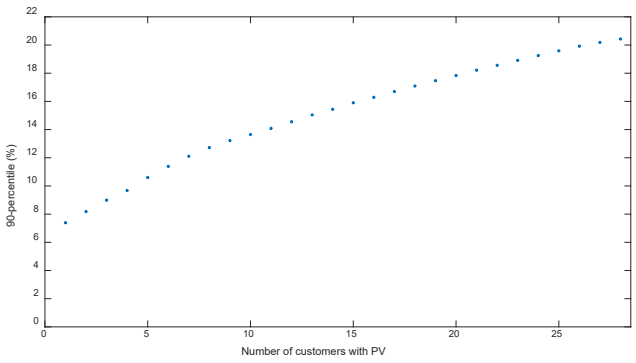

Figure 3-19. Range of voltage for the 28-customer network as a function of the number of customers with PV.

3.5.4 Cable cabinets

The cable cabinets are the de-facto points-of-common-coupling between customers and between existing and possible future customers. The voltage at these locations is a measure for the way in which customers are impacted by PV installations at other customers. The distribution of the voltage magnitude at the cable cabinets is shown in Figure 3-20.

The 90th percentile of the voltages is shown in Figure 3-21 (as a function of the number of customers with PV) and in Figure 3-22 (for the individual customers). When 7 customers have PV installed, the 90th percentile exceeds 110% for the cable cabinet that feeds customers 17, 18 and 19. For 10 customers with PV, the 110% overvoltage limit is exceeded for three more cable cabinets.

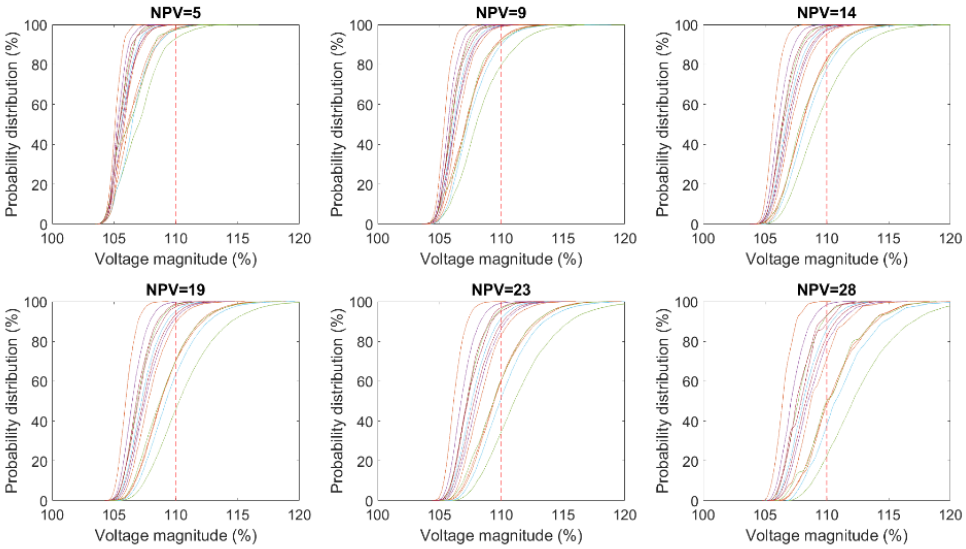

Figure 3-20. Probability distribution function for the highest voltage at the cable cabinets in the 28-customer network.

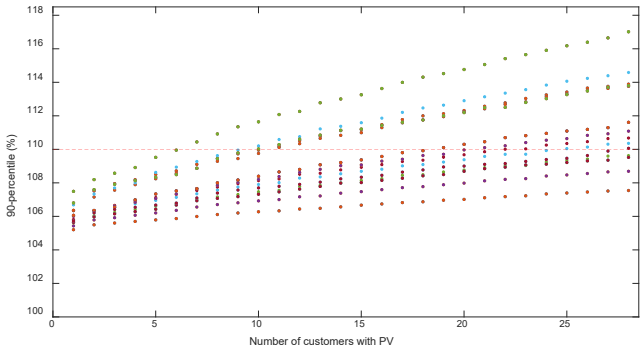

Figure 3-21. 90th percentile of the worst-case overvoltage at the cable cabinets as a function of the number of customers with PV in the 28-customer network.

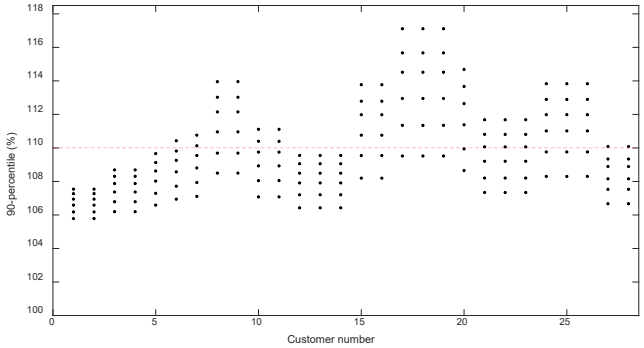

Figure 3-22. 90th percentile of the worst-case overvoltage at the cable cabinets in the 28-customer network, for 5, 9, 14, 19, 23 and 28 (bottom to top) customers with PV.

3.5.5 All inverters connected to the same phase

Like for the 6-customer network, the probability distributions have been calculated for the case when all inverters are connected to the same phase. The result is shown in Figure 3-23. The overvoltage become more severe than with random connection and very high voltages are possible when many customers have PV installed. In the same way as for random distribution over the phases, the 90th percentile has been calculated as a function of the number of customers with PV. The results are shown in Figure 3-24. The hosting capacity, before the 110% limit is exceeded, is actually very similar to the one for random connection. The hosting capacity is already reached for three customers with PV. The 90th percentile is, for one or two customers with PV, similar for connection in the same phase as for random connection.

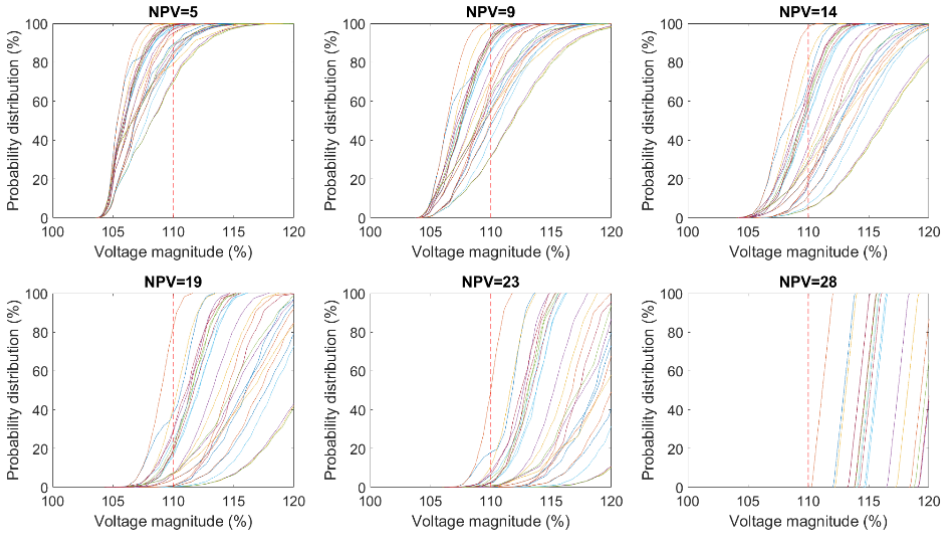

Figure 3-23. Probability distribution function for the highest voltage for increasing amount of solar power in the 6-customer rural network, where all single-phase inverters are connected to the same phase.

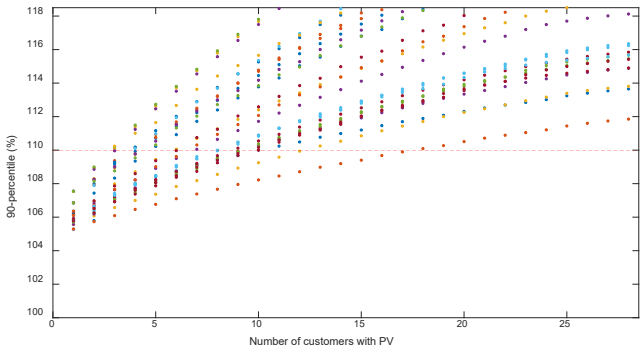

Figure 3-24. 90th percentile of the worst-case overvoltage as a function of the number of customers with PV in the 28-customer network. All inverters connected to the same phase.

3.5.6 Coordinated connection of inverters

Like in Section 3.3.3, the case with coordinated connection of inverters has also been studied for the 28-customer urban network. With coordinated connection, each inverter is connected to the phase with the lowest voltage before connection. This results is a kind of natural spread of the inverters over the three phases.

The resulting distributions and 90th percentile values are shown in Figure 3-25, Figure 3-26 and Figure 3-27. It is shown that coordinated connection results in much lower overvoltages than random connection. For one customer, customer 24, the 110% limit is exceeded already for four customers with PV. However, the 90th percentile remains constant slightly above 110% almost up to 28 customers with PV. Only for 24 customers with PV is the limit exceeded for a second customer as well. As the study is based on a number of assumptions, several of which result in an overestimation of the highest voltage, the conclusion could be that coordinated connection will likely keep the highest voltage below the 110%-limit.

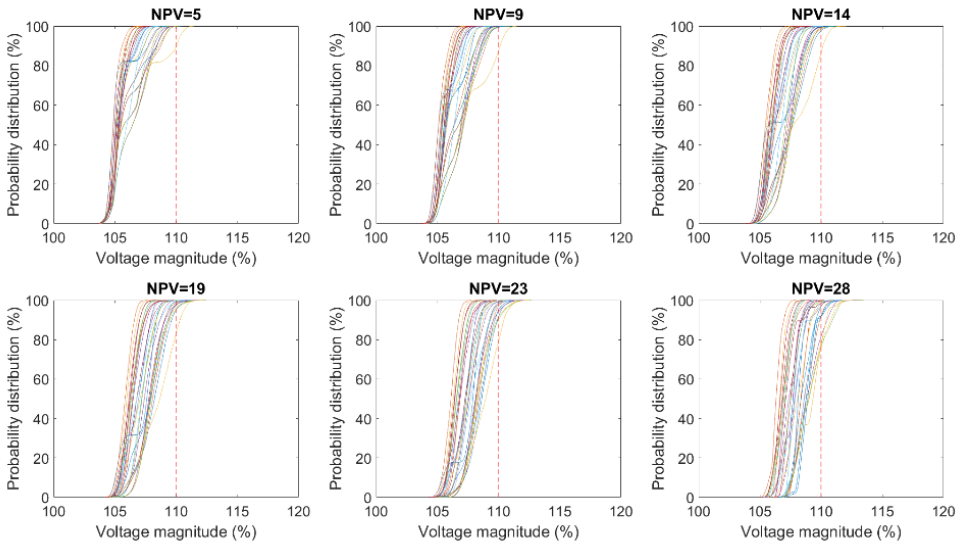

Figure 3-25. Probability distribution function for the highest voltage with the customers in the 28-customer network; coordinated connection of PV.

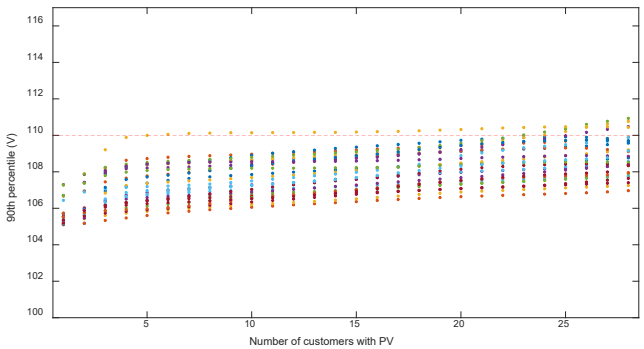

Figure 3-26. 90th percentile of the worst-case overvoltage with the customers, for increasing amount of PV in the 28-customer network; coordinated connection.

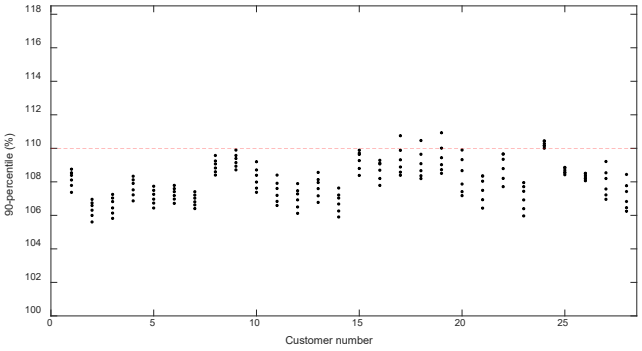

Figure 3-27. 90th percentile of the worst-case overvoltage with the customers, for 5, 9, 14, 19, 23 and 28 customers with PV (bottom to top) in the 28-customer network; coordinated connection.

3.6 CONCLUSIONS

3.6.1 Findings

For a set of about 50 000 low-voltage customers, for which source impedance data was available, it is shown that the hosting capacity for three-phase connected PV is about six times the hosting capacity for single-phase connected PV. With a permissible voltage rise of 5% with maximum production, 99.96% of customers would be able to connect 6-kW three-phase installations. For a single-phase installation of the same maximum production, this would be possible for only 74.7% of the customers. With a permissible voltage rise of 3%, connection would be possible for 95.5% and 49.4% of the customers.

The proposed stochastic approach can be used to estimate the hosting capacity in the planning stage. The outcome of the estimation, together with estimates of future growth of the number of customers with PV, will give feedback to the network operator on the need for network investments.

For single-phase installations injecting 6 kW to the worst-case situation (from an overvoltage viewpoint), the 90th percentile of the overvoltage exceeds the 110% limit already for a small number of customers with PV. This is an extreme case and the actual hosting capacity may be significantly bigger for two reasons:

- It is not expected that all units will inject 6 kW power at the same time. For a PV side of 4 kW, the hosting capacity increases a lot.
- The 90th percentile is a high percentile. For the 75th percentile, the hosting capacity increases as well. The selection of percentile value is strongly related to the amount of risk that the network operator and other stakeholders are willing to take.

Single-phase connected PV inverters not only increase the risk of overvoltage; they also introduce a risk of undervoltage. Undervoltage could occur when high solar-power production coincides with high consumption.

Connecting all inverters in the same phase gives extremely high overvoltage already for a small number of customers with PV.

3.6.2 Recommendations

More experience with the application of the method is needed, which can only be obtained by applying it to more low-voltage networks.

To be able to apply this method more broadly, information should be made available on the consumption of low-voltage customers and on the voltages in medium-voltage networks, with a time resolution of 10 minutes of better.

More data is needed, for example on expected inverter size, but also on differences in production between installations, differences in tilt angle and direction, etc. to estimate what is a suitable inverter size to include in the model.

As a next step, the model should be extended to also include medium-voltage networks.

3.6.3 Modelling assumptions and limitations

Reactive-power production and consumption has not been considered in the study for the following reasons:

- Reactive power consumption of domestic customers is low and shows the tendency to decrease even more.
- Reactive power consumed or produced by PV inverters is small compared to the active power.
- The source and transfer impedances are predominantly resistive, so that the impact of reactive power on the voltage drop or rise is small.

When reactive-power control is used with the PV inverters, larger amounts of reactive power are involved and this can no longer be neglected. This is shown in Section 4.9.

The method used in this study for calculating the voltages is a rather simple method, the transfer-impedance matrix: a multi-dimensional version of Ohm's law. More advanced methods are available and typically used. Many studies on solar-power integration use a load flow method to calculate the voltages. Those methods are however more computationally demanding and its implementation in a flexible tool like Matlab requires a more complicated code. Therefore, the decision was made early on in this project to use the transfer-impedance matrix, despite its limitations.

The main difference between the load flow and the transfer impedance (our model) is that the PV installation is modelled as constant current in our method whereas it is modelled as constant power when using a load flow. For large deviations from the nominal voltage, the error increases; for a 110% voltage at the inverter terminals, the current is overestimated by 10%. Not all inverters will experience a 110% voltage at the same time, so that the error in hosting capacity will be less than 10%. For a complete load-flow study, the voltage dependence of the consumption needs to be included as well. This information is rarely available.

The different uncertainties in the study, like the choice of percentile in the performance indicator, do have a much bigger impact on the results. The choice of

transfer impedance instead of load flow is not expected to have a big impact on the results.

Introducing further uncertainties will likely reduce the overvoltage and increase the hosting capacity. Quantifying this impact is very difficult as very little is known about how things will develop in the future.

In the simulation model, it has been assumed that the range of no-load voltage remains constant with increasing amount of solar power. The no-load voltage is the voltage coming from the medium-voltage grid. With increasing amount of solar power in the low-voltage network under study, it is likely that more solar power will also appear in neighbouring low-voltage networks. This in turn will have an impact of the voltage in the medium-voltage network.

The resistive part of the medium-voltage impedance is about 1 Ω for the 6-customer network. One customer with 6-kW PV, single-phase connected, corresponds to 0.2 A current in two phases in the medium-voltage network. For a 1% voltage rise (57.7 V) a current equal to 57.7 A is needed, or almost 300 installations of 6 kW. With large penetration of solar power, this may become the case. However, as the hosting capacity is already exceeded for much lower values, there is no need to include this in the studies now.

4 Study of Some Mitigation Methods

In this chapter, a number of mitigation methods is studied for reducing the risk of overvoltage. For some of the mitigation methods, the planning approach from Section 3 has been applied. For other methods, only a general discussion is presented.

4.1 STRENGTHENING OF THE NETWORK

Three ways of strengthening the network have been studied: a transformer with a lower impedance; service cables with a larger cross-section; feeder cables with a larger cross-section.

4.1.1 Transformer

A distribution transformer with a bigger rating has a lower impedance; both short-circuit impedance and earth-fault impedance. It is even possible to construct transformers with a smaller zero-sequence impedance. All this will reduce both the source impedance and the transfer impedance and make that the voltage rise due to single-phase connected PV is less.

The source and transfer impedances are however mainly determined by the cable impedances, especially where it concerns the resistive part. The impact of a smaller transformer impedance is therefore small.

To illustrate the potential impact, the extreme case was considered where the transformer impedance is equal to zero. (A very small value, equal to 0.1 μΩ, was used in the calculations to ensure convergence of the matrix inversion.) The results are shown in Figure 4-1 for the 6-customer network, where each dot is obtained from 100 000 simulations. As can be seen from the figure (compare left-hand and right-hand plots), the improvement is small. The difference increases with increasing number of customers with PV because each PV installation contributes to the voltage rise over the transformer impedance.

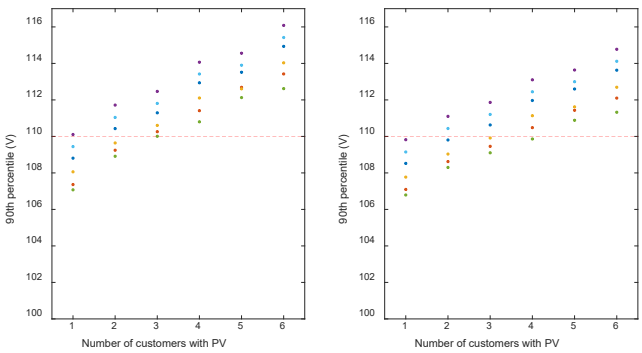

Figure 4-1. 90th percentile of the worst-case overvoltage; 6-customer network; Base case (left) and case with zero transformer impedance (right).

The results for the 28-customer network are shown in Figure 4-2. The results are only shown for up to 10 customers with PV. The impact of the transformer impedance is shown to be even smaller than for the 6-customer network. It is concluded that replacing the transformer by one with a lower impedance does not have any noticeable impact on the hosting capacity.

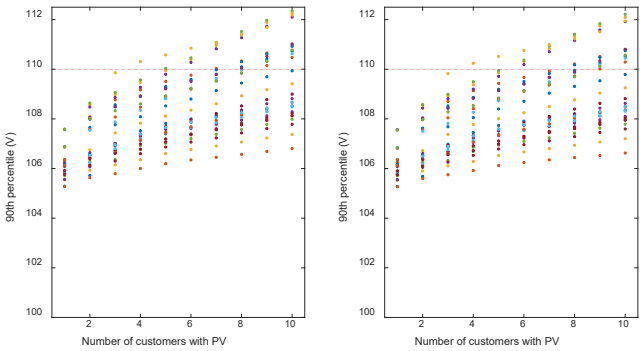

Figure 4-2. 90th percentile of the worst-case overvoltage; 28-customer network; Base case (left) and case with zero transformer impedance (right).

4.1.2 Service cable

The existing service cables have been replaced in the simulation by service cables with 25 mm² and 35 mm² cross-section. This reduces the resistive part of the source impedance and thus the voltage rise. The results are shown in Figure 4-3 and Figure 4-4 for the 6-customer network; in Figure 4-5, Figure 4-6 and Figure 4-7 for the 28-customer network.

Comparing with the base-case shows that the overvoltage is reduced for most customers, with the exception of customers 8 and 9 as well as customers 17, 18 and 19. There is a clear improvement (reduced overvoltage; increased hosting capacity) from 10 mm² (the base case) to 25 mm²; the increase from 25 to 35 mm² is very limited.

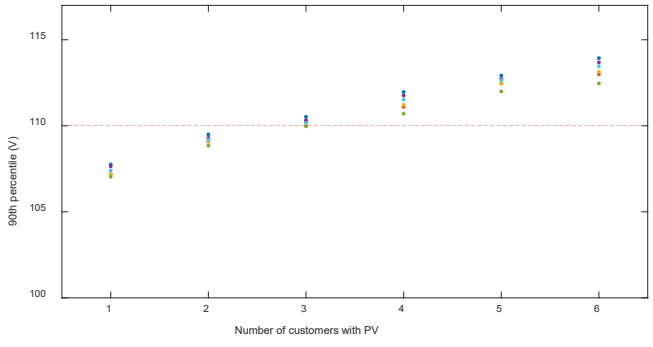

Figure 4-3. 90th percentile of the worst-case overvoltage; 6-customer network; 25 mm² service cables to all customers

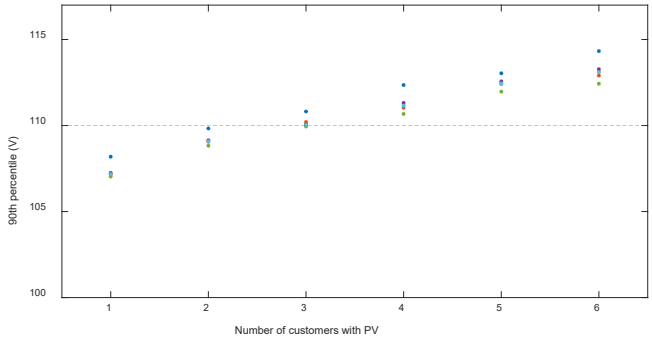

Figure 4-4. 90th percentile of the worst-case overvoltage; 6-customer network; 35 mm² service cables.

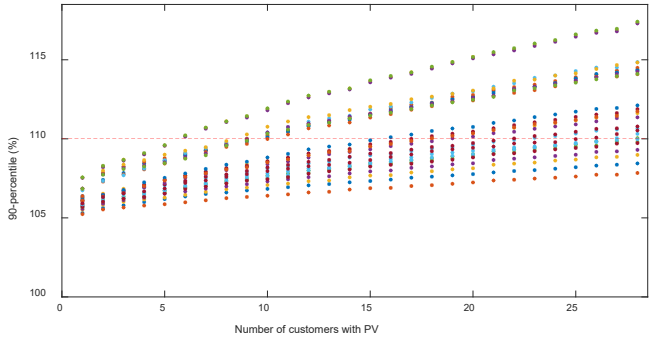

Figure 4-5. 90th percentile of the worst-case overvoltage; 28-customer network; 25 mm² service cables

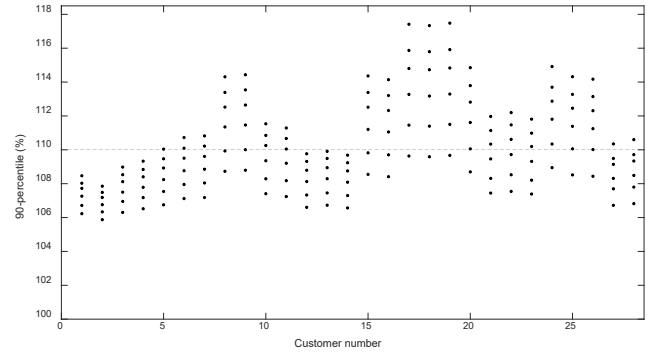

Figure 4-6. 90th percentile of the worst-case overvoltage for the customers on the 28-customer network, for 5, 9, 14, 19, 23 and 28 (bottom to top) customers with PV. 25 mm² service cables

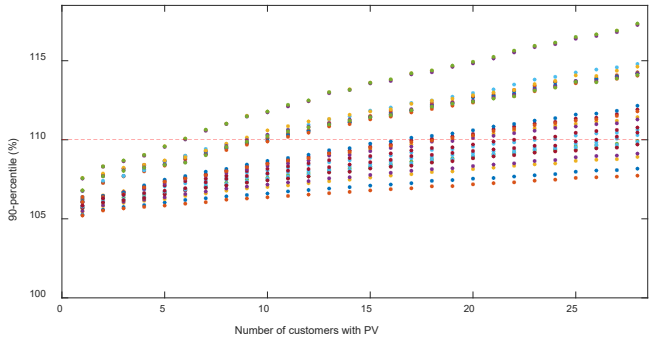

Figure 4-7. 90th percentile of the worst-case overvoltage; 28-customer network; 35 mm² service cables

4.1.3 Feeder cables

As a next step, after upgrading the service cables, the feeder cables can be upgraded. The feeder cables, and the cable cabinets that they are connecting, are shown in Figure 4-8, without the service cables. Most feeder cables are 150 mm² in area, with two exceptions. Both exceptions are indicated in the figure.

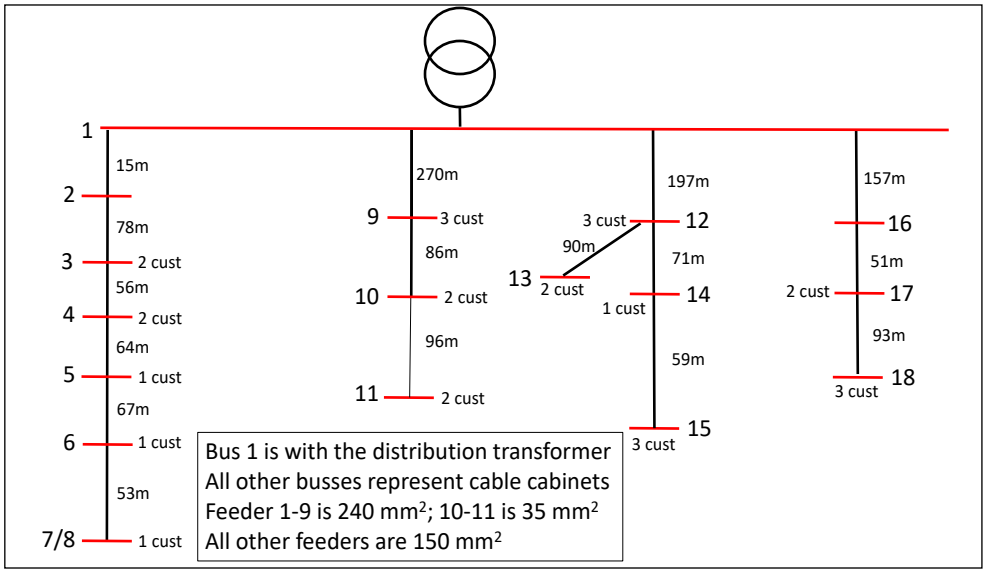

Figure 4-8. Distribution transformer, cable cabinets (2 through 18) and feeder cables with length for the 28-customer urban network. Note that the cable lengths are not shown to scale in the figure.

The supply to customers 8 and 9 (connected to cable cabinet 11) is specifically studied here. As a first step, the upgrade of cable 10-11 to 150 mm² has been simulated, with the 90th percentiles for the different customers shown in Figure 4-9. In the base case, (see Figure 3-17 in Section 3.5.1) customers 8 and 9 (fed from this cable) were among the ones with highest overvoltage (similar to customers 17 to 19). The cable upgrade significantly reduced the overvoltage; only for 14 customers with PV is the 110% overvoltage limit reached (this occurred already between 4 and 9 customers with PV in the base case).

As an additional measure, the upgrade of cable 9-10 to 240 mm² has been simulated, with the results shown in Figure 4-10. The voltages with customers 9 and 10 are somewhat further reduced, but the additional impact of this upgrade remains limited.

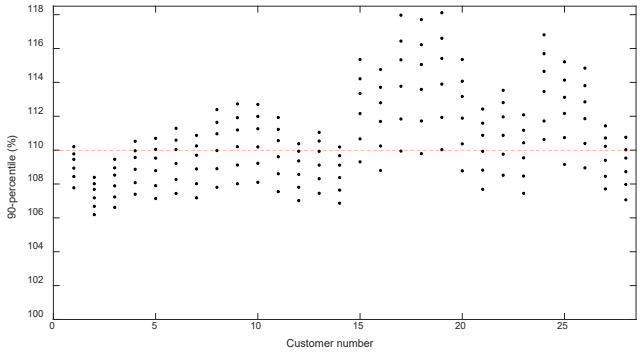

Figure 4-9. 90th percentile of the worst-case overvoltage for the customers in the 28-customer network, for 5, 9, 14, 23 and 28 (bottom to top) customers with PV; cable 10-11 upgraded from 35 mm² to 150 mm².

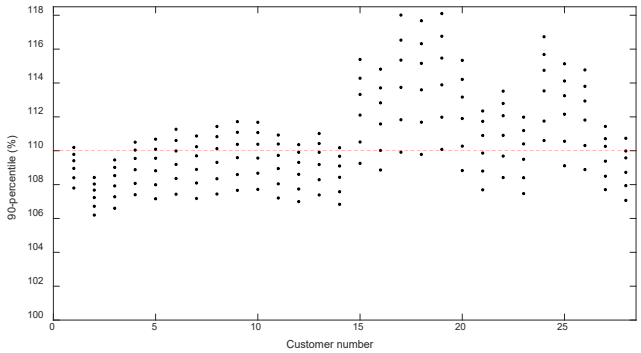

Figure 4-10. 90th percentile of the worst-case overvoltage for the customers in the 28-customer network, for 5, 9, 14, 23 and 28 (bottom to top) customers with PV; cable 10-11 upgraded from 35 mm² to 150 mm²; and cable 9-10 upgraded from 150 mm² to 240 mm².

Further improvements in the low-voltage network as a whole would require the attention to be directed to customers 17, 18, 19 (the ones that experience the highest overvoltage) but also to customer 24 (the one for which the 110 % overvoltage limit is first exceeded). The latter can be solved by upgrading the service cable (see Figure 4-6).

The main issue for customers 17, 18 and 19 is the presence of nine customers that may possibly have PV, downstream of feeder cable 1-12 (197 meter, 150 mm²). Upgrading this cable may be the next step to be considered.

Note, customers 17, 18 and 19 are serviced from cable cabinet 15; customer 24 is serviced from cable cabinet 18 through 76 m of cable. The two other customers with cable cabinet 18 are serviced through 29 and 37 m of cable.

4.2 DISTRIBUTION TRANSFORMER WITH ON-LOAD TAP CHANGER

Distribution transformers are normally equipped with off-load tap changers, where the transformation ratio is set when the transformer is installed. This allows the compensation of the average voltage drop along the medium-voltage feeder. Variations in the voltage on the medium-voltage feeder however directly affect the voltage with the customers. Equipping the distribution transformer with on-load

tap changers makes that these variations are blocked; this gives a bigger overvoltage and/or undervoltage margin.

The main issue to decide about is the setting of the tap changer control. A too high setting reduces the hosting capacity for new production. A too low setting introduces a serious risk of undervoltage during high consumption. The initial value chosen for the simulations was equal to 238 V, the lower limit of the original range in background voltage. The resulting voltages are presented in Figure 4-11 and Figure 4-13. The increased overvoltage margin increases the hosting capacity.

The simulations were repeated for a 240 V setting; 1% above the lowest value of the original range. In this way, the lower limit of the dead-band is still sufficiently high to avoid unacceptable undervoltage. The results for this setting are shown in Figure 4-12 and Figure 4-14.

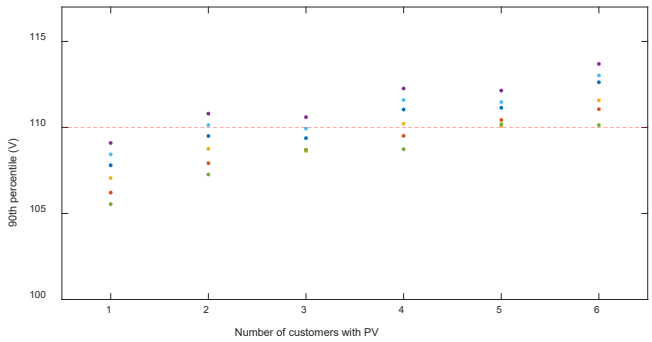

Figure 4-11. 90th percentile of the worst-case overvoltage as a function of the number of customers with PV in the 6-customer network; On-line tap changers on the distribution transformer with upper limit of the controller dead-band set at 238 V.

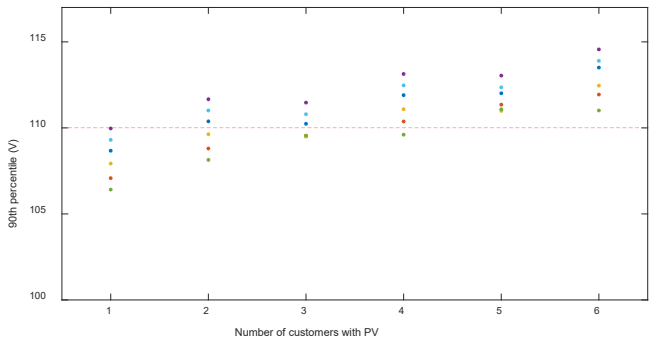

Figure 4-12. 90th percentile of the worst-case overvoltage as a function of the number of customers with PV in the 6-customer network; On-line tap changers on the distribution transformer with upper limit of the controller dead-band set at 240 V.

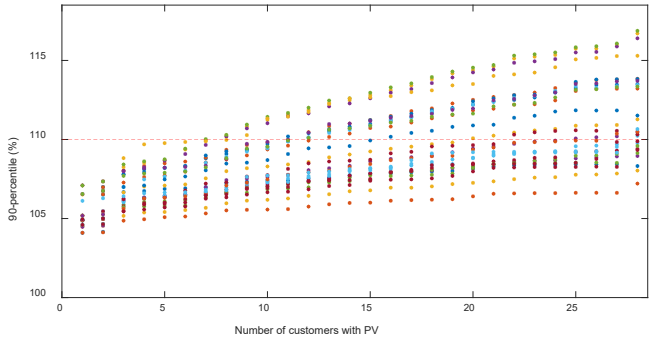

Figure 4-13. 90th percentile of the worst-case overvoltage as a function of the number of customers with PV in the 28-customer network; On-line tap changers on the distribution transformer with upper limit of the controller dead-band set at 238 V.

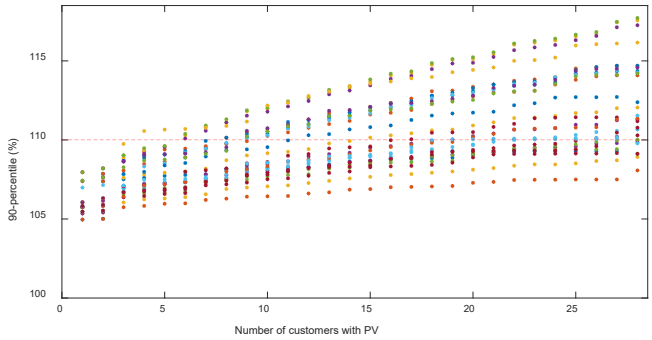

Figure 4-14. 90th percentile of the worst-case overvoltage as a function of the number of customers with PV in the 28-customer network; On-line tap changers on the distribution transformer with upper limit of the controller dead-band set at 240 V.

More advanced control algorithms are possible, where line-drop compensation would be a first approach. Line-drop compensation does however assume that all feeders have a similar production or consumption. The control algorithm is limited when some of the feeders have high consumption whereas others have high production at the same time. How common such a situation is, remains unclear and requires more data collection and simulations.

The most advanced algorithms, discussed in the literature, use measurements of the voltage with a selected number of customers to control the tap changer. Such remains possible as long as the difference between the highest and the lowest voltage, anywhere with any of the customers, is less than 20% of the nominal voltage. As shown in Figure 3-19, this is the case up to almost all customers with PV.

4.3 CAPACITOR BANKS IN THE LOW-VOLTAGE NETWORK

The use of a switchable capacitor on the low-voltage side of the distribution transformer allows for two operational states of the low-voltage network:

- A state with low no-load voltage (no consumption and no production) allowing extra overvoltage margin for high production;

- A state with high no-load voltage allowing extra undervoltage margin for high consumption.

The idea studied here is to drop the voltage on the low-voltage side of the distribution transformer by 2.5% using the off-load tap changer. During periods of high consumption, the capacitor bank is switched in to provide for a 2.5% voltage rise, compensating the voltage drop due to the off-load tap changer. During periods of high consumption, the voltages are the same as before; during periods of high production, they are 2.5% lower.

During periods with high consumption, the capacitor bank is off. For the calculations, it was therefore assumed that the no-load voltage was 2.5% lower than the value used in the earlier calculations. The results are shown in Figure 4-15 for the 6-customer network and in Figure 4-16 for the 28-customer network. The 2.5% extra overvoltage margin gives a significant increase in hosting capacity.

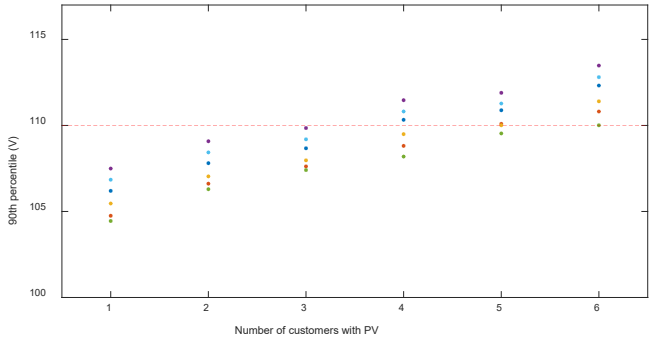

Figure 4-15. 90th percentile of worst-case overvoltage for the 6-customer network; background voltage reduced by 2.5% representing the use of a capacitor bank on low-voltage side of the distribution transformer.

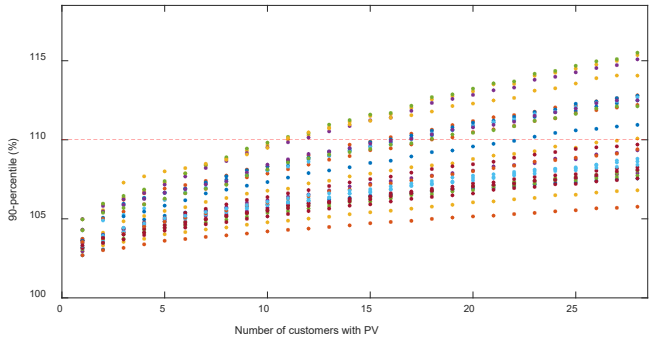

Figure 4-16. 90th percentile of worst-case overvoltage for the 28-customer network; background voltage reduced by 2.5% representing the use of a capacitor bank on low-voltage side of the distribution transformer.

To allow for a 2.5% voltage rise, the capacitor bank should inject sufficient reactive power in relation to the reactive part of the source impedance. Using the data given in Section 2.2, the following sizes are obtained:

- 62,5 kvar for the 6-customer network
- 251 kvar for the 28-customer network

A quick survey was made of low-voltage capacitor banks available on the market. A major manufacturer offered two types:

- 37.5 to 100 kvar, weight less than 40 kg; dimensions 80 x 91 x 48 cm
- 125 to 400 kvar, weight up to 550 kg, dimensions 72x72x239 cm

The first one would fit near a distribution transformer, the second one possibly not depending on the size of the housing around the transformer.

An additional challenge would be the control of the capacitor. An approach similar to "line-drop compensation" could be used to sense the general flow of power through the transformer. The limitation would be during periods with high consumption in some part of the network and high production in another part of the network. The results on the range of voltage magnitudes in Section 3.5.3 show that the likelihood for this happening is low up to about 20 customers with PV.

Another possible disadvantage that require further study are the occurrence of harmonic resonances, switching transients and voltage steps ("individual rapid voltage changes"). Concerning the resonance frequency, this can be estimated from the voltage step ΔU using the following simple expression:

$$f_{res} = f_0 \cdot \frac{1}{\sqrt{(\Delta U)}} \qquad (40)$$

With $f_0 = 50$ Hz. With a voltage step equal to 2.5%, the estimated resonant frequency is 315 Hz. Additional capacitance in the low-voltage network will somewhat reduce the resonant frequency, so that it is expected to be around 300 Hz. There is very limited emission around this frequency, so that no major amplification of harmonic distortion in the low-voltage network will occur.

Energizing the capacitor bank will give an oscillation frequency also somewhat below 315 Hz. The switching of the capacitor bank is however not expected to occur more than a few times a year, so that these occasional transients and the voltage steps are not a major issue.

A related issue, that could become serious and therefore would require further studies, is amplification of the oscillations due to capacitor-bank energizing at a higher voltage. Such switching may occur more often (like once a day) and the nearness of the resonant frequencies could result in high switching overvoltages.

4.4 SHUNT REACTORS IN THE LOW-VOLTAGE NETWORK

Instead of a capacitor bank, a shunt reactor can be used. The setting of the off-load tap changer will not be changed with this solution; instead the shunt reactor will be used to drop the voltage by 2.5% during a period of high production and low consumption.

The impact on the hosting capacity will be the same as for the capacitor bank, so that Figure 4-15 and Figure 4-16 also hold here. Also the size of the reactor will be the same as the size of the capacitor bank: 62.5 kvar in the 6-customer network; 215 kvar in the 28-customer network.

The use of a reactor instead of a capacitor bank will however solve some of the potential problems: harmonic resonance; switching transients; amplification of oscillations from capacitor bank energization.

A search after low-voltage shunt reactance found just one manufacturer that would offer reactors up to 90 kvar for use in 600-V networks. No information was found on the physical size of such reactors.

4.5 CENTRAL ENERGY STORAGE

A storage installation close to the distribution transformer allows for the storage of power when solar power production would result in an unacceptable voltage rise.

The control approach to be used would be similar to the one discussed in the previous two sections. Instead of injecting or consuming reactive power, the energy storage would be used to consume additional active power and in such a way reduce the voltage on low-voltage side of the distribution transformer.

Using the resistive part of the source impedance (as given in Section 2.2), the following extra consumption is needed to give 1% drop in voltage:

- 6-customer network: 56 kW
- 28-customer network: 415 kW

It was shown in Section 4.3 that 2.5% additional overvoltage margin would result in a significant increase in hosting capacity. To obtain the same increase using energy storage, the following storage size would be needed (where it has been assumed that the voltage drop is needed for 2 hours in a row and that the storage can be completely discharged between periods of high voltage):

- 6-customer network: 280 kWh
- 28-customer network: 2075 kWh

As a reference, an installation in operation in Falköping has a storage capacity of 75 kWh. A normal (lead-acid) car battery has a storage capacity around 750 Wh (60-70 Ah, 12 V). The storage capacity needed correspond to:

- 6-customer network: 4 times Falköping; 375 car batteries
- 28-customer network: 28 times Falköping; 2800 car batteries

This would not be impossible sizes, but still on the large size for a distribution network.

4.6 REACTIVE-POWER CONTROL WITH THE DISTRIBUTION TRANSFORMER

The converter with the storage (see previous section) would also be able to control the voltage by reactive-power control. This may in fact be a more effective method than using the energy storage.

To obtain 2.5% extra overvoltage margin requires the following converter ratings with energy storage:

- 6-customer network: 140 kVA
- 28-customer network: 1050 kVA

Using instead only reactive power (as in Section 4.3 and 4.4) the following converter ratings are needed:

- 6-customer network: 62.5 kVA
- 28-customer network: 215 kVA

The same advantages can be obtained as when using a switched capacitor or reactor, but a more smooth voltage control is obtained. The use of a converter instead of a capacitor bank will also avoid harmonic resonances, switching transients and amplification of switching transients. The converter will however inject harmonics and especially supraharmonics into the low-voltage grid[8]. The impact of solar power on harmonics and supraharmonics is studied in a parallel project[9].

4.7 DISTRIBUTED ENERGY STORAGE

Storage of surplus power with the customers allows for control of the voltage at the location where it directly matters. All of the earlier discussed methods control the voltage on the low-voltage side of the transformer. Those methods require some estimation of the voltage with the customers. All those methods will further have their limitations during periods with high consumption in one part of the network and high production in another part of the network. Voltage control directly at the customer terminals does not suffer from this limitation.

Three sizes of energy storage have been studied here:

- 1 kW extra consumption (charging) during two hours;
- 2 kW during two hours;
- 3 kW during two hours.

Storage with more than 3 kW charging capacity would shift the problem to periods with high discharging of the storage. From a grid viewpoint, the impact of high discharging would be the same as the impact of high production.

The results are shown in Figure 4-17 through Figure 4-22. The effect of the storage is an effective reduction of the inverter size. During the worst case, the contribution from PV installation is at most the PV size minus the charging capacity of the storage. The impact of 1 kW charging capacity is small. However, for 3 kW charging capacity, it is possible for almost all customers to have single-phase connected PV.

[8] TB 672 – Power quality aspects of solar power (Technical Brochure), JWG C4/C6.29, 2016

[9] Övertoner i lågspänningsnät vid anslutning av solpaneler, Elforsk rapport, 2018.

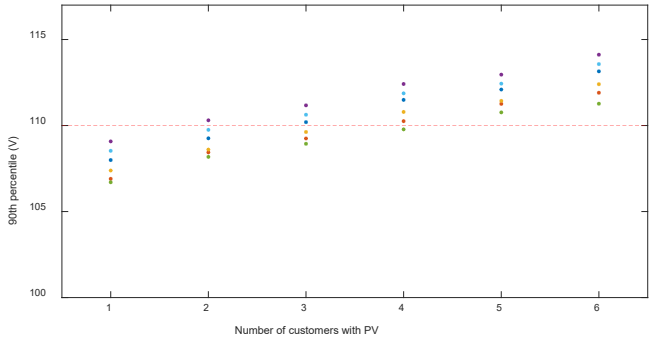

Figure 4-17. 90th percentile of worst-case overvoltage for the 6-customer network; local energy storage with 1 kW charging capacity.

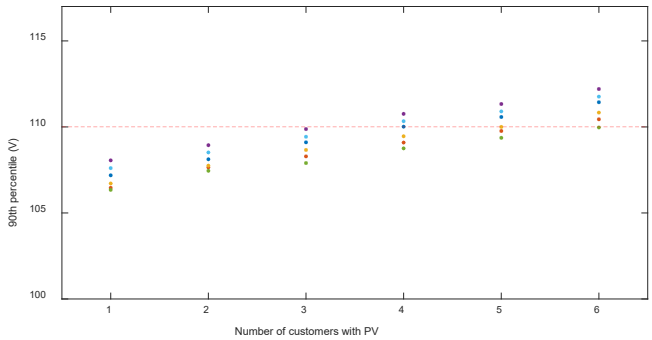

Figure 4-18. 90th percentile of worst-case overvoltage for the 6-customer network; local energy storage with 2 kW charging capacity.

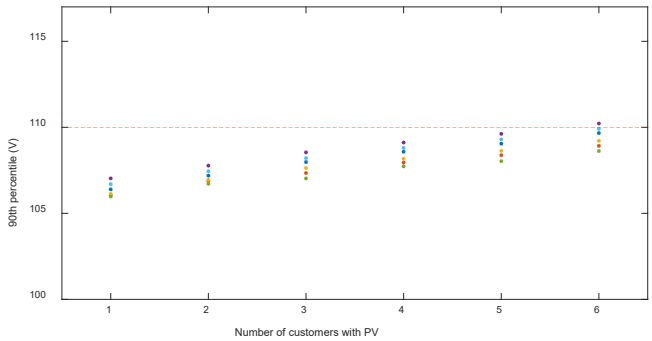

Figure 4-19. 90th percentile of worst-case overvoltage for the 6-customer network; local energy storage with 3 kW charging capacity.

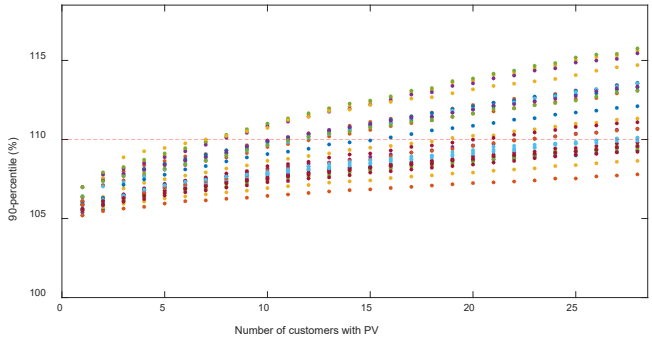

Figure 4-20. 90th percentile of worst-case overvoltage for the 28-customer network; local energy storage with 1 kW charging capacity.

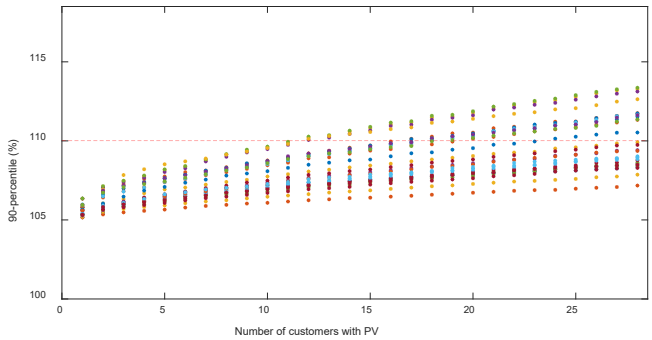

Figure 4-21. 90th percentile of worst-case overvoltage for the 28-customer network; local energy storage with 2 kW charging capacity.

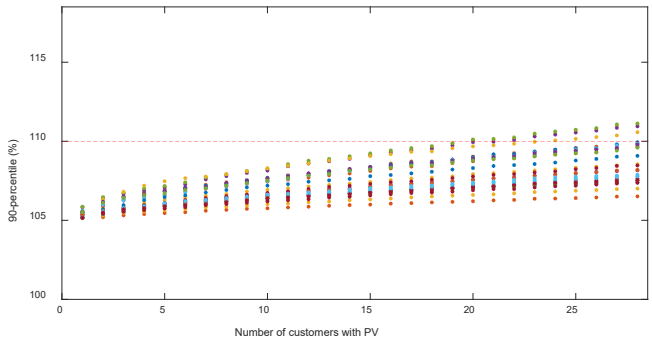

Figure 4-22. 90th percentile of worst-case overvoltage for the 28-customer network; local energy storage with 3 kW charging capacity.

The storage capacity needed to achieve the above is relatively limited. Consider the 3-kW case and the need for storage during three hours. This would require 9 kWh of storage capacity. The Swedish company Box of Energy offers battery storage in the range 2.5 kWh to 28kWh. The Tesla Powerwall is, with 14 kWh, in the same range. Both companies offer commercial solutions to individual domestic customers.

4.8 CURTAILMENT

What matters to the network operator is the power injected into the grid. A reduction of injected power can be due to

- Charging of a local energy storage
- Increased local consumption
- Reduction of production by the PV installation

The latter solution (referred to as "curtailment") allows for an infinite amount of installed production capacity. When the production at a certain moment in time gets too high, the production is simply curtailed. In this case, such curtailment would be triggered by the voltage at the customer terminals exceeding a certain overvoltage threshold.

For curtailment up to 3 kW, the results are the same as for local storage, as shown in the previous section. For completeness, the case with 3.5 kW curtailment is shown in Figure 4-23. It is shown that 3.5 kW curtailment is enough to maintain the voltages within the 110% overvoltage limit.

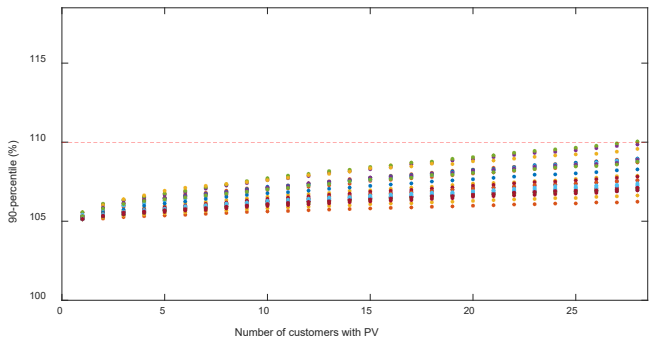

Figure 4-23. 90th percentile of worst-case overvoltage for the 28-customer network; 3.5 kW curtailment possibility.

Curtailment will result in loss of energy, as the actual produced power is less than the available power. The loss of energy can become significant rather quickly. Once the overvoltage limit would be exceeded and curtailment is needed, it will be needed for several days in the year. Both production and consumption have a daily pattern and the voltages will be similar for all sunny days throughout a large part of the year (see the measurement data in Chapter 5).

It was shown in earlier studies[10] that it is important to distinguish between hard and soft curtailment. With hard curtailment, the production is reduced by a fixed amount (1, 2, 3 or 3.5 kW in the above examples) once a certain criterion is fulfilled

[10] N. Etherden, M.H.J. Bollen, Overload and overvoltage in low-voltage and medium-voltage networks due to renewable energy - some illustrative case studies, Electric Power Systems Research, Vol.114 (September 2014), pp.39-48.

Math Bollen, The smart grid – Adapting the power system to the new challenges, Morgan and Claypool Publishers, September 2011.

(in this case, voltage comes too close to 110%). With soft curtailment, the production is reduced only as much as necessary (in this case to keep the voltage at or below 110%).

Soft curtailment requires a control system and has some possible stability issues when many units are equipped with such control. It does however minimize the amount of energy that is lost.

Hard curtailment is much easier to implement, but it could result in repetitive steps in production. A rather long delay may be needed between the switching off and the switching back again. The energy loss is much bigger than with soft curtailment and with increasing installed capacity, the total amount of delivered energy may actually decrease.

4.9 REACTIVE-POWER CONTROL WITH THE INVERTER

4.9.1 6-customer network – source impedance

The source impedances at the customer locations in the 6-customer network are shown in Figure 4-24 and listed in Table 4-1.

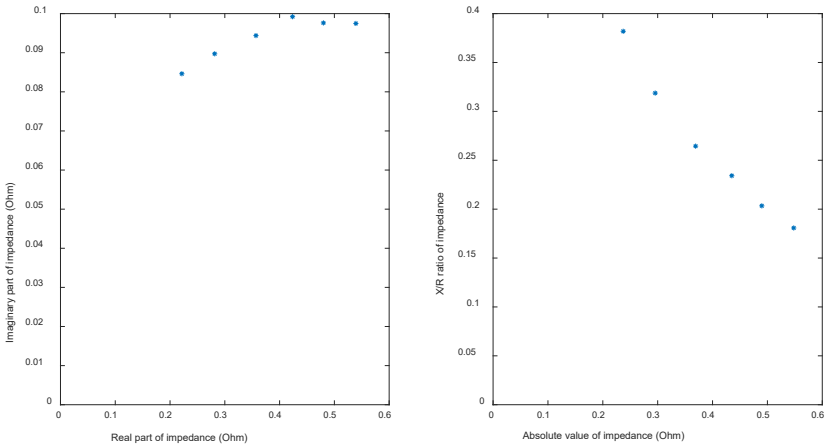

Figure 4-24. Complex source impedance (left) and relation between absolute value and X/R ration of the source impedance (right) at the customer locations in the 6-customer network.

Table 4-1. Source impedance (phase-to-neutral) at the customer locations in the 6-customer network.

Customer	Complex impedance (Ohm)	Absolute value (Ohm)	X/R	R/X
1	0.4236 + 0.0992i	0.4351	0.2342	4.2699
2	0.2815 + 0.0897i	0.2955	0.3187	3.1376
3	0.3569 + 0.0944i	0.3691	0.2645	3.7814
4	0.5393 + 0.0975i	0.5480	0.1808	5.5321
5	0.2216 + 0.0846i	0.2372	0.3819	2.6184
6	0.4800 + 0.0976i	0.4898	0.2034	4.9168

The voltage rise due to injection of active power P and consumption of reactive power Q, is approximately equal to:

$$\Delta U = RP - XQ \tag{41}$$

Where all values are given in per unit. To compensate the voltage rise due to injection of active power, the inverters needs to consume an amount of reactive power equal to:

$$Q = \frac{R}{X} \cdot P \tag{42}$$

The R/X ratio is between 2.6 and 5.5, for the customers connected to the 6-customer network. The amount of reactive power that needs to be injected, to obtain zero voltage rise, is thus between 2.6 and 5.5 times the active power. This would require a significant overrating of the inverter.

4.9.2 6-customer network – impact of reactive-power consumption

To illustrate the impact of reactive-power consumption on the voltages, an installation with customer 4 in the 6-customer network is assumed. The results are shown in Figure 4-25. In the left-hand plot, 6 kW active power is injected in phase A of costumer 4. The plot shows that the voltage rises in phase A with customer 4 and less in this phase with the other customers. The voltages in the other two phases show a slight drop, with the highest drop again with customer 4.

In the right-hand plot, the installation is assumed to produce 6 kW active power and at the same time consume 15 kW reactive power. The impact of the voltage in phase A with customer 4 is small, but the reactive-power consumption does compensate the voltage rise for the other customers. At the same time the reactive-power consumption in phase A results in a voltage rise in phase C and a voltage drop in phase B. As a result, the case with reactive-power compensation is equally bad or even worse than the case without reactive-power compensation.

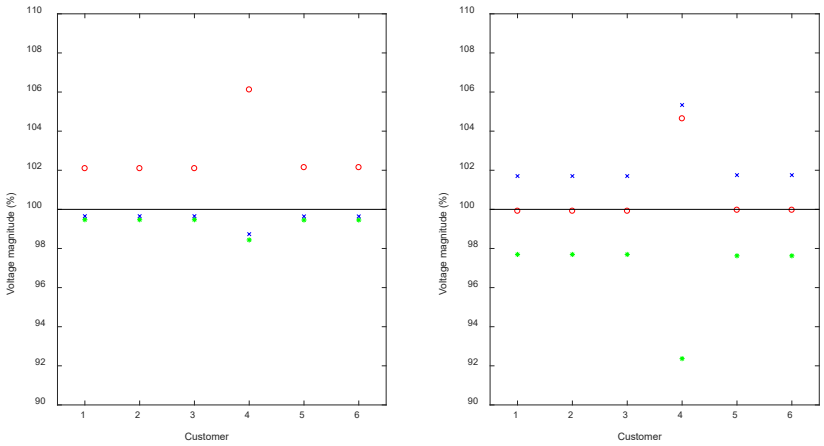

Figure 4-25. Voltage magnitudes in the three phases (red, green, blue) for the customers in the 6-customer network with 6 kW production in phase A with customer 4: no reactive power (left); 15 kvar reactive power consumption (right).

4.9.3 28-customer network – source impedance

The calculations of the source impedance were repeated for the 28-customer network, with the results shown in Figure 4-26 and Table 4-2.

The R/X ratio for this network varies between 4.6 and 11.6. The reactive part of the source impedance (dominated by the transformer impedance) is lower than for the 6-customer network; the resistive part (dominated by the cable impedance) is similar as for the 6-customer network; hence the higher R/X ratio for the 28-customer network.

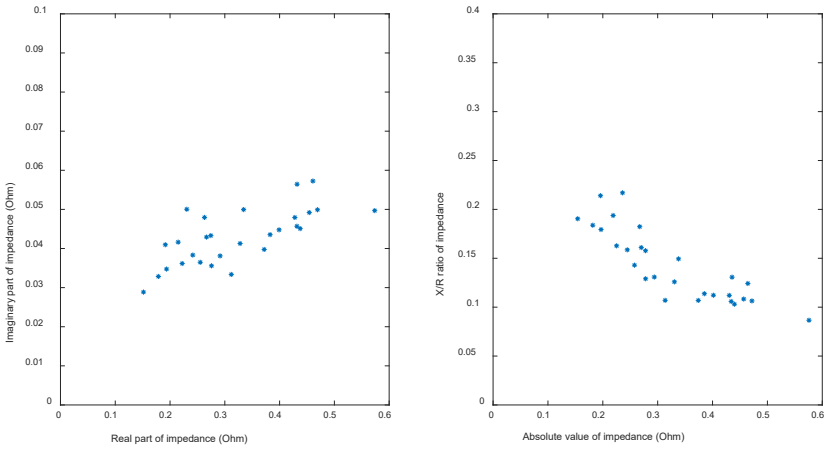

Figure 4-26. Complex source impedance (left) and relation between absolute value and X/R ratio of the source impedance (right) at the customer locations in the 28-customer network.

Table 4-2. Source impedance (phase-to-neutral) at the customer locations in the 6-customer network.

Customer	Complex impedance (Ohm)	Absolute value (Ohm)	X/R	R/X
1	0.3118 + 0.0334i	0.3136	0.1070	9.3464
2	0.1515 + 0.0289i	0.1542	0.1904	5.2517
3	0.1787 + 0.0329i	0.1817	0.1838	5.4403
4	0.2757 + 0.0356i	0.2780	0.1291	7.7489
5	0.2415 + 0.0383i	0.2446	0.1586	6.3034
6	0.2666 + 0.0429i	0.2701	0.1610	6.2125
7	0.2306 + 0.0500i	0.2360	0.2170	4.6089
8	0.4319 + 0.0564i	0.4355	0.1307	7.6525
9	0.4608 + 0.0572i	0.4643	0.1242	8.0488
10	0.3343 + 0.0500i	0.3380	0.1494	6.6927
11	0.2629 + 0.0479i	0.2673	0.1823	5.4844
12	0.2148 + 0.0416i	0.2188	0.1938	5.1609
13	0.2745 + 0.0433i	0.2779	0.1578	6.3385
14	0.1914 + 0.0410i	0.1957	0.2140	4.6721
15	0.4375 + 0.0451i	0.4399	0.1030	9.7045
16	0.3826 + 0.0435i	0.3851	0.1138	8.7880
17	0.4542 + 0.0492i	0.4568	0.1083	9.2320
18	0.4278 + 0.0479i	0.4305	0.1120	8.9249
19	0.4692 + 0.0499i	0.4718	0.1064	9.3999
20	0.3279 + 0.0413i	0.3305	0.1259	7.9427

21	0.2551 + 0.0365i	0.2577	0.1429	6.9955
22	0.3719 + 0.0398i	0.3740	0.1069	9.3540
23	0.1937 + 0.0347i	0.1968	0.1794	5.5741
24	0.5736 + 0.0497i	0.5758	0.0866	11.5451
25	0.4316 + 0.0457i	0.4340	0.1059	9.4468
26	0.3990 + 0.0448i	0.4015	0.1122	8.9127
27	0.2914 + 0.0381i	0.2939	0.1308	7.6455
28	0.2222 + 0.0362i	0.2251	0.1628	6.1443

4.9.4 28-customer network – impact of reactive power compensation

An installation has been assumed with customer 24 in phase A, injecting 6 kW and consuming 12 kvar. The left-hand plot in Figure 4-27 shows the resulting voltages when the reactive power consumption is zero. The voltage rise is biggest with customer 24, and decreases when moving up along the feeder. Customers not connected to this feeder are not affected by the installations. When that same installation also consumes 12 kvar of reactive power, this will give a voltage drop over the distribution transformer, affecting all customers. The overvoltage in phase A with customer 24 is not reduced much, but voltages in phase B show a large drop and in phase C a large increase.

In addition, in this case the consumption of reactive power does not result in any improvement of the voltage quality.

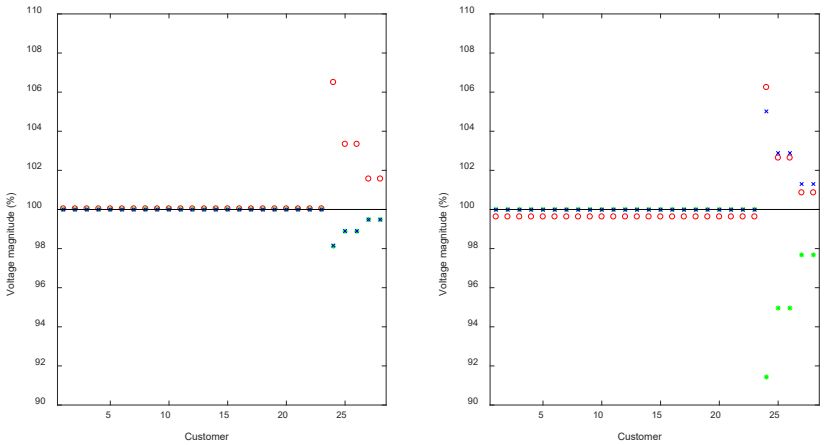

Figure 4-27. Voltage magnitudes in the three phases (red, green, blue) for the customers in the 28-customer network with 6 kW production in phase A with customer 24: no reactive power (left); 12 kvar reactive power consumption (right).

4.10 CONCLUSIONS

A number of mitigation methods have been studies in this chapter and one (coordinated connection) has been studied in the previous chapter.

Reducing the transformer impedance has very limited impact on the overvoltage and on the hosting capacity.

Upgrading the service cables from 10 mm² to 25 mm² has a big impact for most customers. However, this upgrading only improves the voltage for the customers with PV; it does not do anything in reducing the impact on other customers.

Upgrading the feeder cable has additional positive impact on the voltage both for customers with PV and for other customers.

The use of an on-line tap changer with the distribution transformer has the ability to increase the hosting capacity. The resulting increase strongly depends on the voltage control algorithm used and the corresponding settings. The risk of overvoltage should be balanced against the risk of undervoltage during periods with high consumption. Simulations in Chapter 3 have shown that the range in voltage (difference in voltage magnitude between the highest and lowest phase-to-neutral voltage for any of the customers) remains within 20% up to almost all customers with PV. This implies that it is in theory possible to increase the hosting capacity by using a suitable control algorithm. Further studies and algorithm development are needed here.

The use of a switched capacitor bank or shunt reactor on the low-voltage side of the distribution transformer allows for 2.5% extra overvoltage margin with the resulting increase in hosting capacity. Further studies are needed on unintended adverse consequences, especially on the risk that the low-voltage capacitor bank amplifies switching transients originating at higher voltage levels.

Storage with the customers and curtailment of production are solutions that give a serious improvement in overvoltage and increase in hosting capacity. If production can be curtailed to 2.5 kW maximum, all customers can be equipped with single-phase PV.

This reduction is only needed during a limited number of hours per year. No estimation has been made for this specific case of the number of hours per year during which curtailment is needed and how much non-delivered energy this would result in. Local battery storage makes it less disruptive for the customer (most of the energy can be sold later) but from the grid viewpoint, it is the same.

A control algorithm for curtailment needs to be developed; an algorithm where curtailment starts whenever the voltage comes close to the overvoltage limit is a suitable candidate to be studied first. The present role of the overvoltage protection of the PV installation should be considered here as well. To avoid uncontrolled islanding, PV inverters are disconnected whenever the voltage exceeds 111% of nominal for more than one minute (in Sweden, other countries may have different settings). The consequence is that the inverters will start tripping whenever the 10-minute rms voltage moves towards 110%, as one-minute values are somewhat higher than ten-minute values. This is not a desired method, but it does protect the customers against overvoltage.

Storage near the distribution transformer and reactive-power control at the inverter terminals are no suitable solutions.

Coordinated connection (connecting the single-phase inverter to the phase with the lowest pre-connection voltage) is a good and simple way of allowing much more

single-phase PV to be connected. The simulations used the voltage during high production, low consumption and high background voltage, to compare with. This voltage is typically not available during the installation of a single-phase PV inverter. Some guidelines need to be developed on how to determine the "phase with the lowest voltage" in a fast and easy way.

Despite these uncertainties, it is recommended to start propagating this method, as there are no indications that coordinated connection could result in worse voltage quality than random connection.

5 Measurements

This chapter presents the measurements that were done as part of this project, including a limited amount of analysis of the measurement data.

5.1 MEASUREMENT SETUP

Measurements have been performed of voltage and power at a number of locations:

- With one domestic customer in the 28-customer network. This customer is connected through an 89-m service cable to bus 9. Its transfer-impedance properties are most similar to CB13 in the example network.
- With one domestic customer in the 6-customer network. This is customer CB6 in the example network.
- With PV installation 1; a single-phase installation with 2.5 kW rated power.
- With PV installation 2; a three-phase installation with 20 kW rated power.

The locations of the two PV installations and the two example networks are shown in Figure 5-1.

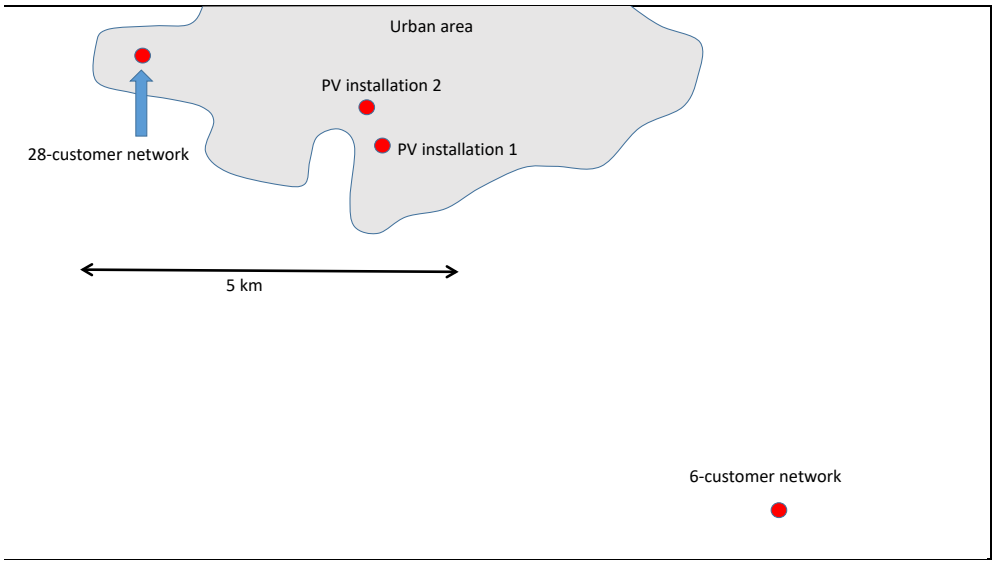

Figure 5-1. Location of the two example networks and the two PV installations. The grey area in the figure is the build-up area of a Swedish city.

5.2 URBAN NETWORK - 2016

Measurements were performed with one of the customers in the 28-customer suburban network in the period 17 August through 12 October 2016. 10-minute values were used for the analysis for active power, reactive power and voltage in the three phases.

5.2.1 Variations over the whole measurement period

The variations in active power, reactive power and voltage, over the whole measurement period, are shown in Figure 5-2, Figure 5-3, and Figure 5-4. The figures show a slight increase in consumption towards the end of the measurement period, associated with a slight decrease in the voltage magnitude. This could be due to the increased use of electric heating when it gets colder. The data also shown an increase in spread in the blue-phase reactive power, towards the end of the measurement period. There is no clear explanation for this, but as this increase corresponds clearly with the increase in active-power consumption there may also here be a relation with the increased use of electric heating.

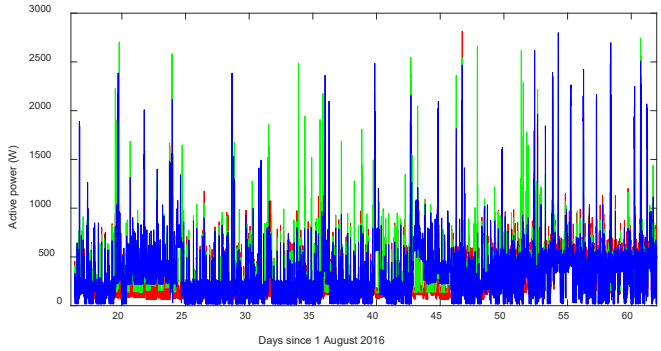

Figure 5-2. Active power versus time, over the whole measurement period. The three colours refer to the three phases.

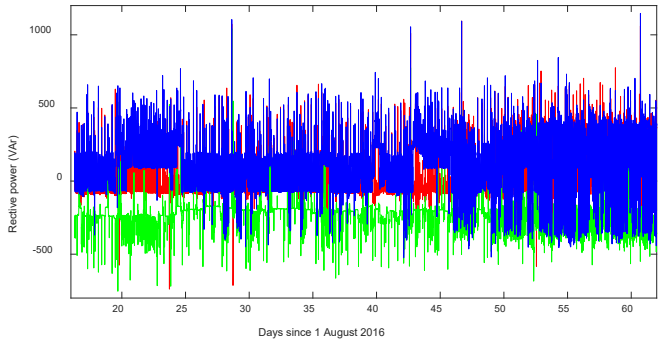

Figure 5-3. Reactive power versus time, over the whole measurement period.

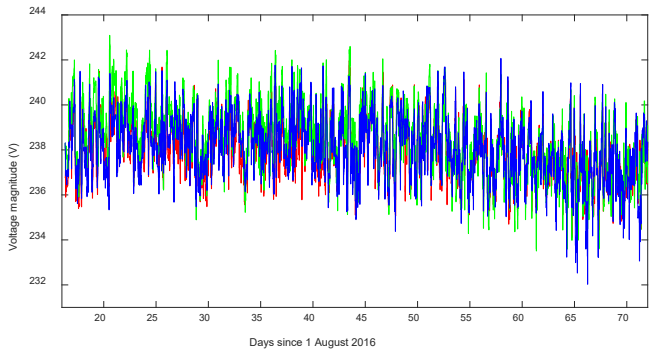

Figure 5-4. Voltage magnitude (10-minute rms) versus time.

5.2.2 Variations versus time of day

The same data has been plotted in a different way in Figure 5-5 and Figure 5-6. In this case, the horizontal axis gives the time of day. The figures show that the voltage has no obvious correlation with the time of the day. Power consumption is bigger in the morning and in the late afternoon and evening hours.

Important for estimating the hosting capacity for PV are the lowest values of the power consumption and the highest values of the voltage. These are independent of the time of day.

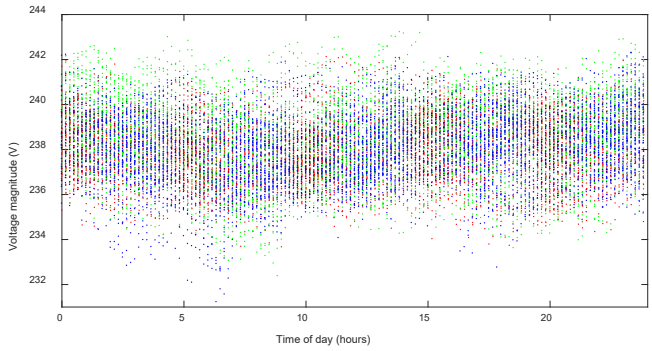

Figure 5-5. Voltage magnitude versus time of day, for a customer in the 28-customer network.

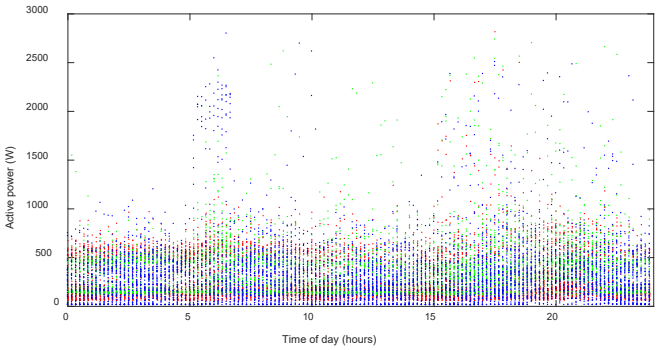

Figure 5-6. Active power versus time of day, for a customer in the 28-customer network.

5.2.3 Probability distribution of the active power

The probability distribution function of the active power for this customer, over the whole measurement period, is shown in Figure 5-7. The active power in the green phase is somewhat higher than in the other two phases, but the difference is small. Statistical indicators obtained from this probability distribution function are shown in Table 5-1.

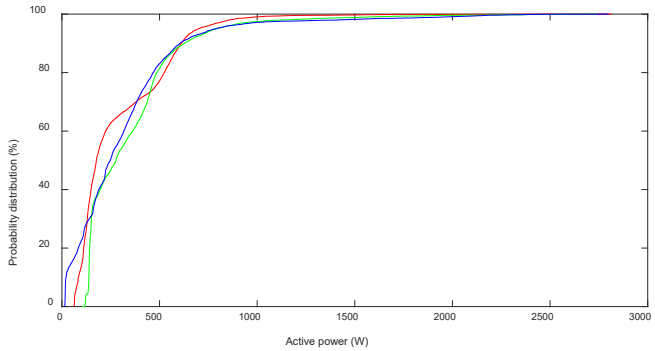

Figure 5-7. Probability distribution of the active power in the three phases, over the whole measurement period.

Table 5-1. Table 51. Statistical indicators of the consumed active power per phase

	Mean	Min	5%	10%	50%	90%	95%	99%	Max
P1	290 W	59 W	70 W	85 W	176 W	612 W	700 W	985 W	2816 W
P2	350 W	102 W	134 W	138 W	277 W	627 W	791 W	1555 W	2740 W
P3	316 W	14 W	17 W	21 W	248 W	604 W	789 W	1950 W	2800 W

5.2.4 Active power versus time of day and time of year

The variations with time of day and time of year, of the active-power consumption are shown in Figure 5-8, Figure 5-9 and Figure 5-10. The values are translated into a colour scheme, where dark blue is lowest and red is highest value. With some minor exceptions, the consumption is lowest during the middle of the day, during summer.

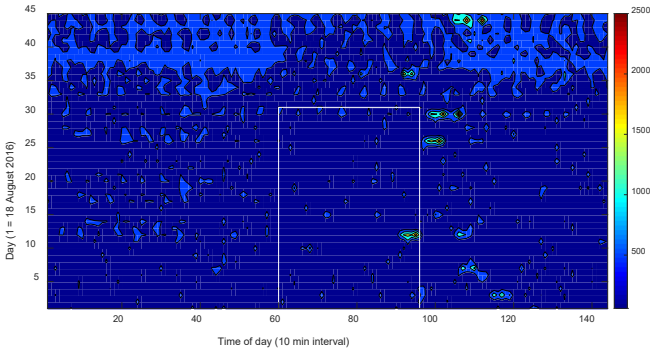

Figure 5-8. Colour-contour chart of consumption in phase A in Watt. The horizontal scale gives the number of 10-minute intervals; where 60 is 10 am, 72 is noon, 84 is 2 pm, 96 is 4 pm. The white box indicates the period during which high solar-power production can be expected.

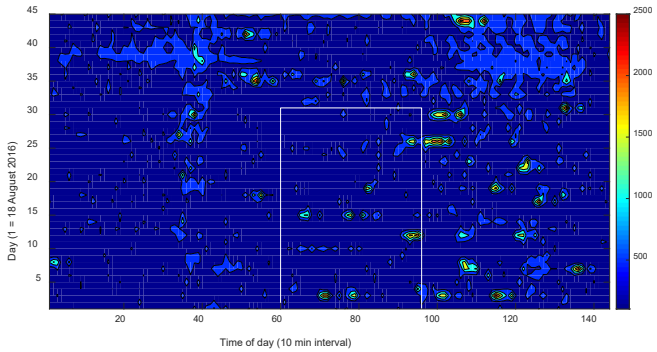

Figure 5-9. Contour-colour chart of consumption in phase B in Watt.

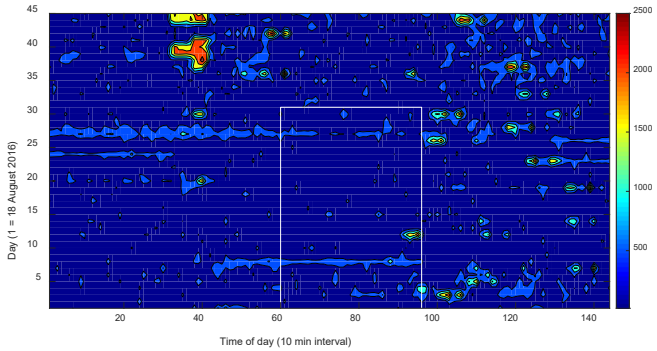

Figure 5-10. Contour-colour chart of consumption in phase C in Watt.

5.2.5 Voltage magnitude variations

Probability distribution functions for the phase-to-neutral voltages are shown in Figure 5-11. Variations with time of day and time of year are shown in Figure 5-12, Figure 5-13 and Figure 5-14. Lower voltages occur more often in the evening hours and towards the end of the measurement period.

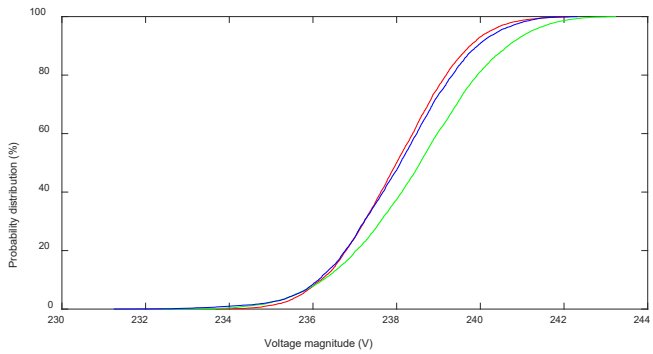

Figure 5-11. Probability distribution of the voltage magnitude in the three phases; whole measurement period.

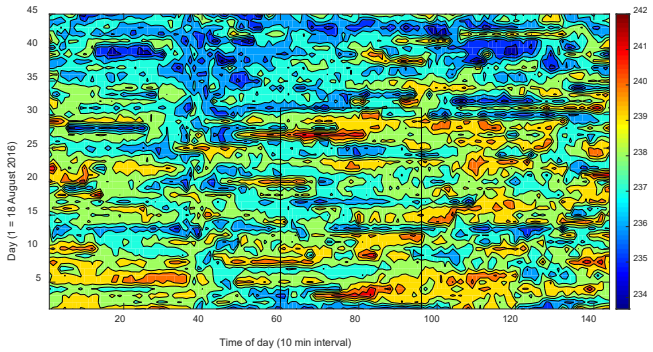

Figure 5-12. Contour-colour chart for the voltage magnitude in phase A.

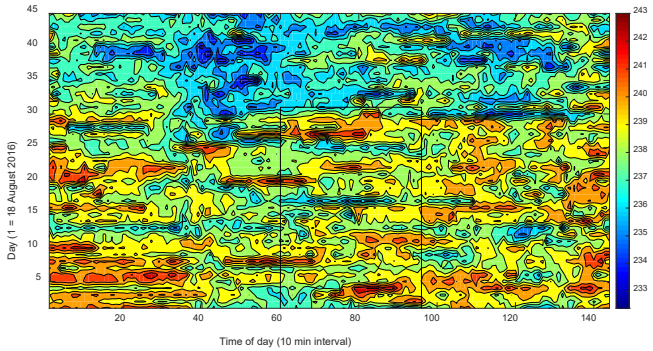

Figure 5-13. Contour-colour chart for the voltage magnitude in phase B.

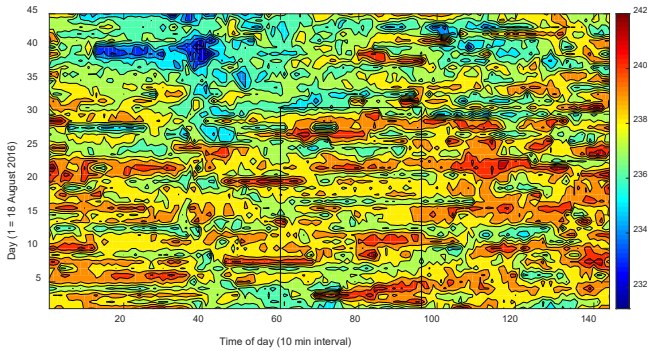

Figure 5-14. Contour-colour chart for the voltage magnitude in phase C.

5.2.6 Relation between voltage and active power consumption

Voltage and active power consumption, for the customer in the 28-customer network, are plotted against each other in Figure 5-15. A light reducing trend is visible, related to the resistive part of the source impedance. The figure also shows that the voltage variations with this customer are mainly due to other customers and only to a limited extent to the load variations by the customer itself.

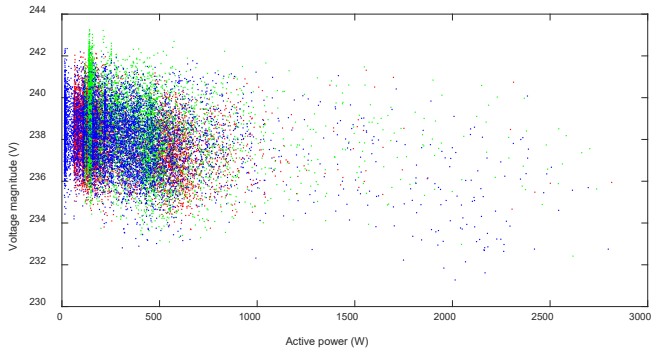

Figure 5-15. Relation between active power and voltage magnitude.

5.2.7 Consumption around the middle of the day

In the studies presented in Chapter 3 and Chapter 4, probability distribution functions have been assumed for the consumption. The same probability distribution function has been assumed for all customers, i.e. equal to the one for the customer at which the measurements were performed. As we are interested in the hours during which the solar-power production is expected to be high, we only consider measurement points between 10 am and 4 pm, and during the first 30 days of the measurement period. These are the values within the white area in the figures shown in Section 5.2.4.

The probability distribution function obtained from only these data is shown in Figure 5-16. As shown in Figure 5-17, this distribution is different from the one based on values over the whole measurement period. The consumption during the sunny hours is clearly less; this will make that the impact of solar power on overvoltage would be underestimated if the data over the whole measurement period had been used.

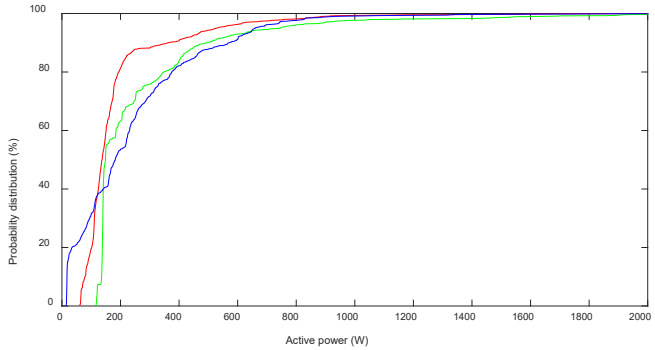

Figure 5-16. Probability distribution of the active power during the hours around noon, middle of August though middle of September.

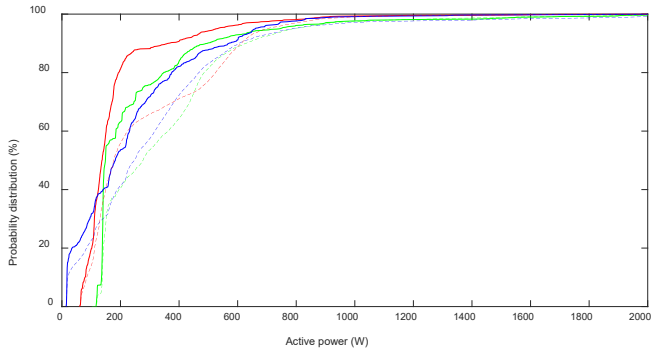

Figure 5-17. Probability distribution function of the active power during the first month of measurement around noon (solid lines) with the one during the whole measurement period (dashed lines).

In Chapter 3 of this report, a probability distribution function of the consumption has been used to estimate the risk of overvoltage. What matters for this, are low values of consumption during the hours in which high production of solar power can be expected. The maximum production will occur over a period of one to two hours, so that short-duration peaks in consumption do not reduce the risk of overvoltage. However, on the other hand, short duration drops in consumption do increase the risk of overvoltage. The other way around, short duration peaks in consumption will increase the risk of undervoltage.

A different distribution for the "background consumption" therefore have to be used to assess the risk of overvoltage than to assess the risk of undervoltage.

In Figure 5-18, the probability distribution functions for the highest and lowest 10-minute values per hour are shown. There is a big difference between these two distributions. One of the conclusions from this is that hourly value are not a good base for calculating the hosting capacity when 10-minute rms voltages are used in the performance criterion.

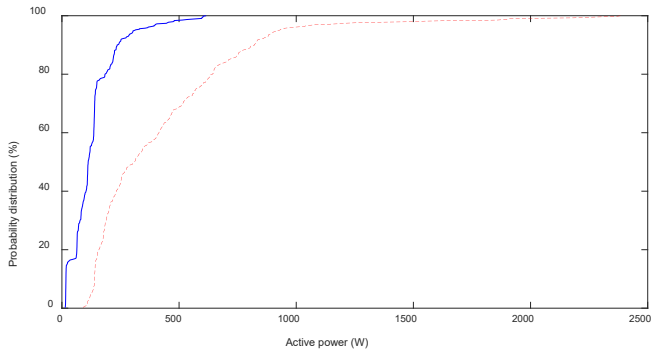

Figure 5-18. Distribution of the highest and lowest 10-minute value of the active power during a one-hour window.

To assess the risk of overvoltage (where it is the lowest consumption that matters) an appropriate distribution is [0, 250 W]. A uniform distribution over this interval has been used for the overvoltage studies in Chapter 3 and Chapter 4. For the risk

of undervoltage the distribution [100, 1000 W] appears more appropriate. The measurement period did however not cover the whole year; even higher consumption values might well occur even during periods when solar-power production can be high. We will for example see later in this chapter that high solar power production can occur as early in the season as March or April. In the simulations in Section 2.4 (where the risk of undervoltage was estimated), a uniform distribution over the interval [1000 W, 2500 W] has been used.

5.2.8 Voltage magnitude around the middle of the day

In Figure 5-19, the distribution for the rms voltage is compared for the sunny hours of the year and the whole year. The voltage during the sunny hours is generally higher than during the whole measurement period.

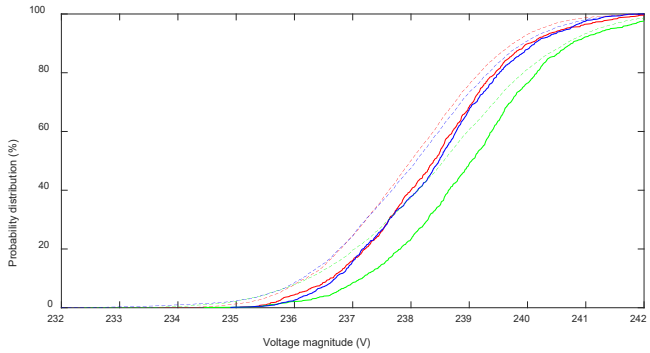

Figure 5-19. Comparison of the distribution of the voltage magnitude during the first month around noon (solid lines) and during the whole measurement period (dashed lines).

The customer at which the measurement has been performed is connected to the cable cabinet through 89 m of service cable with a resistance (phase conductor plus neutral conductor in series) of 3.66 Ω/km. That allows us to estimate the voltages at the cable cabinet, by adding the voltage drop over the cable. The results are shown in Figure 5-20.

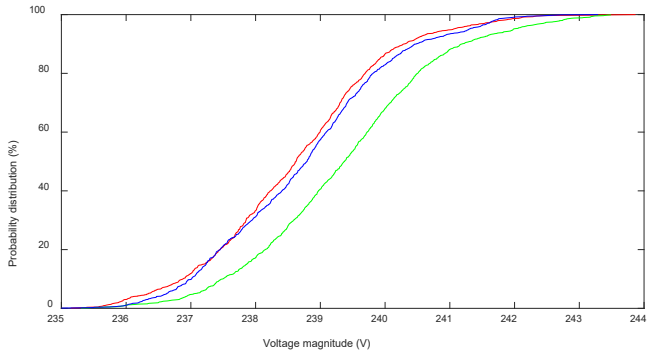

Figure 5-20. Distribution of the voltage during the sunny hours at the cable cabinet. Calculated from measured voltage and active power with the customer at the end of 89 meter of service cable.

This voltage is not the value on the medium side of the transformer, but it is as close as we will come without having to do additional measurements. For the simulations, to generate the background voltage distortion without PV (in Chapter 3), a uniform distribution between 238 V and 242 V has been used.

5.3 MEASUREMENTS IN 6-CUSTOMER NETWORK 2016

Similar measurements as in the 28-customer network have been performed for a customer in the 6-customer rural network. Some of the results from those measurements are presented in this section.

5.3.1 Active power

The active power, in the three phases, is presented in Figure 5-21 as a function of time and in Figure 5-22 versus time of day. Statistics obtained from the probability distribution function are shown in Table 5-2. This customer shows a stable base consumption with peaks that occur especially during daytime and in the evening.

The variation of active-power consumption with time of day and time of year is also shown in Figure 5-23, Figure 5-24 and Figure 5-25. The probability distributions (for the whole measurement period and for the period around noon during the summer months) are shown in Figure 5-26.

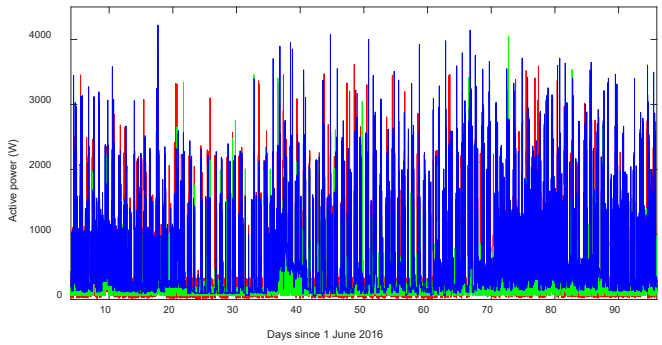

Figure 5-21. Measured active-power consumption for a customer in the 6-customer network.

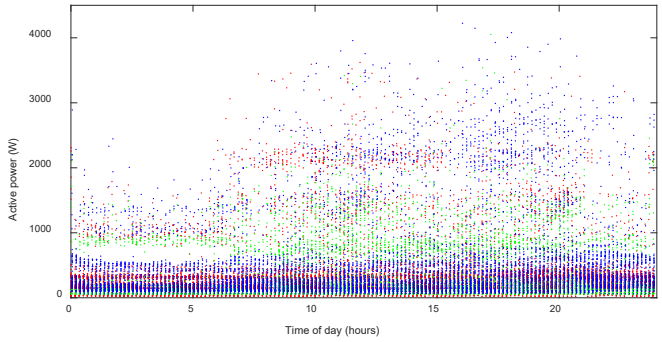

Figure 5-22. Active-power consumption as function of the time of day.

Table 5-2. Statistical indicators of the consumed active power per phase.

	Mean	Min	5-perc	10-perc	50-perc	90-perc	95-perc	99-perc	Max
A	367 W	19 W	39 W	118 W	215 W	849 W	1506 W	2275 W	3620 W
B	272 W	54 W	59 W	60 W	134 W	814 W	1080 W	1616 W	4049 W
C	440 W	55 W	91 W	103 W	214 W	1106 W	2093 W	2817 W	4221 W

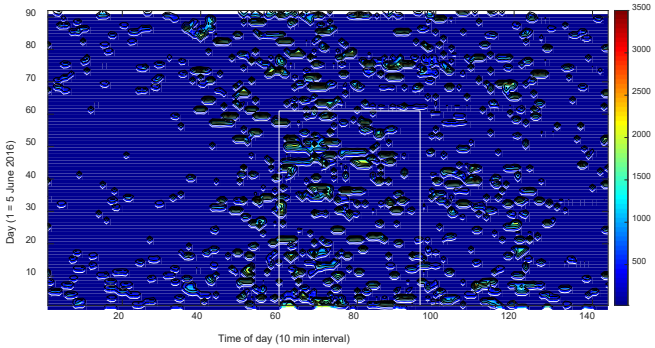

Figure 5-23. Active power for phase A during the day and during the year.

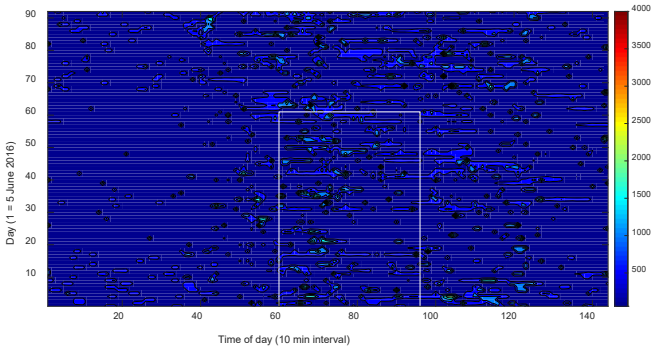

Figure 5-24. Active power for phase B during the day and during the year.

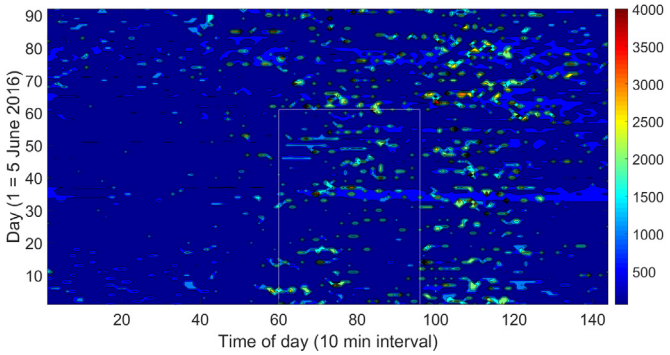

Figure 5-25. Active power for phase C during the day and during the year.

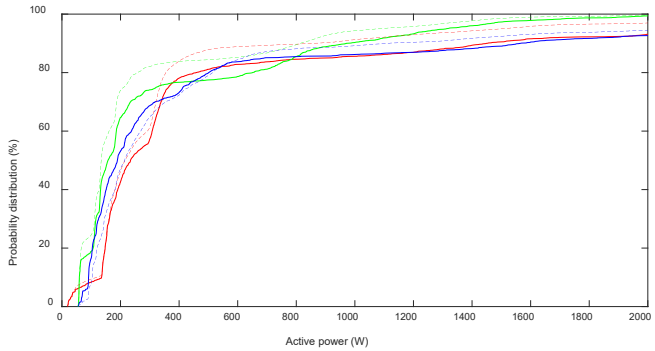

Figure 5-26. Probability distribution function of the active power during the first two months around noon (solid lines) and during the whole measurement period (dashed lines).

The probability distribution functions of the highest and lowest 10-minute values for each hour are shown in Figure 5-27. It is obvious that these two distributions are distinctively different and that using the hourly value would result in inaccurate estimations of the hosting capacity.

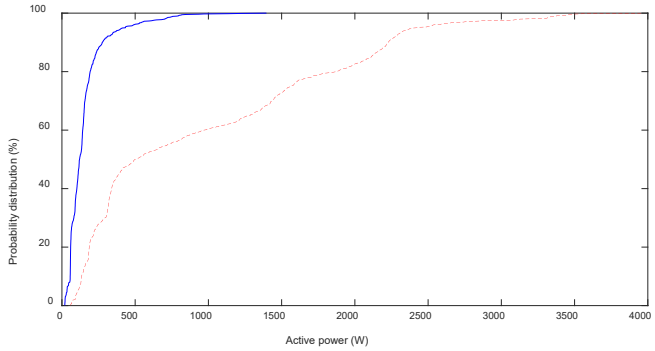

Figure 5-27. Comparing the probability distribution functions for the highest (red dashed) and lowest (blue solid) 10-minute active-power values for a one-hour period during the sunny periods of the year.

Appropriate distributions for the consumption found from this are [0, 250 W] for overvoltage studies, [0, 2000 W] for undervoltage studies. See the comments with the measurements for the customer in the 28-customer network.

5.3.2 Voltage magnitude variations

The voltage magnitude variations, for the customer in the 6-customer network, are shown in Figure 5-28 (as a function of time), in Figure 5-29 (versus time of day) and in Figure 5-30 (as a probability distribution function).

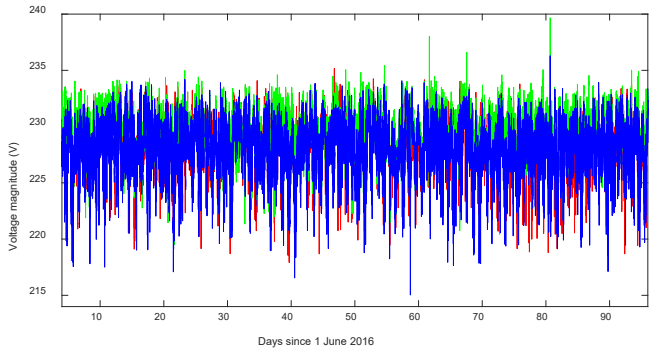

Figure 5-28. Voltage versus time in the three phases, for the customer in the 6-customer network.

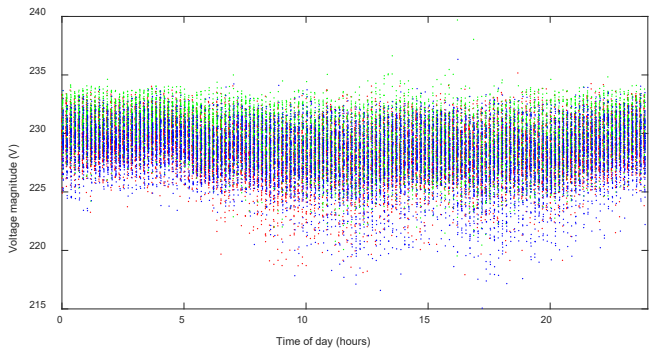

Figure 5-29. Voltage magnitude in the three phases, versus time of day, for the customer in the 6-customer network.

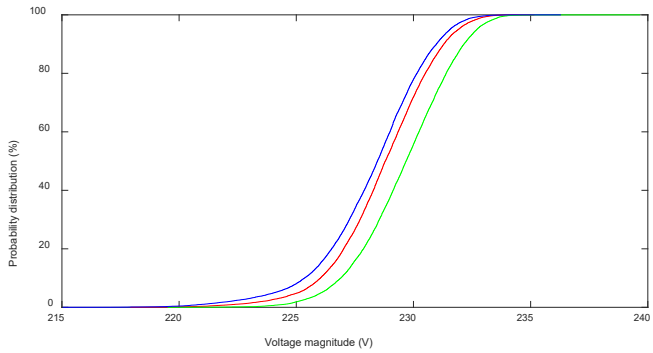

Figure 5-30. Probability distribution function of the voltage magnitude in the three phases, for the customer in the 6-customer network.

5.3.3 Relations between voltage and active-power consumption

The drop in voltage with increasing consumption with this customer is visible in Figure 5-31. As this is a weaker network, the drop is more clearly visible than with the customer in the 28-customer network.

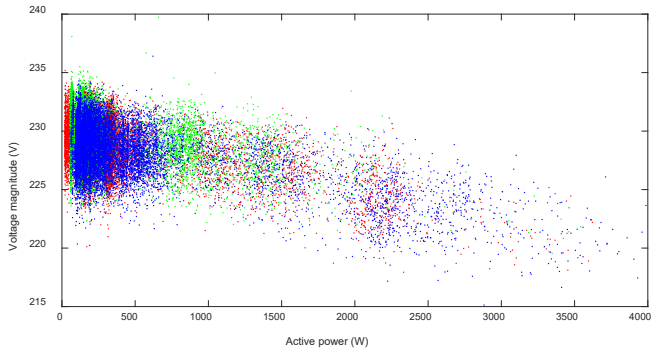

Figure 5-31. Relation between active-power consumption and voltage magnitude.

5.4 RURAL NETWORK - 2017

The voltage measurements for the customer in the rural network were repeated during 2017. Only voltages were measured, no currents. Therefore, no data is available on power consumption. Measurement data was available for the period 15 April through 1 September 2017.

The rms voltage, over each 10-minute window, for the whole measurement period, is shown in Figure 5-32.

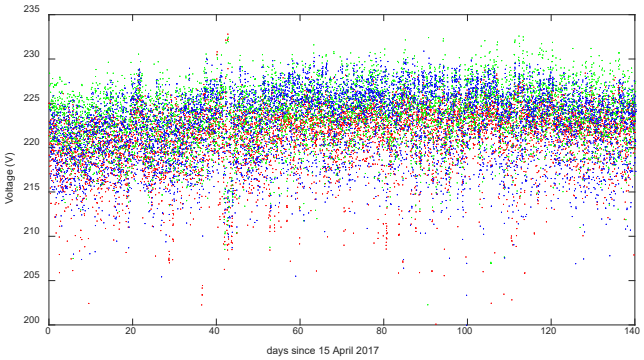

Figure 5-32. Voltage magnitude versus time with the customer in the 6-customer network, for the whole measurement period.

The rms voltage is shows versus time of day in Figure 5-33. The highest voltages are independent of the time of day, but the lowest voltage get lower during the afternoon and evening. It is the highest voltage that matters to estimate the risk of overvoltage.

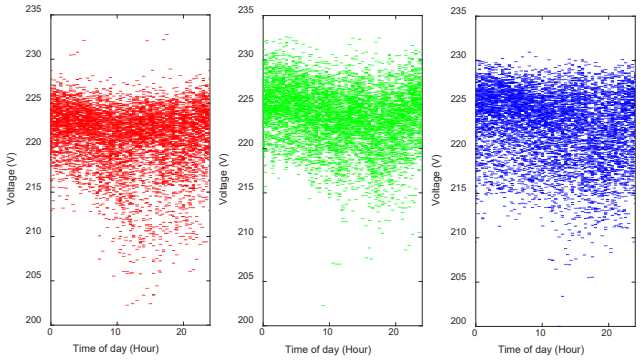

Figure 5-33. Voltage magnitude versus time of day, for the whole measurement period. The three subplots refer to the three phases.

The probability distribution functions of the rms voltages in the three phases are shown in Figure 5-34. Voltages outside of the range 210 V to 230 V are uncommon.

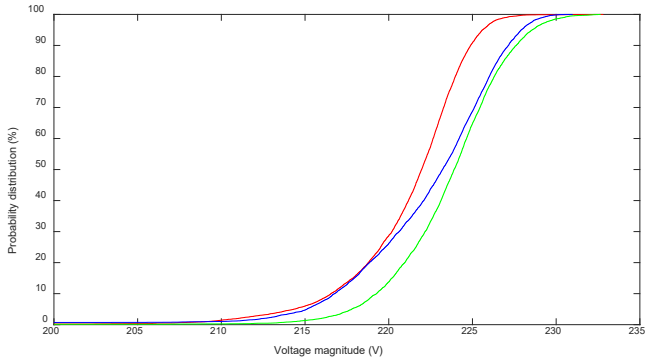

Figure 5-34. Probability distribution (CDF) of the rms voltage, for the whole measurement period.

5.5 PRODUCTION AT LOCATION 1, 2016

The solar power production was obtained[11] during the period June 1st through 3 September 2016, 10-minute averages of both active and reactive power. The active power production as a function of time is shown in Figure 5-35; the reactive-power production in Figure 5-36. The reactive power cannot be neglected (being between 60 and 140 var), but as the resistive part of the grid by far dominates over the reactive part, the reactive power will have a negligible impact on the voltage variations due to solar power.

The active-power and reactive power are shown as a function of the time of day in Figure 5-37 and Figure 5-38, respectively. Both figures show a clear daily variation. The relation between active and reactive power (Figure 5-39) shows a minor decay in reactive power with increasing amount of active power.

[11] Both location 1 and 2 are permanently monitored with a high time resolution. The data presented here has been extracted from the database to correspond with periods at which measurements were performed with two domestic customers.

Figure 5-40 presents how the maximum production per day varies throughout the year. There are clearly “good days” and “bad days” for solar-power production at this location. However, high production can occur anywhere during the measurement period. This is an important observation for hosting capacity studies, as it implies that the highest overvoltage also can occur anywhere during this period.

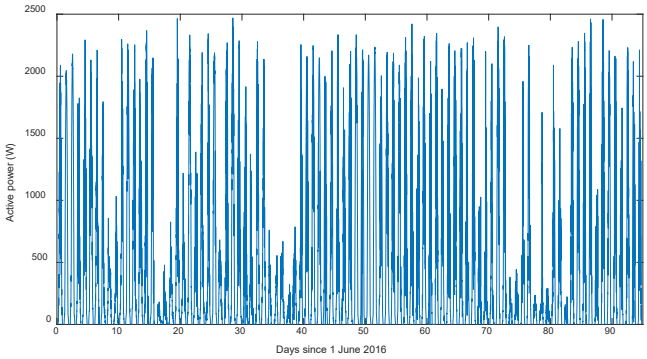

Figure 5-35. Active power production (10-minute averages) at location 1.

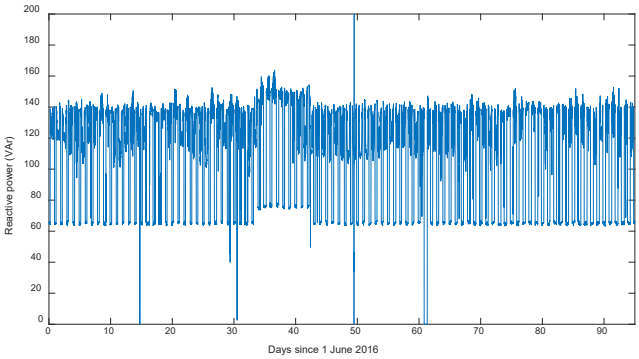

Figure 5-36. Reactive power production (10-minute averages) at location 1. Note the different vertical scale compared to Figure 5-35.

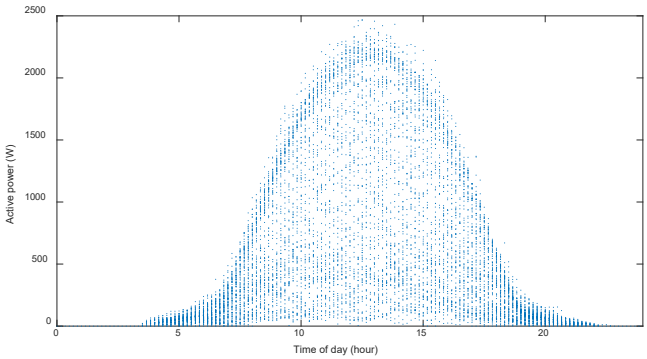

Figure 5-37. Active power production (10-minute averages) versus time of day, at location 1.

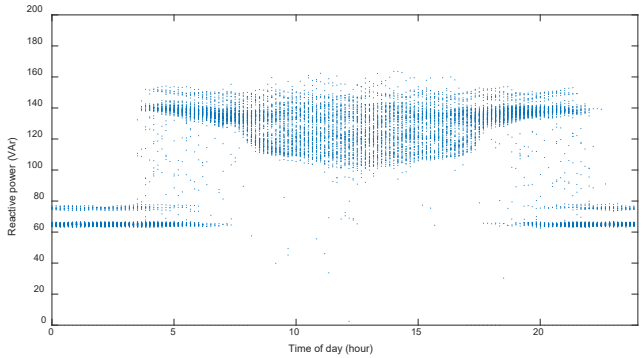

Figure 5-38. Reactive power production (10-minute averages) versus time of day, at location 1.

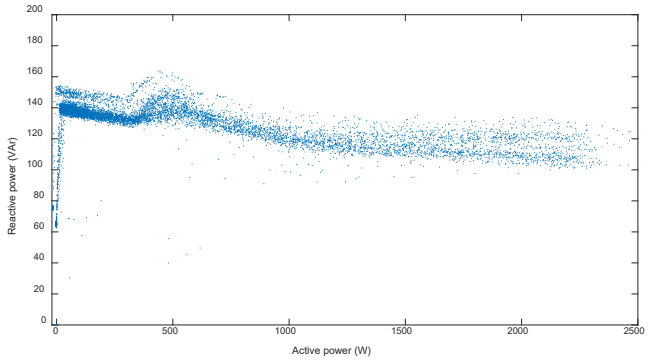

Figure 5-39. Active versus reactive power (10-minute averages), at location 1.

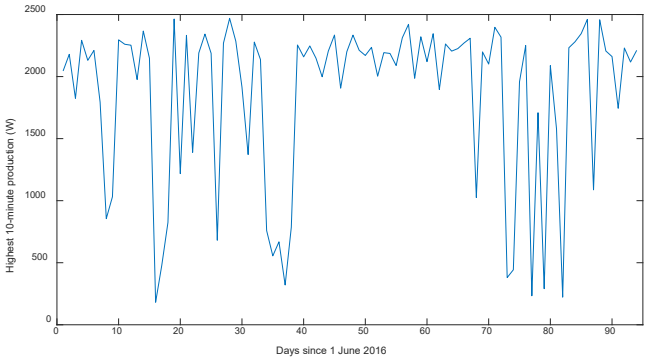

Figure 5-40. Highest 10-minute average production per day, between 1 June and 15 September 2016, at location 1.

5.6 PRODUCTION – LOCATION 1, 2017

The measurements of the production at location 1 have been repeated during spring and summer 2017. The active power production as a function of time is shown in Figure 5-41.

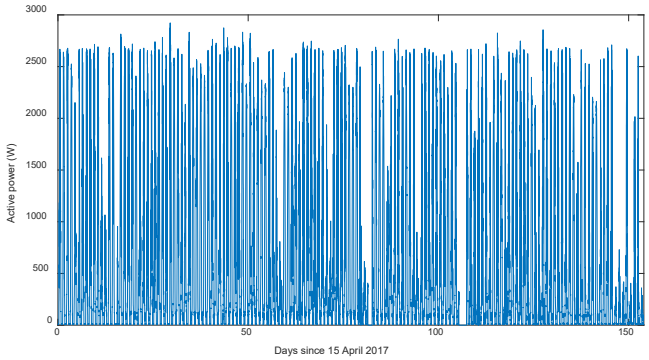

Figure 5-41. Active power production (10 minute averages) at location 1 during 2017.

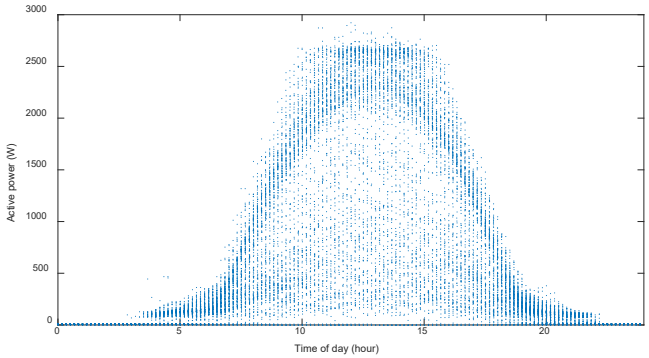

Figure 5-42. Active power production (10 minute averages) as a function of time of day at location 1 during 2017.

The highest daily 10-minute average value has been calculated and is shown in Figure 5-43. High production can occur throughout the period and tends to be even somewhat higher during March and April than during summer. This is possibly due to the lower temperatures resulting in an increased efficiency. The period during which the highest production can occur reaches at least from middle of April through early September.

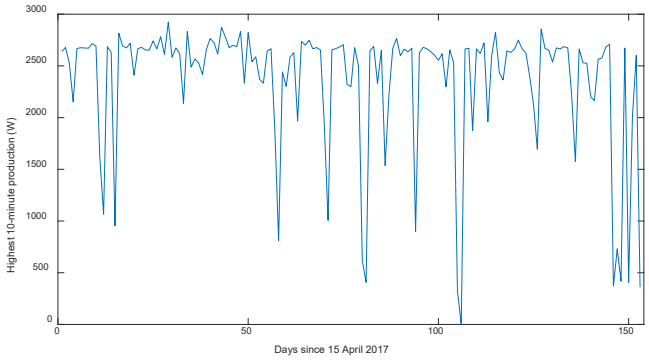

Figure 5-43. Highest 10-minute average per day, between 15 April and 15 September 2017.

5.7 PRODUCTION – LOCATION 2, 2016

The active power as a function of time is shown in Figure 5-44 for the period 1 June through 13 September 2016. The distance between location 1 and location 2 is about 500 m, so that a high correlation is expected between the 10-minute production values.

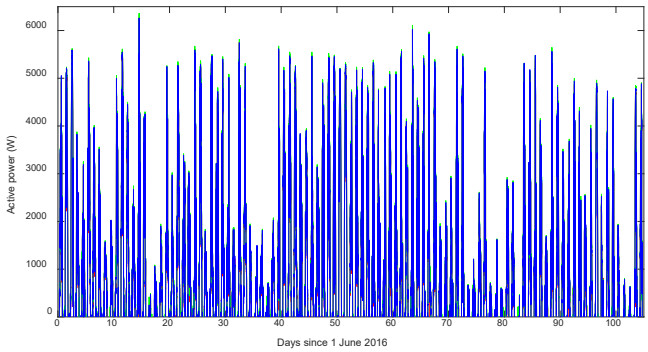

Figure 5-44. Active power production per phase (10-minute averages) at location 2; 1 June through 13 September 2016.

Location 2 is a three-phase installation. The power unbalance is defined here as the difference between the highest production per phase and the lowest production per phase, over each 10-minute interval. This power unbalance is shown in Figure 5-45 versus the total produced power (sum of the power over the three phases). The figure shows that the power unbalance is especially large during low production, where only one or two phases are active. The power unbalance is however never more than 3.4% of the maximum production. The figure also shows that the production in the three phases is rarely exactly equal; for production above about 2 kW, an unbalance of 50 to 100 W remains.

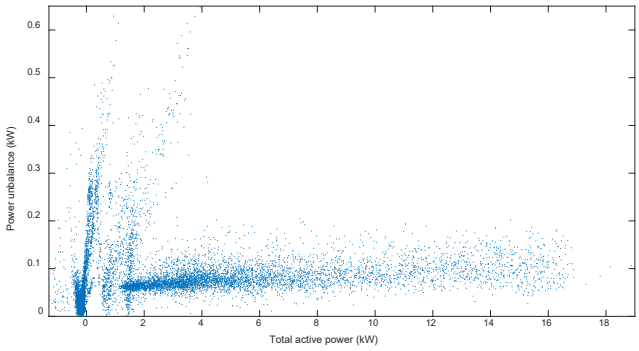

Figure 5-45. Relation between power unbalance and total active power (10-minute averages) at location 2.

Figure 5-46 shows the total active power production (the sum of the production in the three phases) versus time of day. The same daily pattern is visible as for the production at location 1. Figure 5-47 shows the highest daily 10-minute value of

production for each day during the measurement period. High values are obtained throughout the measurement period.

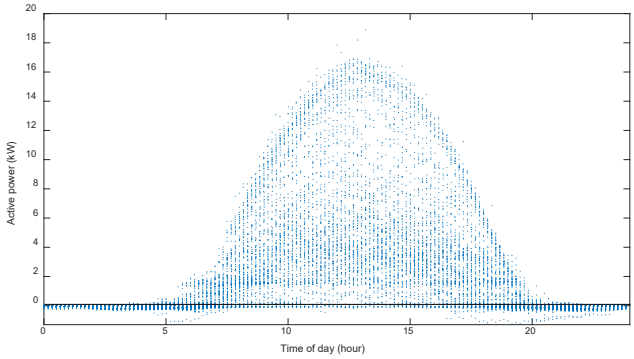

Figure 5-46. Total active power production (10-minute averages) versus time of day, at location 2.

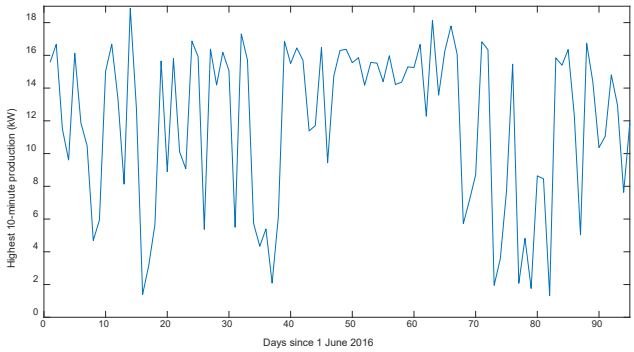

Figure 5-47. Highest 10-minute average production per day, between 1 June and 15 September 2016, at location 2.

The production at the two locations in compared in Figure 5-48. For reasons yet unknown, the production at location 2 is often a lot higher than at location 1 (in percent of the maximum production at that location). The opposite situation is less common. The comparison is made, as a function of time, in Figure 5-49 during five consecutive days.

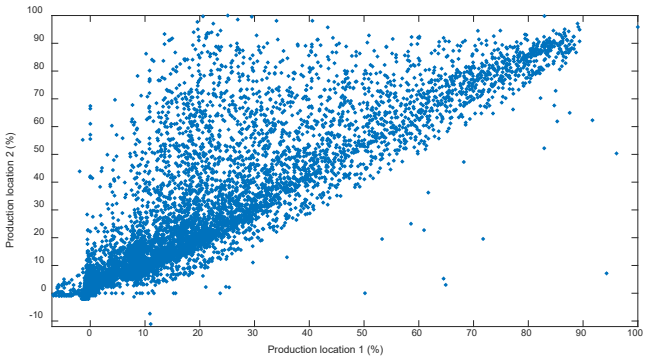

Figure 5-48. Correlation between production at location 1 and at location 2 (both in percent of the maximum production at that location).

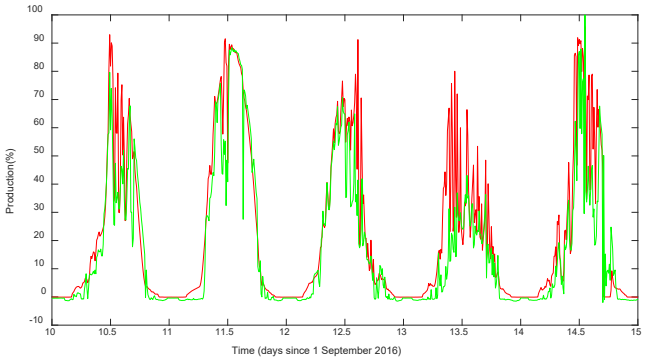

Figure 5-49. Comparison in production between location 1 (green) and location 2 (red) during five consecutive days.

In Figure 5-50, the comparison is made in a somewhat different way. The horizontal axis is the sum of the percentage values (percent of maximum production) for each of the two locations. The two installations are (mathematically) scaled to represent the same size of installation. The vertical axis is again the production at location 2. The diagonal line corresponds to the case where the combined production would be twice the production from one installation. Due to the diversity between the two installations, the maximum of the total production is less than the sum of the maxima (each at 100%). The maximum of the total is 97.9%. The error for the worst case of the assumption that different installations produce the same amount of power at any moment is small.

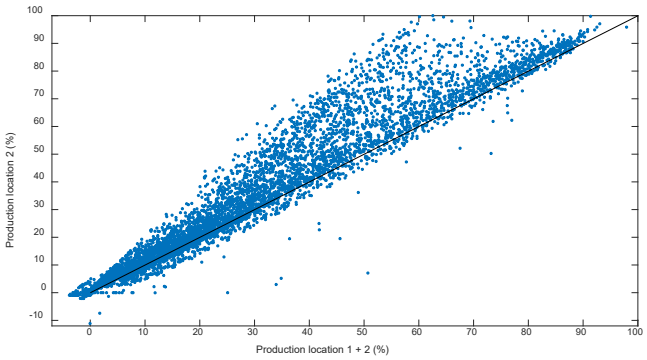

Figure 5-50. Comparing the sum of the production at the two locations (horizontal scale) with the production at location 2 (vertical scale).

5.8 CONCLUSIONS

The measurements presented in this chapter show that different distributions have to be used for considering the risk of overvoltage and for considering the risk of undervoltage. Highest and lowest 10-minute values during a period of a few hours around noon during summer hours are needed for this. From the measurements with two customers (10-minute values), the following ranges were concluded:

For overvoltage studies a consumption between 0 and 250 W, and a no-load voltage between 238 V and 242 V.

For undervoltage studies a consumption between 1000 and 2500 W, and a no-load voltage between 232 V and 236 V.

The probability distribution function for voltage and power should be considered during the sunny periods of the year (the hours around noon, April through August), not over the whole year. It is also shown that the hourly data is not appropriate for hosting capacity studies considering overvoltage and undervoltage.

The measurements of power production show that high levels of production can occur during any day in the period April through August.

The two production units, at a distance of about 500 m from each other, show a strongly correlated but not the same production at a 10-minute time scale.

6 Calculation of new time series

This chapter contains the results of some simulations where the time series data from Chapter 5 has been used as input. The measured voltages, without solar power, have been combined with the produced power to calculate the voltage in the case with solar power.

6.1 RURAL NETWORK - 2016

Time series for the 6-customer network, summer 2016, were available over the following periods, 10-minute averages.

- Voltage in the three phases for customer 6 in the six-customer network, 4 June 13:10 through 5 September 08:20.
- Power produced by a 2.5-kW solar power installation, 1 June 00:00 through 3 September 23:50

The overlapping period (4 June 13.10 – 3 September 23:50) was used to obtain time series of voltage variations for customer 6 with increasing amount of solar power.

The measurement values were scaled by multiplication with a constant factor such that the maximum production equalled 6 kW.

Results are shown in Figure 6-1 and Figure 6-2 for a single-phase installation connected with customer 6 in phase A. There is a significant rise in voltage in phase A and a minor drop in the two other phases.

The probability distribution functions are shown in Figure 6-3 and some statistical indicators in Table 6-1. For phase A, the voltage rise is especially visible for maximum and 95th percentile. But even minimum and 5th percentile show an increase.

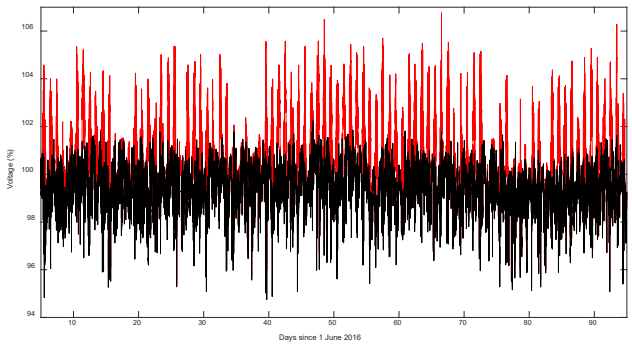

Figure 6-1. Voltage in phase A for customer 6, during summer 2016, measured without solar power (black) and calculated with 6 kW solar power connected locally in phase A (red).

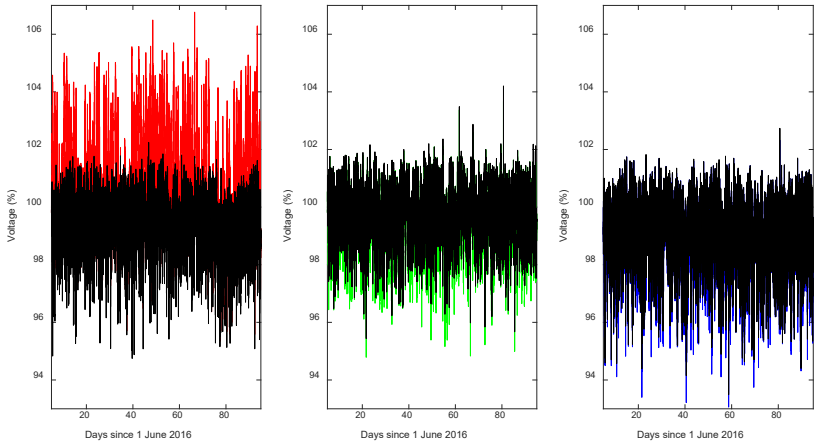

Figure 6-2. Voltage in phase A, B and C (left to right) for customer 6, during summer 2016, measured without solar power (black) and calculated with 6 kW solar power connected locally in phase A (red, green, blue).

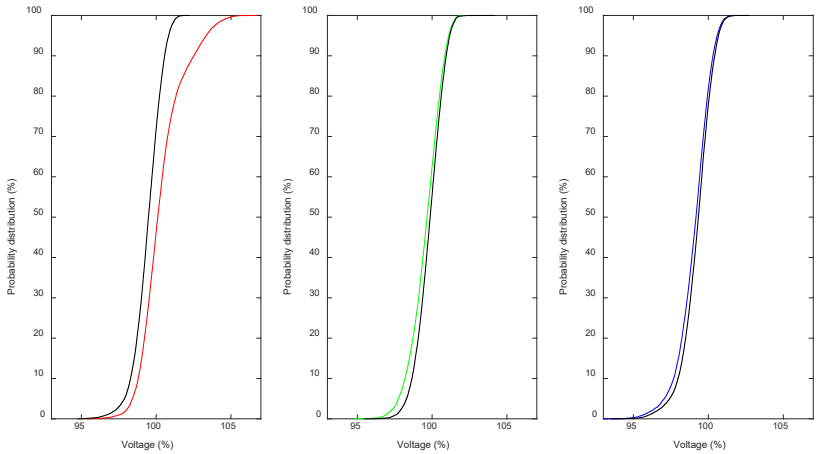

Figure 6-3. Probability distribution (CDF) of the voltage in phase A, B and C (left to right) for customer 6, during summer 2016, measured without solar power (black) and calculated with 6 kW solar power connected locally in phase A (red, green, blue).

Table 6-1. Statistical values of the calculated voltages with customer 6 due to connection of 6 kW solar power, locally in phase A (the values between brackets are the changes compared to the situation without PV).

	Minimum	5th percentile	95th percentile	maximum
Phase A	95.3% (+0.6%)	98.4% (+0.5%)	103.3% (+2.5%)	106.8% (+4.5%)
Phase B	94.8% (-0.7%)	97.7% (-0.5%)	101.1% (-0.1%)	103.7% (-0.5%)
Phase C	93.1% (-0.4%)	97.1% (-0.4%)	100.6% (-0.1%)	102.3% (-0.4%)

Next, the calculations are repeated for the situation with one and two of the neighbours on the same cable cabinet (CB4 and CB5) also having a 6-kW PV

installation, also single-phase connected. It is assumed that the production from the three PV installations follows exactly the same variation with time.

The second case considered is for a 6-kW PV connected to phase A with both customer 5 and 6. The results are shown in Figure 6-4 and Table 6-2. The maximum and the 95th percentile in phase A show a further increase compared to Table 6-1; the minimum and 5th percentile are increased less.

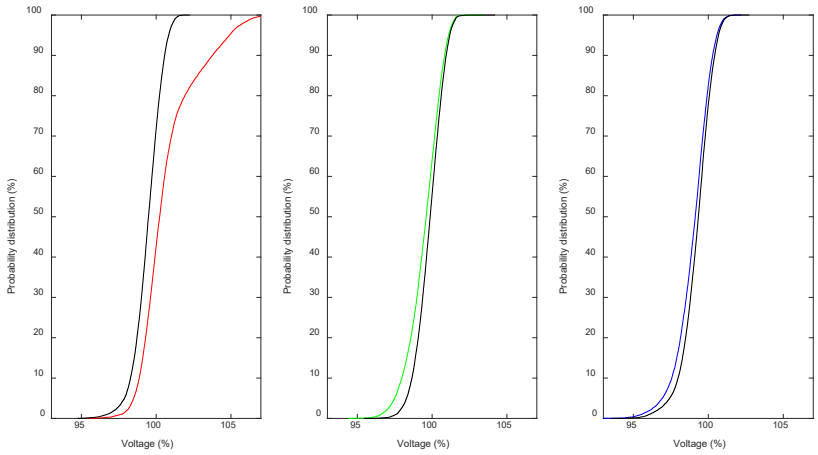

Figure 6-4. Probability distribution (CDF) of the voltage in phase A, B and C (left to right) for customer 6, during summer 2016, measured without solar power (black) and calculated with 6 kW solar power connected with customers 5 and 6 in phase A.

Table 6-2. Statistical values of the calculated voltages with customer 6 due to connection of 6 kW solar power, with customer 5 and 6 in phase A (the values between brackets are the changes compared to the situation without PV).

	Minimum	5th percentile	95th percentile	maximum
Phase A	95.4% (+0. 7%)	98.5% (+0.6%)	104.9% (+4.1%)	108.8% (+6.5%)
Phase B	94.4% (-1.0%)	97.5% (-0.8%)	101.1% (-0.1%)	103.5% (-0.7%)
Phase C	92.9% (-0.6%)	96.9% (-0.5%)	100.6% (-0.1%)	102.2% (-0.5%)

The third case considered is again for 6 kW PV with customer 5 and 6, but now in phase A for customer 6 and in phase B for customer 5. The voltages are again calculated for customer 6. The results are shown in Figure 6-5 and Table 6-3. Comparing with Table 6-2 shows among others that the PV with customer 5 slightly reduces the overvoltage for customer 6.

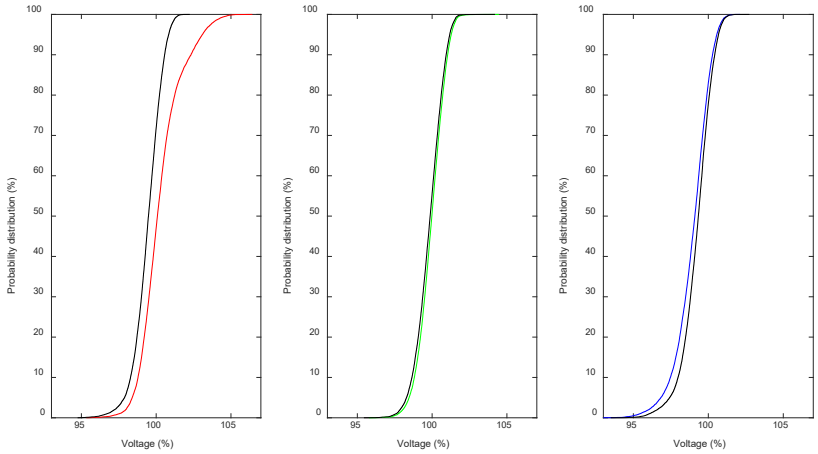

Figure 6-5. Probability distribution (CDF) of the voltage in phase A, B and C (left to right) for customer 6, during summer 2016, measured without solar power (black) and calculated with 6 kW solar power connected with customer 5 in phase B and with customer 6 in phase A.

Table 6-3. Statistical values of the calculated voltages with customer 6 due to connection of 6 kW solar power, with customer 5 in phase B and with customer 6 in phase A (the values between brackets are the changes compared to the situation without PV).

	Minimum	5th percentile	95th percentile	maximum
Phase A	95.3% (+0. 6%)	98.4% (+0.6%)	103.1% (+2.3%)	106.4% (+4.2%)
Phase B	95.8% (+0.3%)	98.5% (+0.2%)	101.3% (+0.1%)	104.5% (+0.3%)
Phase C	92.7% (-0.8%)	96.8% (-0.6%)	100.6% (-0.1%)	102.1% (-0.6%)

Case number four concerns PV with customers 4, 5 and 6, all of 6 kW size, all in phase A. The results are shown in Figure 6-6 and Table 6-4. The voltage rise (in phase A) and the voltage drop (in phase B) further increase compared to Table 6-2.

Table 6-4. Statistical values of the calculated voltages with customer 6 due to connection of 6 kW solar power, with customer 4, 5 and 6 in phase A (the values between brackets are the changes compared to the situation without PV).

	Minimum	5th percentile	95th percentile	maximum
Phase A	95.5% (+0.7)	98.5% (+0.7%)	106.5% (+5.6%)	110.7% (+8.5%)
Phase B	94.0% (-1.5%)	97.2% (-1.1%)	101.1% (-0.1%)	103.3% (-0.9%)
Phase C	92.6% (-0.9%)	96.8% (-0.6%)	100.6% (-0.1%)	102.1% (-0.7%)

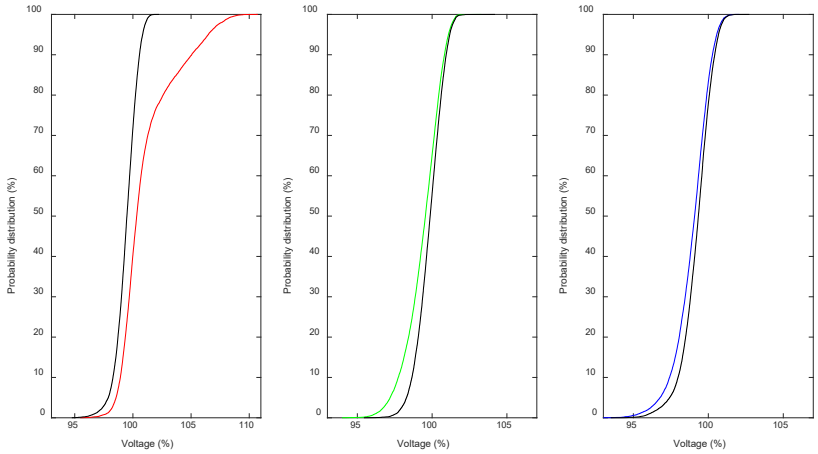

Figure 6-6. Probability distribution (CDF) of the voltage in phase A, B and C (left to right) for customer 6, during summer 2016, measured without solar power (black) and calculated with 6 kW solar power connected with customer 4, 5 and 6 in phase A. Note the difference in horizontal scale with the left-hand plot.

With the fifth and final case, again three PV installations are installed with customers 4, 5 and 6. However, in this case they are spread over the three phases: phase A with customer 6; phase B with customer 5; phase C with customer 4. The results are shown in Figure 6-7 and Table 6-5. The voltage rise is less than when all installations are connected to the same phase; also is there no longer any voltage drop.

Table 6-5. Statistical values of the calculated voltages with customer 6 due to connection of 6 kW solar power, with customer 4, 5 and 6 in phase C, B and A (the values between brackets are the changes compared to the situation without PV).

	Minimum	5th percentile	95th percentile	maximum
Phase A	95.3% (+0.6)	98.4% (+0.5%)	102.7% (+1.8%)	105.9% (+3.7%)
Phase B	95.6% (+0.2%)	98.4% (+0.1%)	101.2% (+0.0%)	104.3% (+0.1%)
Phase C	93.7% (+0.2%)	97.5% (+0.1%)	100.8% (+0.1%)	102.9% (+0.2%)

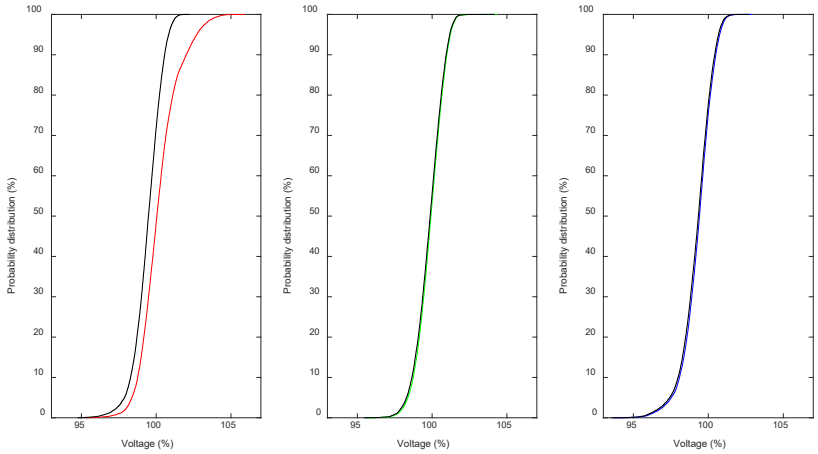

Figure 6-7. Probability distribution (CDF) of the voltage in phase A, B and C (left to right) for customer 6, during summer 2016, measured without solar power (black) and calculated with 6 kW solar power connected with customer 4, 5 and 6 in phase C, B and A.

6.2 RURAL NETWORK – 2017

The calculations over 2016 have been repeated using the data gathered during 2017. Data had been available from 15 April through 15 September. The voltages showed many values that were far below 200 V and sometimes even zero in one or two of the phases. All values below 200 V were removed from the data to enable a comparison with the results from the 2016 data.

Comparisons are made for one, two and three customers with PV, all connected in phase A. The results are shown in Table 6-6 (to be compared with Table 6-1); Table 6-7 (to be compared with Table 6-2), and Table 6-8 (to be compared with Table 6-4).

Table 6-6. Statistical values of the calculated voltages with customer 6 due to connection of 6 kW solar power, locally in phase A (the values between brackets are the changes compared to the situation without PV).

	Minimum	5th percentile	95th percentile	maximum
Phase A	88.0% (+1.0%)	94.2% (+0.9%)	101.2% (+3.1%)	104.4% (+3.2%)
Phase B	87.9% (-0.1%)	94.2% (-0.5%)	99.2% (-0.1%)	101.2% (-0.0%)
Phase C	86.0% (-1.0%)	93.4% (-0.3%)	99.0% (-0.1%)	100.3% (-0.1%)

Table 6-7. Statistical values of the calculated voltages with customer 6 due to connection of 6 kW solar power, with customer 5 and 6 in phase A (the values between brackets are the changes compared to the situation without PV).

	Minimum	5th percentile	95th percentile	maximum
Phase A	88.0% (+1.0%)	94.3% (+1.1%)	102.9% (+4.8%)	106.4% (+5.2%)
Phase B	87.8% (-0.2%)	94.0% (-0.7%)	99.2% (-0.2%)	101.2% (-0.0%)
Phase C	85.7% (-1.2%)	93.2% (-0.4%)	98.9% (-0.2%)	100.3% (-0.1%)

Table 6-8. Statistical values of the calculated voltages with customer 6 due to connection of 6 kW solar power, with customer 5 in phase B and with customer 6 in phase A (the values between brackets are the changes compared to the situation without PV).

	Minimum	5th percentile	95th percentile	maximum
Phase A	88.0% (+1.0%)	94.1% (+0.9%)	100.9% (+2.8%)	104.1% (+2.8%)
Phase B	88.0% (-0.0%)	94.9% (-0.2%)	99.5% (+0.1%)	101.4% (+0.2%)
Phase C	85.5% (-1.4%)	93.1% (-0.2%)	98.9% (-0.2%)	100.3% (-0.2%)

A comparison between the two years in done in Table 6-9, for one to three customers with PV (6 only; 5 and 6; 4, 5 and 6). In all cases has the inverter been connected to phase A; the statistics in the table are for phase A, i.e. the phase with the biggest increase in voltage. The tables shows that there are large differences between the two years, both in absolute value and in differences compared to the case without PV (shown between brackets in the table). Data from just one year is thus not a good predictor for the values that can be expected the next year. It is not clear if this is due to the differences in voltages with the customer or due to differences in produced power. It is however possible to conclude that drawing conclusions from one year of measurements is difficult.

Table 6-9. Comparison between 2016 and 2017 statistics for one, two and three customers with PV; all voltages are taken in Phase A, where also all inverters are connected.

	Minimum	5th percentile	95th percentile	Maximum
1 PV, 2016	95.3% (+0.6%)	98.4% (+0.5%)	103.3% (+2.5%)	106.8% (+4.5%)
1 PV, 2017	88.0% (+1.0%)	94.2% (+0.9%)	101.2% (+3.1%)	104.4% (+3.2%)
2 PV, 2016	**95.4% (+0.7%)**	**98.5% (+0.6%)**	**104.9% (+4.1%)**	**108.8% (+6.5%)**
2 PV, 2017	**88.0% (+1.0%)**	**94.3% (+1.1%)**	**102.9% (+4.8%)**	**106.4% (+5.2%)**
3 PV, 2016	95.5% (+0.7%)	98.5% (+0.7%)	106.5% (+5.6%)	110.7% (+8.5%)
3 PV, 2017	88.0% (+1.0%)	94.1% (+0.9%)	100.9% (+2.8%)	104.1% (+2.8%)

6.3 RURAL NETWORK – INDEPENDENT SOURCES

As mentioned before, measurements were performed at two locations, at about 500 m distance from each other. The two measurements series were used to estimate how the difference between two production units affects the overvoltage. The results are shown in Table 6-10 which should be compared with Table 6-2.

- The 95th percentile of the voltage in phase A drops from 104.9% to 103.8% when the difference between production units is included.
- The maximum voltage in phase A drops from 108.8% to 107.8% when the difference between production units is included.

Table 6-10. Statistical values of the voltages with customer 6 due to connection of 6 kW solar power, with customer 5 and 6 in phase A (the values between brackets are the changes compared to the situation without PV).

	Minimum	5th percentile	95th percentile	maximum
Phase A	95.2% (+0.4%)	98.4% (+0.5%)	103.8% (+3.0%)	107.8% (+5.6%)
Phase B	94.6% (-0.8%)	97.7% (-0.6%)	101.1% (-0.1%)	103.8% (-0.4%)
Phase C	92.9% (-0.6%)	97.1% (-0.4%)	100.6% (-0.1)	102.5% (-0.3%)

The results from the two simulations are compared in Table 6-11. Voltage rise and drop become less when considering two independent sources than when assuming the two sources to have the same variations versus time. This is however for just one summer of data; when using multiple years of data, it is expected that the maximum values will move closer to each other.

Table 6-11. Comparison in obtained statistics between assuming two identical sources and two independent sources (bold).

	Minimum	5th percentile	95th percentile	maximum
Phase A	**95.2% (+0.4%)**	**98.4% (+0.5%)**	**103.8% (+3.0%)**	**107.8% (+5.6%)**
Phase A	95.4% (+0.7%)	98.5% (+0.6%)	104.9% (+4.1%)	108.8% (+6.5%)
Phase B	**94.6% (-0.8%)**	**97.7% (-0.6%)**	**101.1% (-0.1%)**	**103.8% (-0.4%)**
Phase B	94.4% (-1.0%)	97.5% (-0.8%)	101.1% (-0.1%)	103.5% (-0.7%)
Phase C	**92.9% (-0.6%)**	**97.1% (-0.4%)**	**100.6% (-0.1)**	**102.5% (-0.3%)**
Phase C	92.9% (-0.6%)	96.9% (-0.5%)	100.6% (-0.1%)	102.2% (-0.5%)

6.4 CONCLUSIONS

Using time series, over a period of just a few months, the hosting capacity is exceeded (maximum voltage above 110% of nominal) for just three customers with PV in the six-customer network. This corresponds reasonably well with the results from Chapter 3, where the hosting capacity was found to be one or two customers with PV. The short measurement period gives an underestimation of the maximum voltage and thus an overestimation of the hosting capacity.

Data from two different years gives rather different results for overvoltage statistics. Using data from just one year is insufficient to do a hosting-capacity estimation. Several years' of data should be used, but that requires long

measurement periods. The planning approach in Chapter 3 and 4 does not suffer from this disadvantage, although also this one requires some measurement data as input.

When considering the aggregation between two PV installations (measurements obtained for both installations about 500 m separated) overvoltage and undervoltage becomes less. This general trend is expected, as there will always be some aggregation affects. The size of the effect was however somewhat of a surprise. Further studies are needed to verify this and to obtain general guidelines. The fact that one installation had more often a higher production that the other may not be a typical case.

7 Conclusions

The hosting capacity of low-voltage networks for single-phase connected PV is limited for the two networks studied under the assumptions made. It was however also shown that several of the parameter values used have a strong influence on the results. This especially holds for the estimated size of the production per installation, the percentile value used in the performance index, and the range of the no-load voltage. The hosting capacity values found in the studies presented in this report are most likely and underestimation.

Several mitigation methods have been studied to increase the hosting capacity. The most promising ones are: coordinated connection of inverters to the phase with the lowest pre-connection voltage; curtailment of production or energy storage close to the PV installations; and capacitor bank or shunt reactor close to the distribution transformer. The first one appears rather simple; it can be applied without much investment. The method does however require a measurement for which some guidelines are needed.

The hosting-capacity based planning tool was shown to be a useful tool for evaluating the need for mitigation actions and for comparing mitigation actions.

The use of time series of production and consumption is an alternative to the stochastic method. This requires data over a number of years, as there are significant year-to-year variations.

Further collection of data from both production and consumption sites is needed. Time resolution should be at least 10 minutes. Using hourly data is not enough for hosting-capacity studies concerning overvoltage and undervoltage.

Annex – origin of figures and tables

Most of the figures and tables in this report were created using the software package Matlab. The table below links the tables and figures in this report with the files containing the Matlab codes.

Section	Figure or Table	Matlab Code
3.1	Figure 3-1	Figure201.m + impedances.txt
	Figure 3-2	Figure202.m + impedances.txt
	Figure 3-3	Figure203.m + impedances.txt
	Figure 3-4	Figure204.m + impedances.txt
	Figure 3-5	Figure205.m + impedances.txt
3.3	Figure 3-6	Figure052.m + Figure052sub.m
	Figure 3-7	Figure054.m + Figure054sub.m
	Figure 3-8	Figure055.m + Figure054sub.m
	Figure 3-9	Figure056.m + Figure054sub.m
	Figure 3-10	Figure109.m + Figure109a.m
	Figure 3-11	Figure120.m + Figure120a.m
	Figure 3-12	Figure121.m + Figure121a.m
3.4	Figure 3-13	Figure058.m + Figure058sub.m
	Figure 3-14	Figure112.m + Figure112a.m
3.5	Figure 3-15	Figure062.m + Figure062sub.m
	Figure 3-16	Figure065.m + Figure065sub.m
	Table 3-4	See table below
	Figure 3-17	Figure117.m + Figure117a.m
	Figure 3-18	Figure113.m + Figure113a.m
	Figure 3-19	Figure114.m + Figure114a.m
	Figure 3-20	Figure115.m + Figure115a.m
	Figure 3-21	Figure116.m + Figure116a.m
	Figure 3-22	Figure118.m + Figure116a.m
	Figure 3-23	Figure110.m + Figure110a.m
	Figure 3-24	Figure111.m + Figure111a.m
	Figure 3-25	Figure122.m + Figure122a.m
	Figure 3-26	Figure123.m + Figure123a.m
	Figure 3-27	Figure240.m + Figure240a.m
4.1	Figure 4-1	Figure211.m + Figure211a.m
	Figure 4-2	Figure212.m + Figure212a.m + Figure212b.m
	Figure 4-3	Figure130.m + Figure130a.m
	Figure 4-4	Figure131.m + Figure131a.m
	Figure 4-5	Figure132.m + Figure132a.m
	Figure 4-6	Figure262.m + Figure262a.m
	Figure 4-7	Figure133.m + Figure133a.m
	Figure 4-9	Figure260.m + Figure260a.m
	Figure 4-10	Figure261.m + Figure261a.m
4.2	Figure 4-11	Figure134.m + Figure134a.m
	Figure 4-12	Figure135.m + Figure135a.m
	Figure 4-13	Figure136.m + Figure136a.m
	Figure 4-14	Figure137.m + Figure137a.m

4.3	Figure 4-15	Figure138.m + Figure138a.m
	Figure 4-16	Figure139.m + Figure139a.m
4.7	Figure 4-17	Figure140.m + Figure140a.m
	Figure 4-18	Figure141.m + Figure140a.m
	Figure 4-19	Figure142.m + Figure140a.m
	Figure 4-20	Figure143.m + Figure143a.m
	Figure 4-21	Figure144.m + Figure143a.m
	Figure 4-22	Figure145.m + Figure143a.m
4.8	Figure 4-23	Figure146.m + Figure143a.m
4.9	Figure 4-24	Figure124.m
	Figure 4-25	Figure126.m
	Figure 4-26	Figure125.m
	Figure 4-27	Figure127.m
5.2	Figure 5-2	Figure002.m + DATA28.mat
	Figure 5-3	Figure003.m + DATA28.mat
	Figure 5-4	Figure004.m + DATA6.mat
	Figure 5-5	Figure005.m + DATA28.mat
	Figure 5-6	Figure006.m + DATA28.mat
	Figure 5-7	Figure007.m + DATA28.mat
	Table 5-1	Figure013.m + DATA28.mat
	Figure 5-8	Figure008.m + DATA28.mat
	Figure 5-9	Figure009.m + DATA28.mat
	Figure 5-10	Figure010.m + DATA28.mat
	Figure 5-11	Figure014.m + DATA28.mat
	Figure 5-12	Figure015.m + DATA28.mat
	Figure 5-13	Figure016.m + DATA28.mat
	Figure 5-14	Figure017.m + DATA28.mat
	Figure 5-15	Figure034.m + DATA28.mat
	Figure 5-16	Figure011.m + DATA28.mat
	Figure 5-17	Figure012.m + DATA28.mat
	Figure 5-18	Figure042.m + DATA28.mat
	Figure 5-19	Figure018.m + DATA28.mat
	Figure 5-20	Figure044.m + DATA28.mat
5.3	Figure 5-21	Figure020.m + DATA6.mat
	Figure 5-22	Figure021.m + DATA6.mat
	Table 5-2	Figure022.m + DATA6.mat
	Figure 5-23	Figure023.m + DATA6.mat
	Figure 5-24	Figure024.m + DATA6.mat
	Figure 5-25	Figure025.m + DATA6.mat
	Figure 5-26	Figure026.m + DATA6.mat
	Figure 5-27	Figure041.m + DATA6.mat
	Figure 5-28	Figure027.m + DATA6.mat
	Figure 5-29	Figure028.m + DATA6.mat
	Figure 5-30	Figure029.m + DATA6.mat
	Figure 5-31	Figure033.m + DATA6.mat
5.4	Figure 5-32	Figure215.m + VoltageC62017.txt
	Figure 5-33	Figure216.m + VoltageC62017.txt
	Figure 5-34	Figure217.m + VoltageC62017.txt
	Figure 5-35	Figure220.m + LTUPV2016.txt
	Figure 5-36	Figure224.m + LTUPV2016.txt

	Figure 5-37	Figure221.m + LTUPV2016.txt
	Figure 5-38	Figure225.m + LTUPV2016.txt
	Figure 5-39	Figure226.m + LTUPV2016.txt
	Figure 5-40	Figure223.m + LTUPV2016.txt
5.6	Figure 5-41	Figure241.m + LTUPV2017.txt
	Figure 5-42	Figure242.m + LTUPV2017.txt
	Figure 5-43	Figure244.m + LTUPV2017.txt
5.7	Figure 5-44	Figure245.m + BrinkenPV2016.txt
	Figure 5-45	Figure246.m + BrinkenPV2016.txt
	Figure 5-46	Figure247.m + BrinkenPV2016.txt
	Figure 5-47	Figure248.m + BrinkenPV2016.txt
	Figure 5-48	Figure249.m + BrinkenPV2016.txt + LTUPV2016.txt
	Figure 5-49	Figure250.m + BrinkenPV2016.txt + LTUPV2016.txt
	Figure 5-50	Figure251.m + BrinkenPV2016.txt + LTUPV2016.txt
6.1	Figure 6-1	Figure230.m + dataC62016.mat + LTUPV2016.txt
	Figure 6-2	Figure231.m + dataC62016.mat + LTUPV2016.txt
	Figure 6-3	Figure232.m + dataC62016.mat + LTUPV2016.txt
	Table 6-1	Figure233.m + dataC62016.mat + LTUPV2016.txt
	Figure 6-4; Table 6-2	Figure234.m + dataC62016.mat + LTUPV2016.txt
	Figure 6-5; Table 6-3	Figure235.m + dataC62016.mat + LTUPV2016.txt
	Figure 6-6; Table 6-4	Figure236.m + dataC62016.mat + LTUPV2016.txt
	Figure 6-7; Table 6-5	Figure237.m + dataC62016.mat + LTUPV2016.txt
6.2	Table 6-6	Figure263.m + LTUPV2017.txt + VoltageC62017.txt
	Table 6-7	Figure264.m + LTUPV2017.txt + VoltageC62017.txt
	Table 6-8	Figure265.m + LTUPV2017.txt + VoltageC62017.txt
6.3	Table 6-10	Figure266.m + dataC62016.mat + BrinkenPV2016.txt + LTUPV2016.txt
	Table 6-11	Figure267.m + dataC62016.mat + BrinkenPV2016.txt + LTUPV2016.txt

Origin of data inTable 3-4

Table 1 case 0	Figure065.m + Figure065sub.m
Table 1 case 1	Figure075.m + Figure075sub.m
Table 1 case 2	Figure076.m + Figure075sub.m
Table 1 case 3	Figure077.m + Figure075sub.m
Table 1 case 4	Figure078.m + Figure075sub.m
Table 1 case 5	Figure079.m + Figure075sub.m
Table 1 case 6	Figure080.m + Figure075sub.m
Table 1 case 7	Figure081.m + Figure075sub.m
Table 1 case 8	Figure082.m + Figure075sub.m
Table 1 case 9	Figure083.m + Figure075sub.m
Table 1 case 10	Figure084.m + Figure075sub.m
Table 1 case 11	Figure085.m + Figure075sub.m
Table 1 case 12	Figure086.m + Figure075sub.m

ÖVERSPÄNNING FRÅN ENFASANSLUTNA SOLPANELER

När solkraft ansluts till ett lågspänningsnät leder det till en spänningsökning för de kunders om är anslutna till nätet. När mängden ansluten solkraft orsakar en spänningsökning som överstiger överspänningsgränsen har man nått den så kallade acceptansgränsen och för att då kunna ansluta ytterligare solkraft krävs det åtgärder för att minska spänningshöjningen.

Här har påverkan av enfasanslutna solcellsinstallationer till överspänning i lågspänningsnät studerats. Resultaten visar att acceptansgränsen är begränsad för de två befintliga lågspänningsnät som studerads med hjälp av en nyutvecklad planeringsmetod.

Målet har varit att hitta åtgärden för att öka acceptansgränsen. Den mest lovande är en koordinerad anslutning av växelriktare till fas med lägsta spänning innan anslutning. Den här metoden kräver en mätning som det krävs nya riktlinjer för. Det krävs också ytterligare insamling av data, med en tidsupplösning på minst 10 minuter, både från produktion och från förbrukning eftersom timvärden inte räcker för att beräkna acceptansgränser för överspänning och underspänning.

Ett nytt steg i energiforskningen

Energiforsk är en forsknings- och kunskapsorganisation som samlar stora delar av svensk forskning och utveckling om energi. Målet är att öka effektivitet och nyttiggörande av resultat inför framtida utmaningar inom energiområdet. Vi verkar inom ett antal forskningsområden, och tar fram kunskap om resurseffektiv energi i ett helhetsperspektiv – från källan, via omvandling och överföring till användning av energin. www.energiforsk.se

Energiforsk